Evaluation of Soil-Atmosphere Interaction during Evaporation Process

滕, 继東

https://doi.org/10.15017/1398369

出版情報：九州大学, 2013, 博士（工学）, 課程博士
バージョン：
権利関係：全文ファイル公表済

Evaluation of Soil-Atmosphere Interaction during Evaporation Process

Jidong Teng

Evaluation of Soil-Atmosphere Interaction during Evaporation Process

A Thesis Submitted
In Partial Fulfillment of the Requirements
For the Degree of
Doctor of Engineering

By
Jidong Teng

to the
DEPARTMENT OF CIVIL AND STRUCTURAL ENGINEERING
GRADUATE SCHOOL OF ENGINEERING
KYUSHU UNIVERSITY
Fukuoka, Japan
August, 2013

DEPARTMENT OF CIVIL AND STRUCTURAL ENGINEERING
GRADUATE SCHOOL OF ENGINEERING
KYUSHU UNIVERSITY
Fukuoka, Japan

CERTIFICATE

The undersigned hereby certify that they have read and recommended to the Graduate School of Engineering for the acceptance of this thesis entitled, ***"Evaluation of Soil-Atmosphere Interaction during Evaporation Process***" by **Jidong Teng** in partial fulfillment of the requirements for the degree of **Doctor of Engineering**.

Dated: August, 2013

Thesis Supervisor:

_____

Prof. Noriyuki Yasufuku, Dr. Eng.

Examining Committee:

_____

Prof. Takahiro Kuba, Dr. Eng.

_____

Prof. Yasuhiro Mitani, Dr. Eng.

_____

Prof. Noriyuki Yasufuku, Dr. Eng.

ABSTRACT

Nowadays, desertification is one of the world's most alarming global environmental problems. It takes place worldwide in drylands that occupy 41% of earth's land area. The total area affected by desertification is between 6 and 12 million square kilometers, a billion people are under threat from further desertification.

With the knowledge that only environmentally friendly engineering can provide sustainable solutions for combating desertification, the concept of "self-watering system (SWS)" has been proposed from geotechnical view, which aims to develop the greening system without any irrigation as a countermeasure of desertification. In the research program of SWS, geotechnical approach has been dedicated to development of safe and long-term water supply in arid and semi-arid region.

Some important criteria are critical to assess the performance of SWS, such as conservation of soil water, water use efficiency, water content distribution. All these criteria are highly related to the soil-atmosphere interaction. The soil water status in SWS is closely interacted with the ground surface fluxes, particularly the evaporation process, because the evaporation is extremely high and greatly exceeding the annual precipitation in arid and semi-arid region. Many other geotechnical applications also need to evaluate evaporation process. However, little attention was taken from geotechnical researchers to deal with the soil-atmosphere interaction during evaporation process. From academic view, mechanism of soil surface evaporation is not completely understood, how to extend clearly defined potential evaporation to actual evaporation has been a challenge. Moreover, the apparatus capable of truly replicate climate characteristics to evaluate soil evaporation process is really rare.

The primary objective of this thesis is to identify the dominant mechanisms of soil-atmosphere interaction during evaporation process, which is extended from both experimental and analytical approaches. In this thesis, a newly developed climate control apparatus is introduced, based on which soil evaporation properties are evaluated in various conditions. An empirical methodology for determining soil evaporation is presented. The analytical models are developed for simulating water content at any time and any soil depth during evaporation process. Finally, the in-situ soil-atmosphere interaction is investigated by a filed lysimeter test. This dissertation

consists of seven chapters; the specific content of each chapter is described as follows:

Chapter 1 familiarizes the readers with the concept of SWS to combat desertification. It is illustrated that the necessity of the investigation of evaporative flux for evaluating SWS in arid and semi-arid region and other typical problems. The objectives of the thesis to accomplish are briefly outlined. In addition, the original contributions are indicated.

Chapter 2 provides a brief summary of the previous research on the evaporation topics. It reviews from three aspects that are experimental approach for measuring evaporation, methods to compute evaporation and the simulation of soil moisture change. The available information is used to set the stage for further theoretical and experimental evaluation in this research program.

Chapter 3 mainly focuses on the development of laboratory test program. A newly developed climate control apparatus is put forward, which can maintain the atmosphere conditions comprehensively to investigate evaporation behavior. The apparatus is composed of climate control part, evaporation part and data acquisition system. It has the features of flexibly configuring for specimen, accuracy increased and automatic control and visualization. The calibration tests shows that the apparatus is capable to favorably control wind speed and relative humidity, while temperature is stable with a relatively small range.

Chapter 4 presents the methodology for determining soil surface evaporation. Before parameterizing the soil evaporation, the effect of related factors on soil evaporation is evaluated separately by various tests. It is found that, evaporating time would shorten 4% in average for air temperature increasing 1 °C. An increase in wind speed always results in a linear increase in evaporation rate, but average gradient of the increase is related to relative humidity. It would not be a linear relationship between evaporation rate and relative humidity, an inflection point at about 60% properly exists. Soil structure (dry density) has little influence on the evaporation rate, while particle size of soil affects the diffusion of vapor, soil in greater particle size shows longer time of stage 1. Theoretical derivations of E_a/E_p from aerodynamic approach and molecular physics approach indicate that the water content alone cannot be the unique independent variable to formulate the evaporation from all soil surfaces. A parameterizing method is proposed by defining a critical water content θ_c and setting up the formulation of θ_c for different soil textures and wind speeds. Three easily measured indexes are the inputs in this model: the

moisture of top 1cm soil, aerodynamic resistance (wind speed), and field capacity as a constant for specified soil texture. Although this parameterization is in empirical form, its accuracy meets the requirement for estimating evaporation rate from different soil surface.

Chapter 5 develops an analytical model for simulating the temporal and spatial change of soil water content during evaporation process. Based on several assumptions, analytical solutions of Richards' equation are derived in two categories, which are one dimensional evaporation problem from infinite soil domain, and one dimensional evaporation problem with water table. Two groups of column soil evaporation tests are conducted to verify the proposed model, the first group controls the environmental conditions without water supply while the second group controls the water table. The good agreement between the proposed analytical solution and experimental result indicates that the analytical model provides a reliable way to investigate water content redistribution during evaporation process. Finally, the parameter study is performed based on the analytical model, which includes hydraulic parameters, surface evaporative flux, and depth of water table. Some new findings are stated as well in this chapter.

Chapter 6 highlights the in-situ evaluation of soil-atmosphere interaction. A lysimeter test lasted for 81 days is carried out, based on which the thermal and hydrological phenomena of soil are discussed. Finite element simulation is also performed to compare with the measured data. The summary are remarked that the most significant variation of volumetric water content is the near surface area, which is limited in top 35 cm; the lower the soil depth, the greater change in water content responding to evaporation or precipitation. The result also suggests that temperature is more sensitive to climate change than volumetric water content. The rainfall event shows the function of eliminating temperature gradient and unifying the water content profile, while the evaporation process enlarges the gradient of temperature and water content. The comparison between measured data and simulated result indicates that numerical approach provides a rough simulation of the variation of water content and soil temperature. Further effort is required on dealing with the upper boundary.

Chapter 7 concludes the results and achievements of the whole thesis; Also, it indicates the problems to be solved in future studies.

ACKNOWLEDGEMENTS

First and foremost, I express my sincere gratitude to my supervisor, Prof. Noriyuki Yasufuku. He gave me constructive guidance, good supervision, constant encouragement, and many far-reaching thoughts. It is my honor to study with such a talented, capacious-thinking, and amiable person. I would like to say that he made all possible efforts to give me the best research conditions.

I also give my sincere appreciation and respect to Prof. Guangli Xu in China University of Geosciences, who provided me a lot of knowledge and opportunities in engineering practice and academic research. Moreover, his encouragement and help are valuable for both my life and research.

I would also like to extend my sincere appreciation to other academic and technic staffs in geotechnical engineering research group, both past and present, Prof. Hemanta Hazarika, Prof. Kiyoshi Omine, Associ. Prof. Taizo Kobayashi, Assistant Prof. Ryoshi Ishikura, Dr. Kohei Araki, Ms. Aki Ito. Specially, I am indebted to Mr. Michio Nakashima for his great assistance in laboratory and field tests and instruments for this research.

I would like to express my sincerely gratitude to members of my dissertation committee, Prof. Noriyuki Yasufuku, Prof. Takahiro Kuba, and Assoc. Prof. Yasuhiro Mitani for their treasure time in review evaluation and valuable comments on my thesis.

Special thanks are given to my research colleges for their friendship and support throughout my time in Kyushu University, they are: Dr. Manandhar Suman, Dr. Qiang Liu, Dr. Jun Tong, Mr. Shiyu Liu, Ms. Jiali Miao, Mr. Handoko Luky, Mr. Vilayvong, Mr. Zentaro Furukawa, Mr. Zhenbo Jiang, Mr. Yi He, Mr. Guojun Liu, Mr. Shintaro Miyamoto, Mr. Taiga Hashimoto, Mr. Kenichirou Okumura, Mr. Masataka Iwasaki, and Mr. Satoshi Suenaga.

I must also acknowledge my friends who have provided encouragement and kind help to me. Special thanks are given to Mr. Xingwei Ren, Mr. Yanjun Shen, Mr. Shuai Meng, Mr. Changshuai Sun and Mr. Ning Jia.

Finally, my deepest gratitude is due to my family for their continuous encouragement and support in the past years. I appreciate all the things they have done for me.

TABLE OF CONTENT

LIST OF FIGURES

LIST OF TABLES

NOMENCLATURE

C_{sd}	specific heat of dry soil
C_w	specific heat of water
C_p	specific heat of air
C(θ)	specific water capacity
D_{atm}	molecular diffusivity of vapor in air
D_l	hours of daylight
E	evaporation
ET	evapotranspiration
E_a	actual evaporation rate
E_c	cumulative evaporation rate
E_p	potential evaporation rate
G	soil heat flux
G_p	basal percolation
H	sensitive heat transfer
I	the annual heat index
K_0	von Karman's constant
L	water table depth
LE	latent heat transfer
M_w	molecular mass of water
N	the number of days in a given month
P	precipitation
R	gas constant for water vapor
RH	relative humidity
R_h	mean monthly relative humidity
R_s	total solar radiation
R_n	net radiation
R_{off}	surface water runoff
SWS	self-watering system
T_a	air temperature
mean dew point	

TDR	time domain reflectometry
T_m	the modified temperature due to elevation
T_w	water surface temperature
b	a fitting parameter
c	a fitting parameter
d	duration of average monthly daylight in hour
e_a	vapor pressure of air
e_s	vapor pressure of water or soil surface
e^*	vapor pressure at the gas-liquid interface
e_l	vapor pressure from the center of the wet patches
$f(u)$	a function of wind speed
g	acceleration of gravity
h_r	relative humidity of the air next to the water in soil pore
h	pore water pressure head
i	monthly heat index
k	hydraulic conductivity
k_m	a monthly consumptive use coefficient
k_s	saturated hydraulic conductivity
l	pore connectivity parameter
m	the ratio of critical water content to volumetric water content
m_v	one fitting parameters in van Genuchten model
n_v	one fitting parameters in van Genuchten model
p_b	barometric pressure
p_{er}	percentage of total daytime hours to the period used out of total daytime hours of the year
q	volumetric liquid water flux
q_a	specific humidity of air
q_s	specific humidity of air at the soil surface
q^*	saturated specific humidity as a function of temperature
r	radius of parallel pipes
r_a	aerodynamic resistance
r_s	surface resistance
s_1	relative wetted surface area

t	time
u	wind speed
z	vertical coordinate
Δ	slope of the saturation vapor pressure curve
ΔS	changes in moisture storage
ρ_a	density of air
γ	psychromatic constant
θ	volumetric water content
θ_c	critical water content
θ_{fc}	the field capacity
θ_s	saturated water content
θ_r	residual water content
ψ	water potential at soil surface
λ	soil water desorption
δ	thickness of the viscous sublayer
Λ	mean free path of the gas molecules
α	soil pore-size distribution parameter
α_m	adjust parameter in the function of soil wetness
α_v	one fitting parameter in van Genuchten model
β	a positive constant with the unit of one over time
β_m	adjust parameter in the function of soil wetness
Θ	normalized soil water content

CHAPTER 1

INTRODUCTION

1.1 BACKGROUND

1.1.1 CONCEPT OF SELF-WATERING SYSTEM

Desertification is defined as “land degradation in arid, semiarid and sub-humid areas, resulting from climatic various factor including climatic variations and human activities” by the United Nations Convention to Combat Desertification (UNCCD, 1994). Nowadays, desertification is one of the world’s most alarming global environmental problems. It takes place worldwide in drylands that occupy 41% of earth’s land area. It has been estimated that some 10~20% of drylands are already degraded, the total area affected by desertification being between 6 and 12 million square kilometers, that about 1~6% of the inhabitants of drylands live in desertified areas, and that a billion people are under threat from further desertification (Holtz, 2007). At least 90% of the inhabitants of drylands live in developing countries and they suffer the poorest economic and social conditions.

Considering that the world’s dry lands is home to more than 2 billion people and being concerned that many dry lands are subject to desertification as a result of extended droughts, climate change and human activities, new scientific challenges and opportunities for research and development have emerged. With the knowledge that only environmentally friendly engineering can provide sustainable solutions for combating desertification, the concept of “self-watering system” (SWS) has been proposed by geotechnical research laboratory of Kyushu University, which aims to develop the greening system without any irrigation as a countermeasure of desertification. In the research program of SWS, geotechnical approach has been

dedicated to development of safe and long-term water supply in arid and semi-arid region.

The objective of the “self-watering system” (SWS) is introduction of innovative approach in project design and creation of energy efficient, large water supply system, adapted to the prevailing desert environment and integrated with the recovery of depleted and saline regional aquifers in arid and semi-arid region. The SWS is designed to collect and store all kinds of water, comprised of the simple ground is much efficient to support surface vegetation. The system can continually raise the ground water to a certain depth in the sandy ground using the capillary force without extra energy input. Moreover, it can minimize the evaporation from the system, which provides the potential to minimize salinization (Liu et al., 2011).

1.1.2 NECESSITY OF PREDICTING SOIL SURFACE EVAPORATION

Conservation of soil moisture, water use efficiency, water resource distribution and so on are important criteria for the assessment and further improvement of SWS in semi-arid and arid regions. These criteria cannot be carried out without considering the interaction among soil, vegetation, and the atmosphere. The soil water condition is closely related to the ground surface fluxes, especially in the dry climate condition. Therefore, the ability to predict surface flux also plays an important role in operation of SWS. Moreover, an understanding of the process of surface flux in relation to the overall soil water balance is necessary.

Amongst the fluxes that the different actors of the water sector need to assess, soil evaporation and infiltration are of major importance. Infiltration refers to the movement of water into a soil profile, of which the quantification can be determined directly by using the fluxmeters. Evaporation from bare land is a phenomenon in which the aqueous content of the soil is directly transferred into the atmosphere from the ground surface in the gaseous phase, due to vaporization. The mechanics of infiltration is relatively understood and widely discussed in literature. In contrast, the mechanics of evaporation from soil surface is not completely understood. However, Estimating surface evaporation is extremely important for the study of water resources management, environmental studies in arid and semi-arid region where the potential evaporation is very high, greatly exceeding the annual rainfall. Evaluation of evaporation also can significantly improve the modeling of energy balance and water cycle.

From other aspects, numerous practical problems require the prediction of the water flux from soil surface as summarized in Figure 1.1. Especially for geotechnical problems, it includes that regional ground water modeling, the design of light structure on expansive soils, seepage analysis through earth structures such as dams and canals, and the evaluation of pore pressure conditions in natural slopes or manmade embankments (Wilson, 1990). In addition, recent evaluation on hazards caused by droughts showed that evaporation is also an important process to be accounted for natural hazards analysis. However, little attention was taken from geotechnical researchers to deal with the soil-atmosphere interaction, especially the surface evaporative flux. Therefore, a comprehensive research of mechanistic and experimental approaches is requisite to enhance the study of soil-atmosphere inaction.

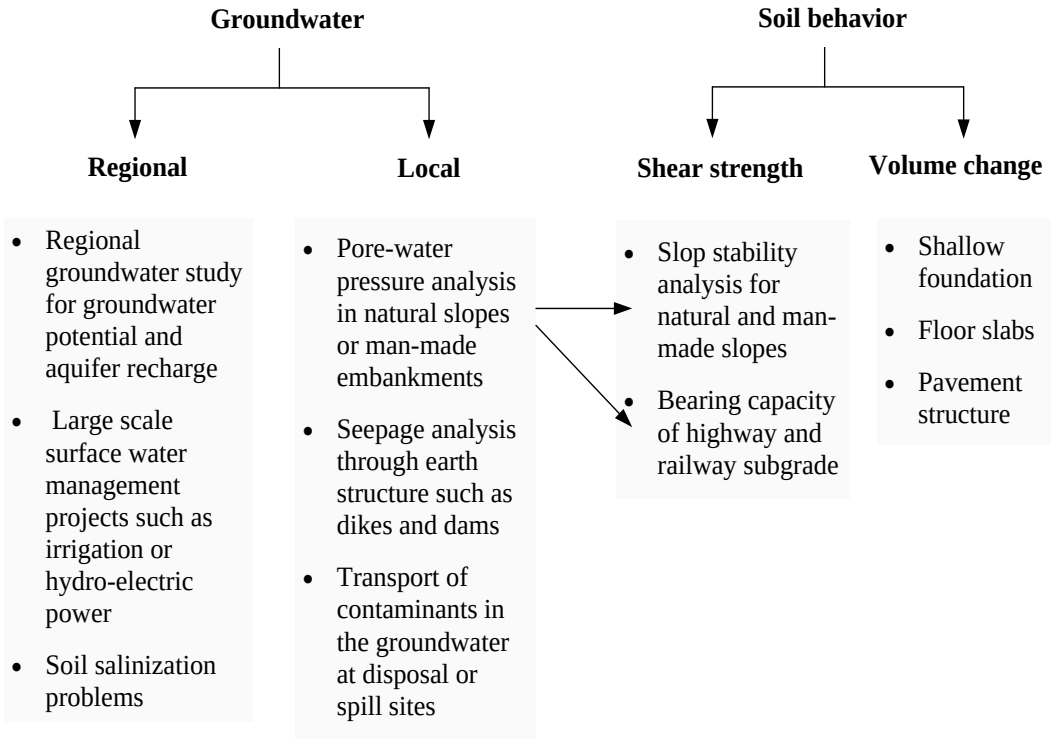

Figure 1.1 Classes of problems requiring the evaluation of moisture fluxes at the soil surface (after Wilson 1990)

1.2 OBJECTIVES AND SCOPES

The objectives of this study are to investigate the evaporative flux from soil

surface particularly unsaturated soil surfaces, which impose the greatest analytical difficulties. To achieve the goal, the mechanism of the evaporation should be investigated from both experimental and analytical or numerical simulation approach. The specific objectives are as follows:

1) To develop a new apparatus with distinguishing features for evaluating the mechanisms involved in evaporation and water content distribution.
2) To explain the physical process of evaporation and to identify the appropriate soil properties and meteorological variables that control evaporation from soil surface.
3) To propose the methodology for parameterizing the acutal evaporation rate from soil surface and analytically model for soil water redistribution during the evaporation process.
4) To carry out laboratory and field tests together with numerical simulation to verify the proposed model, further demonstrate the soil-atmosphere interaction mechanism in field condition.

The research in this thesis is the evaluation of evaporation from non-vegetated soil surfaces, it is understood that soil moisture due to plants uptake (transpiration) may exceed evaporation from a bare soil. However, the presence of a vegetative cover greatly increases the complexity of the problem of evaluation of evaporation. Before the complex evapotranspiration, process from vegetated surface can be examined from geotechnical perspective, the mechanism and processes involved in evaporation from unsaturated soil must be thoroughly understood.

1.3 THESIS ORGANIZATION

To fully achieve the objectives as mentioned above, this dissertation is organized in seven chapters with the framework presented in Figure 1.2. The outlines of each chapter are briefly described as follows:

Chapter 1 familiarizes the readers with the concept of SWS to combat desertification. And it highlights the necessity of investigating evaporative flux for evaluating performance of SWS and other typical geotechnical problems. The objectives of this thesis and research program required to accomplish are briefly outlined. In addition, the original contributions of this study are presented.

Chapter 2 provides a brief summary of pervious research on the evaporation topic. It reviews from the following three aspects: phenomena of evaporation that

mainly discusses the affecting factors of soil evaporation, measurement of soil evaporation, methods to determine evaporation rate and finally the simulation of soil water variation during evaporation process. The academic issues to be solved are also summarized in this chapter. The available information is used to set the stage for further theoretical and experimental development in this research program.

Chapter 3 mainly focuses on the apparatus development. Since the errors related to evaporation measurements are mainly due to the alteration of natural profiles of atmospheric conditions. A climate control apparatus is newly developed and comprehensively introduced from the aspects of instrumentation of the apparatus, features and accuracy calibration. This apparatus is flexible to response to different experimental demands, for example, the pan soil evaporation test, column soil evaporation test with or without water supply. In addition, it provides the soil evaporation rate in higher precision 0.01 mm/h compared with regular evaporation devices.

Chapter 4 proposes a methodology for determining evaporation from soil surface. The influence factors of soil evaporation are firstly evaluated by evaporation test, including the atmosphere variables and soil properties such as relative humidity, temperature, wind speed, and soil dry density. The theoretical formulation of the actual evaporation rate is derived from the approaches of aerodynamic approach and molecular physics approach. Based on the theoretical formulation, the related parameters are identified, and the form of the determining formula is obtained. Finally, the parameterization of the soil evaporation is proposed by defining a critical water content θ_c. The empirical formulation of θ_c for different soil textures and wind speeds is set up. The experimental work verifies the proposed model, which applies 12 different atmosphere conditions on three kinds of soil respectively.

Chapter 5 investigates the water content variation of soil during the evaporation process that is the water flow properties in soil body caused by the surface evaporation. Actually, it provides a connection between soil surface evaporation and the water content distribution. Based on some assumptions, the analytical solutions of Richards' equation for two evaporation problems are developed, which are the evaporation process from infinite soil domain, evaporation process with water table. These two cases are seeks to comprise the normal problem dealing with evaporation problem. Two groups of soil column evaporation experiments are conducted to verify the proposed model. In first group, the atmosphere condition is controlled in three cases with no water supply, while the water table is maintained at two different

depths for the second group. The comparison between the proposed analytical model and laboratory test result shows good agreement and thus validates the proposed model. Finally, the parameter study is performed to investigate the influence of soil hydraulic properties and external factors on soil water distribution during evaporation process.

Chapter 6 evaluates the soil water properties towards soil-atmosphere interaction in natural condition. A lysimeter test conducted in the field of Ito campus of Kyushu University is described, it provides an extensive database of environmental parameters and the reaction of soil properties. Both thermal and hydrological phenomena are discussed in this chapter. HYDRUS-1D code is adopted to simulate the variations of water content, soil temperature and water fluxes, these simulated data is also used to compare with field-measured result.

Chapter 7 summarizes the findings from this dissertation and provides recommendations regarding the direction for future work in this research topic.

1.4 ORIGINAL CONTRIBUTIONS

Current research investigates the soil-atmosphere interaction during evaporation process from both experimental and theoretical approaches; some new findings are obtained which are considered as the original contributions, as follows,

(1) A climate control apparatus is newly developed for investigating the soil evaporation properties, it has function of handling with different experimental demands, providing the soil evaporation rate in higher precision, and auto-testing system.

(2) Two theoretical derivations from aerodynamic approach and molecular physic approach are developed to formulate the ratio of actual evaporation to potential evaporation, which identifies the related parameters and the form for determining soil evaporation.

(3) A methodology for determining soil evaporation is presented by defining a critical water content θ_c and setting up the empirical formulation of θ_c for different soil textures and wind speeds. Three easily measured indexes are inputs in this methodology: water content of top 1cm soil, aerodynamic resistance (wind speed), and field capacity as a constant for specified soil texture.

(4) The analytical model for simulating the soil water redistribution during

evaporation process in two cases is developed respectively, which are the evaporation process from infinite soil domain, and evaporation process with water table. In this model, the basic hydraulic parameters k_s, α, (θ_s -θ_r), constant evaporation rate E, and water table depth L are inputs for simulating instantaneous water content profile. The model in these two cases can comprise the normal problem dealing with evaporation problem.

(5) The filed lysimeter test provides a practical foundation for designing the SWS, moreover the comparison between finite element simulation of HYDRUS-1D code and field measurement also designate the further effort on dealing with the field soil-atmosphere interaction problem.

REFERENCE

Liu, Q., Yasufuku, N., Omine, K., and Hazarika, H. (2011): A geotechnical countermeasure for combating desertification: self-watering system in unsaturated arid ground. The Proceedings of 5th International Symposium on the East Asian Environmental Problems, 209-216.

Holtz, U. (2007): Implementing the united nations convention to combat desertification from a parliamentary point of view-Critical assessment and challenges ahead, 1-28.

UNCCD, (1994): United Nations Convention to Combat Desertification.

Wilson, G. W. (1990): Soil evaporative fluxes for geotechnical engineering problems. Ph.D. dissertation, University of Saskatchewan, Saskatoon.

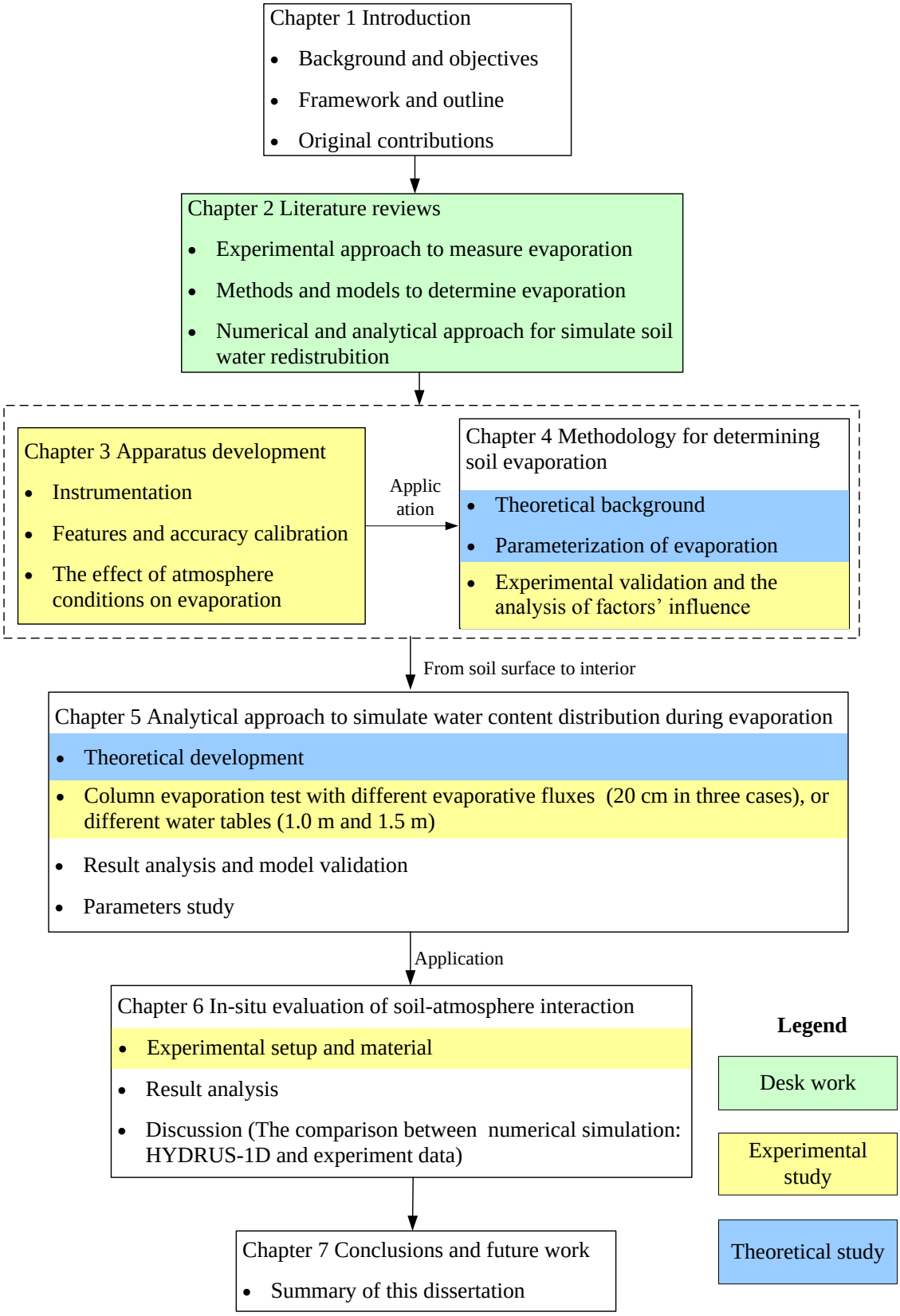

Figure 1.2 Flowchart of this dissertation

CHAPTER 2

LITERATURE REVIEW

2.1 INTRODUCTION

Evaporation is a complex process belonging to a phenomenon of soil-atmosphere interaction in nature, which needs comprehensively consideration of both atmosphere condition and soil water properties. This chapter provides the literature review from the aspects of firstly physical illustration of evaporation process, secondly the experiment approach to measure evaporation, thirdly method to determine evaporation, and finally the simulation of soil water redistribution due to evaporation.

2.2 EVAPORATION PHENOMENON

2.2.1 DEFINITION

Evaporation is the process that liquid water changes to vapor from macroscopic view, while water molecule overcomes the attractive forces between molecules and escapes to atmosphere from microscopic view. Hillel (1980) pointed that three requirements should be satisfied for evaporation occurrence and maintenance, continuous energy supply, the vapor pressure gradient between evaporative surface and atmosphere and sufficient water transfer to evaporative surface.

We usually refer the evaporation process occurring at a free water surface, which actually is the potential evaporation (E_p), the International Glossary of Hydrology (World Meteorological Organization, 1974) defines the E_p as "The quantity of water vapor which could be emitted by a surface of pure water per unit

surface area and unit time under the existing atmosphere conditions". It is a function of meteorological variable. However, the actual evaporation (E_a) that the evaporation takes place on soil surface is the topic specifically dealt with in this thesis. In most simple terms, maximum rate of E_a is stated to be approximately equal to the E_p when the soil is wet or near saturated, then it start to decline as the surface becomes unsaturated and the supply of water to the surface becomes limited (Brutseart, 1982).

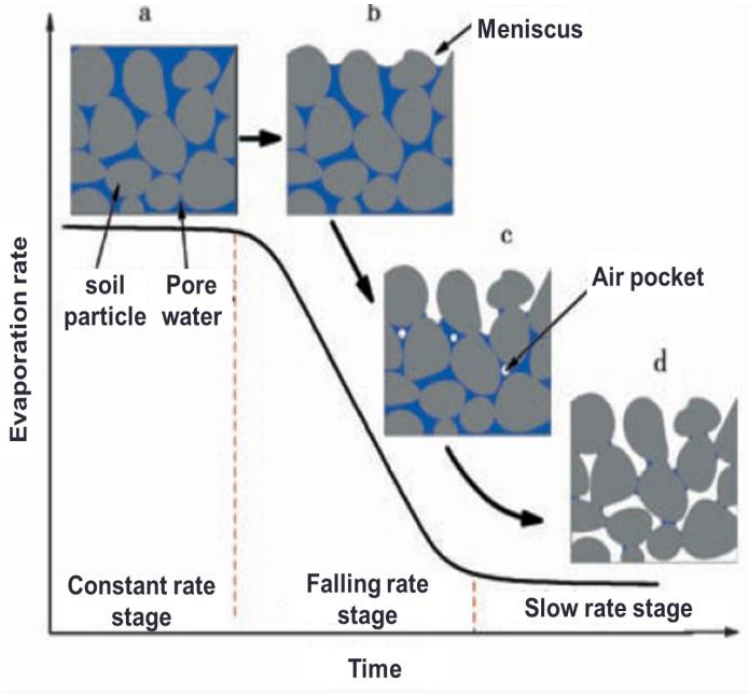

Figure 2.1 Relationship of soil evaporation rate versus time with showing there stages of drying and soil water status

The shape of evaporation curve shown in Figure 2.1 is well known and has been described by many researchers, which has three stages in general. Stage I named as constant rate stage is the maximum or potential rate of drying that occurs when the soil surface is at or near saturated. At that time, the soil is sufficiently conductive to supply water to the evaporative site at a rate equal to the evaporative flux imposed by climatic conditions.

Stage II is the falling rate stage, it starts when the conductive properties of the soil no longer permit a sufficient flow of water to the surface to maintain the maximum potential rate of evaporation. The hydraulic conductivity of the soil decreases with desaturation because the effective cross sectional area of the liquid phase is declining or thinning out. Richie (1972) claim the decline in evaporation

with is proportional to the square root of time elapsed, which was validated by many researchers from experimental work including Yunusa et al. (1994), Brutsaert and Chen (1995), Shokri and Or (2011) and so on.

The rate of evaporation continues to desiccate and reaches a slow residual value defined as Stage III. It is stated by Hillel (1980) that the Stage III occurs after the soil surface becomes sufficiently discontinuous. The flow of liquid water to the surface eases and water molecules may only migrate to the surface through the process of vapor diffusion. The third stage of drying occurs at a point of drying where the residual liquid phase is controlled by the molecular adsorptive forces of the soil particle.

In summary, it can be seen that the rate of actual evaporation from soil surface is controlled by both climate conditions and soil properties.

2.2.2 FACTORS AFFECTING ACTUAL EVAPORATION

Evaporation from soil surface involves very complex mechanisms since water in soil is not freely available. Exchange of water vapor between the surface and the atmosphere not only depends on hydraulic transfers within the deep soil but also on the diffusion of water in a thin layer close to the surface where vaporization of soil water takes places. Hillel (1980) stated that the actual evaporation rate is determined either by external evaporability or by the soils own ability to deliver water, whichever is the lesser (and hence the limiting factor). Evaporation from soil surface is affected by many factors, such as soil hydraulic properties, climate conditions, soil-atmosphere interface behavior and so on. These factors do not function as independent variables, but rather acts as a closely coupled system.

The evaporation rate is controlled by the climate condition, which is indexed by energy availability, humidity and rate of turbulent diffusion. Firstly, the energy provided to evaporation is normally the solar radiation, which supplies the power for the molecule to escape out from water body. And also, it can improve the temperature of subsurface, then the molecules have a higher average kinetic energy, thus evaporation can be accelerated. Secondly, evaporation rate is a function of the humidity difference between the water surface and the overlying air. Only when the vapor pressure deficit exists, the evaporation occurs. Thirdly, vapor pressure deficit soon reaches zero in calm condition for evaporation, so a mixing of air by turbulence is required, air movement is needed to remove the lowest moist layers in contact with

the water surface and to mix them with the upper drier layers. The stronger wind results in greater turbulence. Thus, there will be more convection and more evaporation. In addition to meteorological factors, the physical characteristics of water body also have influence on the rates of evaporation, such as the salinity.

Refer in particular to factors affecting the soil surface evaporation, the most important thing is water availability, which is highly related to the depth of water table. Gardner (1958) developed solutions to the unsaturated flow equation for the case of steady state flow from a water table. He showed that the maximum evaporation rate from a soil is a function of the hydraulic conductivity of the soil and the depth to the water table. The results show that if the water table is located at a shallow depth, a steady evaporation rate will be attained, and that the greater the depth, the lower the steady state evaporation rate will be.

The effect of soil texture and associated hydraulic conductivity on soil evaporation rate were also demonstrated by Gardner (1958). Figure 2.2 shows the relationships between the free water evaporation rate and the computed soil evaporation rate for a medium and a coarse texture soil. In the case of the medium-textured soil, the soil evaporation rate almost equals to the free water evaporation rate at low and moderate evaporative condition. Restriction to flows occurs only when high evaporation rates are imposed. The curve for coarse textured soil shows a decline in the evaporative rate at much lower fluxes. This occurs because the hydraulic conductivity of coarse grained material decreases more rapidly as desaturation occurs.

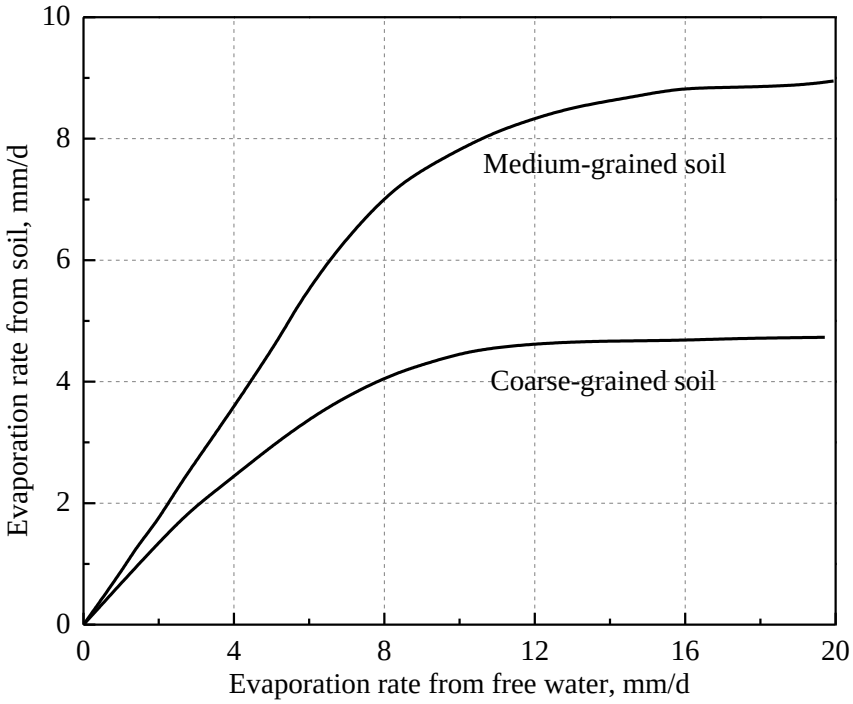

Figure 2.2 Steady state evaporation rates from medium and coarse textured soils versus the evaporation rate from a free water surface (after Gardner, 1958)

Besides that, soil color, temperature and surface roughness also affect the evaporation from soil surface. Soil color affects albedo of solar radiation, normally darker soils tends to absorb more heat. Warmer soils may have higher rates of evaporation as they have more energy that is available. The surface roughness would have influence on the movement of the wind.

2.3 DIRECT MEASUREMENT OF EVAPORATION

Direct measurements of evaporation are commonly performed by meteorologists and hydrologists. Direct measurements typically determine the potential evaporation, the evaporation rate that is controlled by climate conditions rather than by soil and groundwater conditions. The most common direct measurement methods for evaporation are evaporation pans and lysimeters, and also some sophisticated equipment were also adapted in lab or field evaporation test. A comprehensive review is presented in Table 1.1.

Each measurement method has its own application scope. The evaporation pans are likely the most familiar devises in evaluating evaporation. It gives realistic

estimates of potential evapotranspiration in humid regions while it is less reliable in arid climates. Factors such as moisture availability, advected energy and surface roughness are extremely important (Brutseart, 1982).

A lysimeter measures the weight change of a soil mass due to evaporation based on the load cell at bottom. The apparatus is installed or constructed in the field such that its surface is continuous or flush with the natural ground. Lysimeter provides the best estimate of actual evaporation in the field. Many researchers from hydrology and agriculture conducted the lysimeter experiment with different features including Plauborg (1995), Herbst et al. (1996), Benson et al. (2001), Miyamoto et al. (2010) and so on. In addition, Wilson (1990) and Yanful (2003) also carried out laboratory evaporation tests by developing new apparatus, of which the principles are similar to lysimeter. In fact, field tests have limitation including difficulty in imposing predetermined climate conditions (controlling boundary condition) and in making long term measurements. Also it is required for assessing hysteretic behavior of soil as in responds to alternating drying and wetting.

For laboratory evaporation tests, various kinds of apparatus have been developed. Van de Griend (1994), Yamanaka et al. (1997), and Wang (2006) developed the evaporation apparatus based on wind tunnels in different scales. The wind tunnel can provide enough range of wind speed to increase the evaporation rate, but sometimes other variables would change much due to its large scale. Yanful (1997), Aluwihare et al. (2003) and Cui (2012) used environmental chamber to investigate soil surface evaporation with different properties, the working principle of the chambers developed by Aluwihare et al. (2003) and Cui (2012) is similar, which calculate the evaporation rate from the change of air humidity. The environmental chamber can maintain certain climate condition and provide full set of data involving both air and soil at a relatively low cost, thus may be the best devices for studying soil water evaporation (Cui et al., 2012). Blight (1997) introduced a set of devices to monitor the micrometeological parameters thus to indirectly predict evaporation rate. Tristancho et al. (2011) developed equipment combing the climate chamber with a centrifuge, which was designed to simulate tropical weather conditions and respect the scaling laws.

Examination of the existing apparatus shows that most of them only analyze the air conditions, the soil being few instrumented and studied. Moreover, the apparatus capable to control climate conditions for investigating evaporation process is relatively rare; the researchers normally conducted the evaporation test under natural

condition. In other words, no device to date, truly replicate climate characteristics to evaluate soil evaporation process.

2.4 METHODS FOR CALCULATING POTENTIAL EVAPORATION

Potential evaporation is not only an important input in hydrological cycle simulations, but also acts as a base for the estimation of actual evaporation. Therefore, we firstly reviews the methods for calculating potential evaporation in this section. Over the last century, a large number of more or less empirical methods have been developed by numerous scientists and specialists worldwide to estimate potential evaporation from different climatic variables. These methods can be categorized into three groups due to their mechanisms: mass transfer method, radiation based method and radiation based method. However, the use of different methods to estimate potential evaporation influences the simulation accuracy of a given hydrological or environmental model. It should be noted that although this section will review the methods for calculating potential evaporation in detail, not all of them are suitable for geotechnical researchers for estimating evaporative fluxes since a local and micro scale should be considered.

2.4.1 MASS TRANSFER METHOD

The mass transfer approach has the deepest historical roots as its origin is frequently attributed to Dalton at the turn of the nineteenth century. The mass transfer method utilizes the concept of eddy motion transfer of water vapor from an evaporating surface to the atmosphere. Many researchers have proposed empirical methods as briefly shown in Table 2.2 while the generalized form of these equations are summarized in Table 2.3.

Table 2.1 Description of the apparatus for measuring evaporation

Item	Derivation	Characteristic	Comments
Evaporation pan	Wang (2006)	holding water to evaporation while monitor the weight change	(1) simple and convenient (2) only for free water evaporation (3) location limited
	Wilson (1997) Kondo et al. (1990)	(1) thickness:74 mm, diameter: 258mm (2) soil sample as thin as possible (3) monitoring air and soil temperature, humidity, and water loss in laboratory condition	(1) effectively evaluate the soil surface behavior during evaporation (2) atmosphere conditions' influence should be considered
Lysimeter	Benson et al. (2001) Herbst et al. (1996) Miyamoto et al. (2010) Plauborg (1995)	(1) measuring the total weight of soil and the stored water (2) combined with other methods, such as TDR	(1) measure ET and E_a in field (2) fluids could only be gathered under saturated gravity flow
	Wilson (1990) Yanful (2003)	(1) conducted in lab and water supply controlled (2) monitoring temperature and water content of soil column profile (3) multi-layers experiment can be conducted	(1) it is available to investigate evaporation process in lab (2) more modification needed in controlling the atmosphere conditions constant (3) considering radiations effects

Table 2.1 (continued)

Environmental chamber	Yanful (1997) Aluwihare et al. (2003) Cui (2012)	(1) conducting experiment under certain condition (2) monitoring atmosphere indexes together with specimen conditions	(1) the accuracy of the chamber of Aluwihare and Cui should be confirmed (2) climate change's influence need be considered
Wind tunnel	Yamanaka et al (1997) Van de Griend (1994) Wang (2006)	(1) atmosphere conditions controlled or partly controlled (2) monitoring water loss use a lysimeter (3) soil conditions controlled	fluctuation of controlled variables or accuracy need be considered
Others	Blight (1997)	a meteorological station works together with soil heat/moisture flux measurement in filed	E_a or ET value cannot directly obtained, computation from models is needed
	Teng et al. (2011)	(1) temperature, relative humidity and wind speed can be controlled (2) pan soil test and soil column evaporation test can be conducted in one apparatus.	(1) meteorological variables only can be controlled in a small range (2) evaporation rate cannot be measured directly for column evaporation test.
	Tristancho et al. (2011)	(1) climate chamber with centrifuge (2) monitor seasonal cycles of drying and wetting	only tropical weather conditions can be simulated

TDR: time domain reflectometry; ET: evapotranspiration

Table 2.2 Some formulas of mass transfer method to estimate evaporation (after Singh and Xu, 1997)

No.	Equations	Derivation	Note
1	$E_p = a(e_s - e_a)$	Dalton(1802)	a = 15,11 for shallow and large deep water, respectively
2	$E_p = (0.4 + 0.199u)(e_s - e_a)$	Fitzgerald (1886)	
3	$E_p = 11(1 + 0.1u)(e_s - e_a)$	Meyer(1915)	
4	$E_p = 0.4\left[(2 - \exp(-2u))(e_s - e_a)\right]$	Horton(1917)	
5	$E_p = 0.77(1.465 - 0.0186 p_b)\cdot (0.44 + 0.118u)(e_s - e_a)$	Rohwer (1931)	p_b = barometric pressure
6	$E_p = 0.35(1 + 0.24u_2)(e_s - e_a)$	Penman (1948)	
7	$E_p = 0.0578u_8(e_s - e_a)$ $E_p = 0.0724u_4(e_s - e_a)$	Harbeck et al. (1954)	
8	$E_p = 6.0(1 + 0.21u_8)(e_s - e_a)$	Kuzmin (1957)	
9	$E_p = 0.00181u(e_s - e_a)(1 - 0.03(T_a - T_w))$	Harbeck et al. (1958)	T_a = air temperature T_w = water surface temperature
10	$E_p = (0.024(t_w - t_2)/u_1 + 0.166u_1)(e_s - e_a)$	Konstantinov (1968)	
11	$E_p = 0.0018(T_a + 25)^2(100 - h)$	Romanenko (1961)	h = relative humidity
12	$E_p = (0.623\rho_a K_0^2 u_8(e_0 - e_8))/(p(\ln 800/z)^2)$	Sverdrup(1946)	K_0= von Karman's constant ρ_a = density of air P = atmosphere pressure
13	$E_p = (0.623\rho_a K_0^2(u_8 - u_2)(e_2 - e_8))/(p(\ln 4)^2)$	Thornthwaite et al. (1939)	

e_s is vapor pressure of water or soil surface, e_a is vapor pressure of air. The subscripts attached to u refer to height in meters at which the measurements are taken; no subscript refers to measurements near the ground or water surface.

Table 2.3 Generalized equations for the formulas of mass transfer method

No.	Generalized forms	Original equations
1	$E_p = a(e_0 - e_a)$	1
2	$E_p = a \cdot u(e_0 - e_a)$	2, 7, 12, 13
3	$E_p = a \cdot (1 - \exp(-u)) \cdot (e_0 - e_a)$	4
4	$E_p = a \cdot (1 + bu) \cdot (e_0 - e_a)$	3, 6, 8
5	$E_p = a \cdot u(e_0 - e_a) \cdot (1 - b(T_a - T_d))$	9
6	$E_p = a \cdot (T_a + 25)^2 \cdot (100 - h)$	11
7	$E_p = a(1 + bu)(e_0 - e_a) \cdot (1 - c(T_a - T_d))$	10

a, *b*, *c* are parameters, T_d is freely defined as conditions. The No. of original equations are related to Table 2.2.

In Table 2.2, the equations proposed by Dalton (1802), Penman (1948) and Thornthwaite et al. (1939) are commonly used in engineering practice. Singh and Xu (1997) evaluated the seven generalized equations for estimating evaporation as shown in Table 2.3 using climatological data in north-western Ontario, Canada. Calibration results show that all seven equations yield comparable and satisfactory estimates for monthly evaporation, provided the model parameters are calibrated using local meteorological variables. Model complexity is not necessarily a measure of its ability to perform better when using this type of equation.

Generally, the mass transfer method provides good estimates of evaporative flux when the relative humidity of the evaporating surface is 100% and the surface temperature is known. However, difficulties comes once the availability of water at the surface becomes restricted. The actual vapor pressure at the surface drops to some value below the saturated vapor pressure. Evaluation of the suppressed vapor pressure is difficult.

2.4.2 RADIATION-BASED METHOD

The radiation based method for estimating evaporation generally applies the energy balance concept to estimate potential evaporation, and they have wide application in estimation of lake evaporation or potential evaporation of land area. It is reported that the radiation-based method show good results in humid climates, but

performance in arid conditions is erratic and tends to underestimate potential evaporation.

Table 2.4 Generalized equations for radiation-based method (after Xu and Singh, 2000)

No.	Generalized equation forms	Derivation
1	$E_p = a\frac{R_s}{\lambda}$	Abtew (1996)
2	$E_p = a(T_a + b)\frac{R_s}{\lambda}$	Jensen-haise(1963), Hargreaves (1975), McGuinness and Bordne (1972)
3	$E_p = a\frac{\Delta}{\Delta+\gamma}\frac{R_s}{\lambda} + b$	Makkink(1957), Doorenbos and pruitt (1977)
4	$E_p = a\frac{\Delta}{\Delta+\gamma}\frac{R_n}{\lambda} + b$	Priestley and Taylor (1972)
5	$E_p = 0.013\frac{T_a}{T_a+15}(R_s+50)$ for h≥50 $E_p = 0.013\frac{T_a}{T_a+15}(R_s+50)(1+\frac{50-h}{70})$ for h<50	Turc (1961)

R_s is total solar radiation, R_n is net radiation, Δ is slope of the saturation vapor pressure curve, γ is psychromatic constant, a, b are fitting variables.

Owing to the wide-ranging inconsistency in meteorological data collection procedures and standards, many different evaporation methods, which have more or less the same model form, have been used by different authors. For example, by a proper transformation, the equations proposed by Jensen-haise (1963), Hargreaves (1975) and McGuinness and Bordne (1972) can be represented by same model (No.2 in Table 2.4). Xu and Singh (2000) summarized eight evaporation models into five forms as presented in Table 2.4, and then they compare different model forms using the standard meteorological data measured at consistent heights and for the same period. Their conclusions stated that when using the original constant values, of the five original equations valued, the simple Abtew equation result in monthly and annual evaporation value that agree most closely with pan evaporation values. Large errors results for the other four methods. Underestimation was the common problem, especially for cold months. By substituting recalibrated constant values for the original constant values, four of the five equations improved greatly, and all five

equations worked well for determining the mean annual evaporation values. As far as the seasonal and monthly values were concerned, the Hargreaves and Turc equations showed a significant bias when compared with pan evaporation. With properly determined constant values, the Makkink and Priestley and Taylor equations are good choices for calculating evaporation as far as radiation based methods are concerned.

2.4.3 TEMPERATURE-BASED METHOD

This section will review the various popular evaporation equations that belong to the category of temperature-based method. This mechanism of this method is calculating the potential evaporation rate only based on the mean temperature value for a period of one day or one month, thus it is very convenient to be carried out. This method remains empirical and require local calibration in order to achieve satisfactory results. Moreover, Xu and Singh (2001) pointed out that the temperature-based evaporation calculation method, although widely criticized, were still widely used and had often been misused because of their simple nature. They also believes that if we could not avoid using such method the best thing we can do was to analyze and compare them using the standard meteorological data and procedure, so as to provide the best equation forms to the users who have only temperature data. A summary of normally used temperature based method is presented in Table 2.5.

Based on the evaluation of temperature-based method conducted by Xu and Singh (2001), the comments can be stated as follows. In case of using original constant values of original equations evaluated, the Blaney-Criddle equation resulted in mean seasonal evaporation values that agree most closely with pan evaporation values. Large errors results for the Thornthwaite and Hamon methods. Underestimation was the common problem. And all the equations works well for determining the mean seasonal evaporation values. As far as the monthly values were concerned, the modified Blaney-Criddle method produces least percentage error of all the months, followed by the Thornthwaite method. With properly determined constant values, the Blaney-Criddle and Thornthwaite are the recommend method for calculating potential evaporation.

Table 2.5 A summary of normally used temperature-based method to determine potential evaporation

No.	Equations	Derivation	Note
1	$E_p = 1.6(\frac{d}{12})(\frac{N}{30})(\frac{100T_a}{I})^a$	Thornthwaite (1948)	$i = (\frac{T_a}{5})^{1.514}$
2	$E_p = \frac{500T_m / (100 - A) + 15(T_a - T_d)}{(80 - T_a)}$	Linacre (1977)	
3	$E_p = 0.34 p_{er} T_a^{1.3}$	Kharrufa (1985)	
4	$E_p = k_m p_{er}(0.46T_a + 8.13)$	Blaney-Criddle (1959)	
5	$E_p = 0.55D_l \frac{4.95e^{0.062T_a}}{100}$	Hamon (1961)	D_l = hours of daylight
6	$E_p = 0.0018(25 + T_a)^2(100 - Rh)$	Romanenko (1961)	Rh = mean monthly relative humidity

d is duration of average monthly daylight in hour, N is the number of days in a given month, 1-31 (days). I is the sum of 12 monthly heat indices 'i', T_m is the modified temperature due to elevation, T_d is the mean dew point, A is the latitude (degree), p_{er} is percentage of total daytime hours to the period used out of total daytime hours of the year, k_m is a monthly consumptive use coefficient.

2.5 METHODS FOR CALCULATING ACTUAL EVAPORATION

Estimation of evaporation from soil surface not only needs the climatic information, but also is closely related to the soil water status. Therefore, the calculation of actual evaporation is more different than the calculation for potential evaporation. The problem becomes indeterminate because both the temperature and relative humidity are unknown. In general, all conventional climate based methods fail to provide reasonable estimates of actual evaporation from unsaturated soil surface.

Focusing on extending the potential evaporation calculating method to evaluate the actual evaporation, many kinds of methods have been developed with different data input requirements. Moreover, the actual evaporation rate is meaningful for geotechnical application. In the following section, evaporation calculation methods from different disciplines are reviewed from their categories of water balance method,

surface moisture availability method and combined method. Then their differences are analyzed to be classified in accordance with their estimation principles.

2.5.1 WATER BALANCE METHOD

Evaporation can be measured indirectly by quantifying other components in water balance, specifically, precipitation, surface water runoff, changes in moisture storage, and basal percolation. Considering the conservation of mass of water into and out of the soil body, the evaporation can be obtained as follows:

$$E = P - G_p - \triangle S - R_{off} \tag{2.1}$$

where:

E = evaporation.

P = precipitation.

G_p = basal percolation.

ΔS = changes in moisture storage.

R_{off} = surface water runoff.

Due to the basal percolation is normally impossible to measure in natural soil profile, this method is usually adopted together with the lysimeter experiment in practice. In addition, the possible recharge of the soil from the water table may affect water content measurements (Cui, 2008).

2.5.2 AERODYNAMIC METHOD

Aerodynamic method is a simple approach for relating actual evaporation to the surface soil water content, which adopts the parameter of aerodynamic resistance to calculate the restrict for vapor flowing from evaporating surface to air. To establish the relationship between evaporation and soil water content, numerous formulations have been proposed, especially for the discipline of meteorology. All these formulations can be divided into two approaches as summarized in Table 2.6: α_m method and β_m method. The difference for these two approach is that surface specific humidity is assumed to be proportional to saturation specific humidity in α_m method , while the relative humidity of the air in the soil pore is used in β_m method which also adopts surface resistance parameter r_s to adjust the evaporation. The r_s describes the resistance of vapor flow through the soil surface.

Table 2.6 Summary of aerodynamic method to calculate actual evaporation (modified from Mahfouf and Noilhan, 1991)

Item	Generalized equation	Equations	Derivation
α_m	$E_a = \frac{\rho_a}{r_a}[\alpha_m q^*(T_s) - q_a]$	$\alpha_m = \min(1, \frac{1.8\theta}{\theta + 30})$	Barton (1979)
		$\alpha_m = \min(1, \frac{1.8\theta}{0.7\theta + 0.4})$	Yasuda and Toya (1981)
		$\alpha_m = \frac{1}{2}[1 - \cos(\frac{\theta}{\theta_{fc}}\frac{\pi}{2})]$ for $\theta < \theta_{fc}$ $\alpha_m = 1$ for $\theta \geq \theta_{fc}$	Noilhan and Planton (1963)
β_m	$E_a = \frac{\rho_a}{r_a}\beta_m[h_r q^*(T_s) - q_a]$ $\beta_m = \frac{r_a}{r_a + r_s}$	$\beta_m = \min(1, \frac{1.8\theta}{0.75\theta_{sat}})$, $h_r = 1$	Deardorff (1978)
		$r_s = 3.5(\frac{\theta_{sat}}{\theta})^{2.3} + 33.5$, $h_r = 1$	Sun (1982)
		$r_s = 3.81 \times 10^4 \exp(-13.515\frac{\theta}{\theta_{fc}})$	Passerat (1986)
		$r_s = 216(\theta_{sat} - \theta)^{10} / D_m$	Kondo (1990)
		$r_s = 4140(\theta_{sat} - \theta) - 805$ $h_r = \exp(g\psi / RT_s)$	Camillo and Gurney (1986) Dorman and Sellers (1989)
		$r_s = 10e^{0.3563(15-\theta)}$	van de Griend (1994)

α_m, β_m are adjust parameter and function of soil wetness, $q^*(T_s)$ is the saturated specific humidity at the surface temperature T_s, ρ_a is air density, q_a is the air specific humidity, r_a is aerodynamic resistance r_s is surface resistance, θ is volumetric water content, θ_{fc} is the field capacity, θ_{sat} is saturated water content, h_r is the relative humidity of the air next to the water in soil pore, g is the acceleration of gravity, ψ is water potential at soil surface, R is gas constant for water vapor.

Kondo and Saigusa (1990) stated that while there are many ways to represent this surface availability, it has not been established which methodology is generally superior. Mahfouf and Noilhan (1991) reviewd and examined the α_m and β_m method, it is found that the β_m method seemed to overestimate the nocturnal evaporation,

discrepancies in night-time predictions involved differences of cumulative evaporation of about 20% between the α_m and β_m method. According to the research result of Dekic (1995), the Deardorff (1978) method is recommended since its good performance in prediction of evaporation.

2.5.3 COMBINATION METHOD

The definition of combination method is the rational composition of two or three method mentioned before to calculate evaporation. The original form of combination method is the Penman (1948) model, which is developed based on mass transfer method and energy balance, penman method compute the evaporation for an open water surface from standard climatological records of sunshine, temperature, humidity and wind speed. The Penman method may require local calibration of the wind function to achieve satisfactory results. The primary advantage of the Penman method is only routine weather parameters such as air temperature, relative humidity and wind speed are required. The main disadvantage of this method is that it provides only an estimate of potential evaporation assuming water is freely available.

This so-called combination method was further developed by many researchers and extended to cropped surface by introducing resistance factors. A brief summary for combination methods is shown in Table 2.7. Monteith (1965) further develop the penman model by including the parameters of aerodynamic resistance r_a and surface resistance r_s that belong to aerodynamic method. Although the exchange process in soil layer or vegetation layer is too complex to be fully described by the two resistance factors, good correlation can be obtained between measured and calculated evaporation and evapotranspiration rate. For the purpose of generalizing Penman-Monteith method in a wide range of locations and climates, the FAO Penman-Monteith method (1998) is recommended as the standard method. The FAO Penman-Monteith is a close simple representation of the physical and physiological factors governing the actual evaporation or evapotranspiration process. It provides a standard to (1) evapotranspiration (actual evaporation) at different periods of year or in other regions can be compared; and (2) evapotranspiration of other crops can be related.

By introducing a method to compute surface relative humidity whose expression follows Dorman and Sellers (1989) in Table 2.6, Wilson (1990) derived a new formulation of Penman equation. It provide a realistic approach to estimate

evaporation from soil surface, and always act as the upper boundary condition for modeling soil-atmosphere interaction. However, its accuracy depends on the expression of relative humidity that is parameter *A*. And also, Penman-Wilson method is hard to be carried out independently to estimate evaporation since it is highly related to the soil suction at surface.

Table 2.7 A brief summary of combination method for evaluating evaporation

No.	Equations	Derivation	Note
1	$E_p = \frac{\Delta R_n + \gamma f(u)(e_s - e_a)}{\Delta + \gamma}$ $f(u) = 0.35(1 + 9.8\times10^{-3}u)$	Penman (1948)	$f(u)$ is a function of wind speed
2	$E_a = \frac{\Delta(R_n - G) + \rho_a c_p \frac{(e_s - e_a)}{r_a}}{\Delta + \gamma(1 + \frac{r_s}{r_a})}$	Penman -Monteith (1965)	G is soil heat flux c_p is specific heat of air
3	$E_a = \frac{\Delta R_n + \gamma f(u) e_a (B - A)}{\Delta + \gamma A}$ $f(u) = 0.35(1 + 9.8\times10^{-3}u)$	Penman-Wilson (1990)	B = 1/(relative humidity of air) $A = 1/h_r$
4	$E_a = \frac{0.408\Delta(R_n - G) + \gamma \frac{900}{T_a + 273} u_2 (e_s - e_a)}{\Delta + \gamma(1 + 0.34u_2)}$	FAO Penman-Monteith (1998)	$u_2 = u_z \frac{4.87}{\ln(67.8\times z - 5.42)}$
5	$R_n - H - LE_a - G = 0$ $H = \frac{\rho c_p (T_s - T_a)}{r_a}$ $E_a = \frac{M_w (e_s - e_a)}{RT(r_s + r_a)}$ $G = z(\Delta T)(C_{sd} + wC_w)\rho_s$	van Bavel and Hillel (1976) Cui et al. (2008) Blight et al. (2009)	L = 4.618*10^3(607-0.7T$_a$) M_w is molecular mass of water H is sensitive heat transfer

C_{sd} and C_w is specific heat of dry soil and soil water, respectively.

The evaporative process is primarily one of energy consumption. Energy must be supplied to provide the latent heat of vaporization necessary for water to evaporate at the soil surface, and the resultant water vapor must be swept away by air movement or disperse by diffusion to maintain the evaporation gradient and keep the

evaporative process going. If the amount of energy consumed by evaporation can be computed, the corresponding mass of water evaporated can be deduced. Based on this energy balance principle, van Bavel and Hillel (1976), Cui et al. (2008) and Blight et al. (2009) showed the its combination with aerodynamic method. This method can provide the exact evaporation value from soil surface in theory, and it sounds a good choice for geotechnical researchers, however, more verification work need to carry out.

2.6 SIMULATION OF SOIL WATER REDISTRIBUTION DURING EVAPORATION

Multi-phase flow through soils represents an important problem in geotechnical and geo-environmental engineering. The state of practice in prediction of unsaturated flow fields in porous media is based mainly on initial formulations established by Richards (1931). Due to its wide range of applications, Richards' equation has been studied extensively in the literature (Ghotbi et al., 2011). Most solutions that available for the governing equation are based on numerical techniques, as it is rather difficult to derive analytical solutions to the problem. The difficulty in solving Richards' equation stems mainly from the complications introduced by dependence of hydraulic conductivity and diffusivity on moisture content.

2.6.1 NUMERICAL SIMULATION APPROACH

Finite element and finite difference methods have been adopted by several researchers (Clement et al., 1994; Baca et al., 1997; Bergamaschi et al., 1999) for solving practical cases of the application of Richards' equation. Mass lumping was employed in these studies to improve stability. Time stepping schemes such as the Douglas-Jones-predictor-corrector method, Runge-Kutta method and backward difference formulae also fit within this context (Kavetski et al., 2001). Tabuada et al. (1995) used an implicit method and presented equations governing two-dimensional irrigation of water into unsaturated soil based on Richards' equation. The Gauss-Seidel method was then effectively used to solve the resulting equations.

Direct geoenvironmental applications of Richards' equation have been explored by several authors as well. Bunsri et al. (2008) solved Richards' equation accompanied by advective-dispersive solute transport equations by the Galerkin technique. Witelski (1997) used perturbation methods to study the interaction of wetting fronts with impervious boundaries in layered soils governed by Richards'

equation, and was able to obtain reliable solutions. Through comparison with numerical solutions, Witelski concluded that perturbation methods are able to yield highly accurate solutions to Richards' equation. Wiltshire and El-Kafri (2004) also derived the non-classical symmetries of Bluman and Cole as they apply to Richard's equation for water flow in an unsaturated homogenous soil. It was then shown that determining equations for the non-classical case leads to four highly nonlinear equations. A numerical model for 1D flow within unsaturated topsoil was developed by Hsu et al. (2002) and was solved using a two-step Crank‐Nicolson scheme. However, Richards' equation was utilized for the simulations and based on some assumptions, three infiltration-capacity formulas were evaluated for three types of soil. Recently, Omidvar et al. (2010) explored homotopy perturbation method and differential transform method to solve simplified forms of Richards' equation.

Most of the methods mentioned above are the advances of numerical analysis for Richards' equation. Besides that, many commercial codes based on finite element and finite difference methods are competent to model the soil water dynamic, including UNSATH, HYDRUS, SHAW, Vadose/W, SWIM, VS2DTI, and HELP (Fayer, 2000; Scanlon et al. 2002; Benson et al. 2004). Of these codes, HYDRUS, UNSAT-H, LEACHM, and Vadose/W are used most frequently in practice. A comprehensive review and evaluation of these codes can refer to Khire et al. (1997), Scanlon et al. (2002, 2005), Benson et al. (2004) and Ogorzalek et al. (2008).

2.6.2 ANALYTICAL SOLUTION APPROACH

The analysis of soil water dynamic has largely been carried out using numerical methods mainly because of the difficulty in solving the governing nonlinear differential equation. Although the numerical method are powerful in solving complex nonlinear problems, analytical results provide general insights and concisely identify the relationships among the variables from which rational approximations and simplifications can be derived. They can also be useful for checking numerical schemes (Basha, 1999).

During the past decades, many analytical solutions for steady and nonsteady soil water dynamic have been developed. Linear or quasilinear approximations are usually needed to facilitate mathematical formulation. Based on the nature of the linearization and approximation of Richards' equation, the exsiting analytical solutions may be divided into two classes; one uses exponential constitutive

relationships (Garden, 1958; Lomen and Warrick, 1978; Srivastava and Yeh, 1991; Basha, 2000; Chen et al., 2003), the others uses power law forms (van Genucheten, 1980; Broadbridge and White, 1988; Ross and Porlange, 1994; Hogrrth and Porlange, 2000). A complete review of the qusilinear theory of unsaturated flow problem was presented by Pullan (1990).

Most of the analytical approaches mentioned above describe the downward water movement that is induced by infiltration. Mechanism of evaporation is quite different from that of infiltration, and evaporation rate estimated from climate variables would not always be the actual surface fluxes. Therefore, the surface flux is not suitable to define the boundary condition or it only could be simulate the partial stage of evaporation process. The analytical solutions for infiltration cannot be directly applied to handle with the evaporative flux. Only several researchers have presented analytical and qusi-analytical solution of the flow equation for evaporation process of semi-infinite and finite soil (Garden, 1959; Menziani et al., 1999; Wallence et al., 1999; Zarei et al., 2010). These studies mainly focused on the one dimensional diffusion equation, neglecting thermal and gravity effects. Therefore, a comprehensive analytical solution that capable of handling the evaporation processes with different initial and boundary conditions simultaneously are scare.

2.7 SUMMARY AND ACADEMIC ISSUES TO BE SOLVED

This chapter reviews the previous researches that have close relationship with soil surface evaporation. The literature review are expanded from the aspects that the phenomena of evaporation which mainly discusses the affecting factors of soil evaporation, measurement of soil evaporation, models to determine evaporation rate and finally the simulation of soil water dynamic during evaporation process. The academic issues to be solved can be summarized as follows:

(1) For the measurement of soil evaporation, pervious researchers normally conducted evaporation test under natural condition, thus apparatus capable of controlling climate conditions for investigating evaporation process is relatively rare; In other words, no device to date, truly replicate climate characteristics to evaluate soil evaporation process.

(2) For the methodology of computing evaporation rate, varies kinds of methods are available for determining potential evaporation rate and standard method has been commonly received, while how to extend to evaluate actual evaporation rate is

still ambiguous. An easily-employed method with profound theoretical background and high accuracy is called for, and the calibration and evaluation among different methods needs to further conducted.

(3) Although numerical simulation of soil water dynamic during evaporation are available, analytical approach is important as well since it provides important insights into the physics of the evaporation phenomena and concisely identify the relationship among the variables of mechanisms. Moreover, the comprehensive analytical solution that capable of handling the evaporation processes with different initial and boundary conditions simultaneously are scare. The in-situ application of analytical model with comparing with numerical simulation is also leading edge of this topic.

Existing problems are concluded one by one, which consists of the research content of the following chapters. At meanwhile, the objective of this dissertation becomes clear.

REFERENCE

Abtew, W. (1996): Evapotranspiration measurement and modeling for three wetland systems in South Florida. Water Resources Bulletin, 32, 465-473.

Aluwihare, S. and Watanabe, K. (2003): Measurement of evaporation on bare soil and estimating surface resistance. Journal of Environment Engineering. 129(12), 1157-1168.

Baca, R.G., Chung, J.N., and Mulla, D.J. (1997): Mixed transform finite element method for solving the nonlinear equation for flow in variably saturated porous media. International Journal of Numerical Methods in Fluids Mechanism, 24, 441-455.

Barton, I.J. (1979): A parameterization of the evaporation from nonsaturated surfaces, Journal of Applied Meteorology, 18, 43-47.

Basha, H.A. (1999): Mulitdimensional lineared nonsteady infiltration with prescribed boundary conditions at the soil surface. Water Resources Research, 35(1), 75-83.

Basha, H.A. (2000): Multidimensional linearized nonsteady infiltration toward a shallow water table. Water Resource Research, 36, 2567-2573.

Benson, C.H., Abichou, T., Albright, W.H., Gee, G., Roesler, A.C. (2001): Field evaluation of alternative earthen finial covers. International Journal of Phytoremediation. 3(1), 105-127.

Benson, C.H., Bohnhoff, G.L., Apiwantragoon, P., Ogorzalek, A.S., Shackelford, C.D., and Albright, W. H. (2004): Comparison of model predictions and field data for an ET cover. Tailings and Mine Waste ’04, Balkema, Leiden, The Netherlands, 137-142.

Bergamaschi, L., Putti, M. (1999): Mixed finite element and Newton-type linearizations for the solution of Richards’ equation. International Journal of Numerical Methods and Engineering, 45,1025-1046.

Blaney, H.F., Criddle, W.D. (1950): Determining water requirements in irrigated areas from climatological irrigation data. Technical Paper No. 96, US Department of Agriculture, Soil Conservation Service, Washington, D.C., 48.

Blight, G.E. (1997): Interaction between the atmosphere and the earth. Geotechnique, 47(4), 715-767.

Blight, G.E. (2009): Solar heating of the soil and evaporation from a soil surface. Geotechnique, 59(4), 355-363.

Broadbridge, P., and White, I. (1988): Constant rate rainfall infiltration: A versatile nonlinear model. 1. Analytic solution. Water Resource Research, 24, 145-154.

Brutsaert, W. (1982): Evaporation into the atmosphere: Theory, history, and applications. Reidel, Dordrecht, The Netherland.

Brutsaert, W. and Chen, D. (1995): Desorption and the two stages of drying of natural tallgrass prairie. Water Resource Research, 31(5), 1305-1313.

Bunsri, T., Sivakumar, M., Hagare, D. (2008): Numerical modelling of tracer transport in unsaturated porous media. Journal of Applied Fluid Mechnics,1(1),62-70.

Camillo, P. J., and Curney, R. J. (1986): A resistance parameter for bare soil evaporation models. Soil Science, 141, 95-105.

Chen, J.M., Tan, Y.C. and Chen, C.H. (2003): Analytical solutions of one-dimensional infiltration before and after ponding. Hydrological Processes, 17, 815-822.

Clement, T.P., William, R.W., Molz, F.J. (1994): A physically based two-dimensional, finite difference algorithm for modelling variably saturated flow. Journal of Hydrology, 161,71‑90.

Cui, Y.J. and Zornberg, J.G. (2008) Water balance and evapotranspiration monitoring in geotechnical and geoenvironmental engineering. Geotechnical and Geological Engineering, 26, 783-798.

Cui, Y.J., Ta, A.N., Hemmati, S., Tang, A.M., Gatmiri, B.(2012): Experimental and

numerical investigation of soil-atmosphere interaction. Engineering Geology, doi:10.1016/j.enggeo.2012.03.018.

Dalton, J. (1802): Experimental essays on the constitution of mixed gases: on the force of steam or vapor from water or other liquids in different temperatures, both in a Torricelli vacuum and in air; on evaporation; and on expansion of gases by heat. Manchester Lit. Phil. Soc. Mem. Proc., 5, 536-602.

Deardorff, J.W. (1978): Efficient prediction of ground temperature and moisture with inclusion of a layer of vegeatation. Journal of Geophysical Research, 83, 1889-1903.

Dekic, Lj., Mihailovic, D.T., Rajkovic, B. (1995): A study of sensitivity of bare soil evaporation schemes to soil surface wetness, using the coupled soil moisture and surface temperature prediction model, BARESOIL. Meteorological and Atmospheric Physics, 55, 101-112.

Doorenbos, J., Pruitt W.O. (1977): Crop water requirements. Irrigation and Drainage Paper 24, Food and Agriculture Organization of the United Nations: Rome, Italy, 144.

Dorman, J.L. and Sellers, P.J. (1989): A global climatology for albedo, roughness length, and stomatal resistance for atmospheric general circulation models as represented by the simple biosphere model. Journal of Applied Meteorology, 28, 833-855.

FAO (1998): Crop evapotranspiration-Guidelines for computing crop water requirements-FAO Irrigation and drainage paper 56. Chapter 2: FAO Penman-Menoteith, 17-28.

Fayer, M. (2000): UNSAT-H version 3.0: Unsaturated soil water and heat flow model-theory, user manual, and examples. Rep. No. PNNL-13249, Pacific Northwest National Laboratory, Richland, Wash.

Fitzgerald, D. (1886): Evaporation. Trans. Am. Soc. Civ. Eng., 98(HY12), 2073-2085.

Gardner, W.R. (1958): Some steady-state solutions of the unsaturated flow equation with application to evaporation from a water table. Soil Science, 85, 244-249.

Gardner, W.R. (1959): Solution of the flow equation for the drying of soils and other porous media. Soil Sci. Soc. Am. Proc. 23, 183-187.

Ghotbi, A.R., Omidvar, M., and Barari, A. (2011): Infiltration in unsaturated soils-an analytical approach. Computers and Geotechnics, 38, 777-782.

Hamon, W.R. (1961): Estimating potential evapotranspiration. Journal of Hydraulics

Division, Proceedings of the American Society of Civil Engineers, 871, 107-120.
Harbeck, G.E., et al. (1954): Water loss investigations. Vol. 1, Lake Hefner studies. U.S. Geological Survey Paper 269. US Government. Printing Office, Washington, D.C.
Harbeck, G.E., et al. (1958): Water loss investigations, Lake Mead studies. U.S. Geological Survey Professional Paper 298. US Government Printing Office, Washington, D.C.
Herbst, M., Kappen, L., Thamm, F., Vanslow, R. (1996): Simultaneous measurements of transpiration, soil evaporation and total evaporation in a maize field in north Germany. Journal of Experimental Botany, 47, 1957-1962.
Hargreaves, G.H. (1975): Moisture availability and crop production. Transactions of the ASCE 18, 980-984.
Hillel, D. (1980): Introduction to Soil Physical. Academic Press. New York, USA.
Hogarth, W.L., and Parlange, J.Y. (2000): Application and improvement of a recent approximate analytical solution of Richards' equation. Water Resource Research, 36, 1965-1968.
Horton, R.E. (1971): Rainfall interception. Month. Weather Rev., 47(9), 603-623.
Hsu, S.M., Ni, C.F., Hung, P.F. (2002): Assessment of three infiltration formulas based on model fitting on Richards' equation. Journal of Hydrological Engineering, 7(5):373-379.
Jensen, M.E, Haise, H.R. (1963): Estimation of evapotranspiration from solar radiation. Journal of Irrigation and Drainage Division, Proceedings of the American Society of Civil Engineers 89,15-41.
Kavetski, D., Binning, P., and Sloan, S.W. (2001): Adaptive backward Euler time stepping with truncation error control for numerical modeling of unsaturated fluid flow. International Journal of Numerical Methods and Engineering, 53, 1301-1322.
Kharrufa, N.S. (1985): Simplified equation for evapotranspiration in arid regions. Beitrage zur Hydrologie, Sonderheft 5.1, 39-47.
Khire, M.V., Benson, C.H., and Bosscher, P.J. (1997): Water balance modeling of earthen final covers. Journal of Geotechnical and Geoenvironmental Engineering, 123(8), 744-754.
Kondo, J., Saigusa, N. (1990): A parameterization of evaporation from bare soil surface, Journal of Applied Meteorology, 29, 385-389.
Konstantinov, A.R. 1968. Evaporation in Nature. Leningrad.
Kuzmin, P.O. (1957): Hydrophysical investigations of land waters. Int. Assoc. Sci.

Hydrol. Publ., 3, 468-478.

Linacre, E.T. (1977): A simple formula for estimating evaporation rates in various climates, using temperature data alone. Agricultural Meteorology, 18, 409-424.

Lomen, D.O., and Warrick, A.W. (1978): Time-dependent solutions to the one-dimensional linearized moisture flow equation with water extraction. Journal of Hydrology. 39, 59-67.

Mahfouf, J.F. and Noilhan, J. (1991): Comparative study of various formulation of evaporation from bare soil using in situ data. Journal of Applied Meteorology, 30, 1354-1365.

Makkink G.F. (1957): Testing the Penman formula by means of lysimeters. Journal of the Institution of Water Engineers, 11, 277-288.

McGuinness, J.L., Bordne, E.F. (1972): A Comparison of lysimeter-derived potential evapotranspiration with computed values. Technical Bulletin 1452, Agricultural Research Service, US Department of Agriculture: Washington, DC, 71.

Meyer, A.F. (1915): Computing runoff from rainfall and other physical data. Trans. Am. Soc. Civ. Eng., 79, 1055-1155.

Menziani, M., Pugnaghi, S., Pilan, L., Santangelo, R., Vincenzi, S. (1999): Field experiment to study evaporation from saturated bare soil. Phys. Chem. Earth (B) 24 (7), 813-818.

Miyamoto, Y., Kitamura, R. (2011): Measurement of thermodynamic behavior with numerical simulation for unsaturated soil. Proceedings of the 2nd Korea-Japan Joint Workshop on Unsaturated Soils.

Monteith, J.L. (1965): Evaporation and the environment, In: The State and Movement of Water in Living Organisms, 205-234. XIXth Symposium of the Society for Experimental Biology, Swansea. Cambridge, UK, Cambridge University Press.

Noilhan, J. and Planton, S. (1989): A simple parameterization of land surface processes for meterorological models. Monthly Weather Review, 117,536-549.

Ogorzalek1, A.S., Bohnhoff, G.L., Shackelford. C.D., Benson, C. H., and Apiwantragoon, P. (2008): Comparison of field data and water-balance predictions for a capillary barrier cover. Journal of Geotechnical and Geoenvironmental Engineering, 134(4), 470-486.

Omidvar, M., Barari, A., Momeni, M., Ganji, D.D.(2010): New class of solutions for water infiltration problems in unsaturated soils. Geomechanics and Geoengineering: An Interational Journal, 5(2), 127-135.

Passerat de Silans, A. (1986): Transferts de masse et de chaleur dans un soil stratifie soimis a une excitation atmospherique naturelle. Comparision: Modeles-experience, thesis, Institut National Polytechnique de Grenoble.

Penman, H.L. (1948): Natural evaporation from open water, bare soil and grass. Proc. R. Soc. Lond., 193, 120-145.

Plauborg, F. (1995): Evaporation from bare soil in a temperature humid climate-measurement using micro-lysimeters and time domain reflectometry. Agricultural and Forest Meteorology, 76, 1-17.

Pullan, A.J. (1990): The quasilinear approximation for unsaturated porous media flow. Water Resource Research, 26(6), 1219-1234.

Richards, L.A. (1931): Capillary conduction of liquids through porous mediums. Physics, 1: 318-333.

Ritchie, J.T. (1972): Model for predicting evaporation from a row crop with incomplete cover. Water Resource Research, 8, 1204-1213.

Rohwer, C. (1931): Evaporation from free water surfaces. Technical Bulletin 271. US Department of Agriculture, Washington, D.C.

Romanenko, V.A. (1961): Computation of the autumn soil moisture using a universal relationship for a large area Proceedings, Ukrainian Hydrometeorological Research Institute, No. 3. Kiev.

Ross, P.J., and Parlange, J.Y. (1994): Comparing exact and numerical solutions of Richards' equation for one-dimensional infiltration and drainage. Soil Science, 157, 341-344.

Scanlon, B.R., Christman, M., Reedy, R.C., Porro, I., Šimůnek, J., and Flerchinger, G.N. (2002): Intercode comparisons for simulating water balance of surficial sediments in semiarid regions. Water Resource Research, 38(12), 1323-1339.

Scanlon, B.R., Reedy, R.C., Keese, K.E., and Dwyer, S.F. (2005): Evaluation of evapotranspirative covers for waste containment in arid and semiarid regions of the Southwestern USA. Vadose Zone Journal,4(1), 55-71.

Shokri, N. and Or, D. (2011): What determined drying rates at the onset of diffusion controlled stage-2 evaporation from porous media? Water Resource Research, 47, W09513, doi: 10.1029/2010WR010284.

Singh, V.P., Xu, C.Y. (1997): Evaluation and generalization of 13 equations for determining free water evaporation. Hydrological Processes, 11, 311-323.

Srivastava, R., and Jim Yeh, T.C. (1991): Analytical solutions for one-dimensional, transient infiltration toward the water table in homogeneous and layered soils.

Water Resource Research, 27,753-762.

Sun, S.F. (1982): Moisture and heat transport in a soil layer forced by atmosphere conditions. Master thesis, University of Connecticut.

Sverdrup, H. U. (1946): The humidity gradient over the sea surface. J. Meteorol., 3, 1-8.

Priestley, C.H.B., Taylor, R.J. (1972): On the assessment of the surface heat flux and evaporation using large-scale parameters. Monthly Weather Review, 100, 81-92.

Tabuada, M.A., Rego, Z.J.C., Vachaud, G., and Pereira, L.S. (1995): Two-dimensional irrigation under furrow irrigation: modeling, its validation and applications. Agricultural Water Management, 27(2),105-123.

Teng, J.D., Yasufuku, N., Liu, Q. (2012): A newly developed climate control apparatus to investigate evaporation behavior. Proceedings of 8th International Symposium on Lowland Technology, 161-166.

Thornthwaite, C.W. and Holzman, B. (1939): The determination of land and water surfaces. Month. Weather Rev., 67, 4-11.

Thornthwaite, C.W. (1948): An approach toward a rational classification of climate. Geographical Review, 38, 55-94.

Tristancho, J., Caicedo, B., Thorel, L., Obregón, N. (2012): Climatic chamber with centrifuge to simulate different weather conditions. Geotechnical Testing Journal, 35(1),1-13.

Turc, L. (1961): Estimation of irrigation water requirements, potential evapotranspiration: a simple climatic formula evolved up to date. Annals of Agronomy, 12, 13-49.

Van Bavel, C.H.M, Hillel D.I. (1976): Calculating potential and actual evaporation from a bare soil surface by simulation of concurrent flow of water and heat. Agricultural Meteorology, 17, 453-476.

Van de Griend, A.A., Owe, M. (1994): Bare soil surface resistance to evaporation by vapor diffusion under semiarid conditions, Water Resources Research, 30(2), 181-188.

Van Genuchten, M.Th. (1980): A closed-form equation for predicting the hydraulic conductivity of unsaturated soils. Soil Sci. Soc. Am. J. 44, 892-898.

Wallace, J.S., Jackson, N.A., Ong, C.K. (1999): Modeling soil evaporation in an agro forestry system in Kenya. Agric. For. Meteorol. 94, 189-202.

Wang, W.C. (2006): Wind tunnel experiment on bare soil evaporation. Master Thesis, National Central University, Taiwan.

Wilson, G.W. (1990): Soil evaporative fluxes for geotechnical engineering problems. Ph.D. dissertation, University of Saskatchewan, Saskatoon.

Wilson, G.W., Fredlund, D.G., and Barbour, S.L. (1997): The effect of soil suction on evaporative fluxes from soil surfaces, Canadian Geotechnical Journal, 31, 151-161.

Witelski, T.P. (1997): Perturbation analysis for wetting fronts in Richards' equation. Transpiration of Porous Media, 27(2):121-134.

Wiltshire, R., El-Kafri, M. (2004): Non-classical and potential symmetry analysis of Richards'equation for moisture flow in soil. Journal of Physics A: Mathematical and General, 37(3), doi:10.1088/0305-4470/37/3/019.

World Meteorological Organization. (1974): International glossary of hydrology. WMO Report No.385.

Xu, C.Y., Singh, V.P. (2000): Evaluation and generalization of radiation-based methods for calculating evaporation. Hydrological Processes, 14, 339-349.

Xu, C.Y., Singh, V.P. (2001): Evaluation and generalization of temperature-based methods for calculating evaporation. Hydrological Processes, 15: 305–319.

Yamanaka, T., Takeda, A. and Sugita, F. (1997): A modified surface-resistance approach for representing bare-soil evaporation: Wind tunnel experiments under various atmospheric conditions. Water Resources Research. 33(9), 2117-2128.

Yanful, E.K. and Choo, L.P. (1997): Measurement of evaporative fluxes from candidate cover soils. Canadian Geotechnical Journal. 34, 447-459.

Yanful, E.K., Mousavi, S.M. and Yang, M. (2003): Modeling and measurement of evaporation in moisture-retaining soil covers. Advances in Environmental Research, 7, 783-801.

Yasuda, N. and Toya, T. (1981): Evaporation from nonsaturated surface and surface moisture availability. Paper of Meteorological Geophysics, 32, 89-98.

Zarei, G., Homaee, M., Liaghat, A.M., and Horrfar, A.H. (2010): A model for soil surface evaporation based on Compell's retention curve. Journal of Hydrology, 380, 356-361.

CHAPTER 3

DEVELOPMENT OF CLIMATE CONTROL APPARATUS FOR EVAPORATION EXPERIMENT

3.1 INTRODUCTION

The water transfer in soil and at soil surface is a key issue in geotechnical and geo-environmental engineering. Especially, the evaporation process is a multi-phase flow of liquid water-vapor-heat between soil surface and atmosphere, which is effected by many factors, such as soil hydraulic properties, climate conditions, soil-atmosphere interface behavior and so on. These factors do not function as independent variables, but rather act as a closely coupled system. Because of the involvement of these complex processes, it has been a challenge to accurately calculate evaporation rate from soil.

From an experimental point of view, the evaporative flux analysis requires measurement of soil suction or water content. However, as the boundary conditions in the field cannot be controlled and are difficult to be measured prior laboratory tests are often required. Although there are numerous methods for measuring evaporation as reviewed in section 2.3 of Chapter 2, each method is associated with a set of complication and it is rather difficult to find a suitable method to estimate evaporation accurately and continuously. Nevertheless, since the errors related to evaporation measurements are mainly due to the alteration of natural profiles of atmospheric conditions (Aluwihare and Watanabe, 2003), the climatic influences on evaporation should be primarily evaluated.

The objective of laboratory test program revolves two primary objectives. The first objective is to determine the soil properties and characteristics that affect the

evaporative fluxes from soil surface. The secondary objective is to investigate the soil water dynamic during evaporation that is the soil-atmosphere interaction. Specifically for the soil evaporation test of under controlled condition, a new apparatus was developed. The following section will be presented from the aspects of instrumentation of the apparatus, features and accuracy calibration.

3.2 INSTRUMENTATION OF THE APPARATUS

The design of this equipment is to maintain the atmosphere conditions of evaporation chamber comprehensively for investigating evaporation behavior (Teng et al., 2012). A general picture layout of the climate control apparatus is shown in Figure 3.1, while the schematic illustration of the apparatus is displayed in Figure 3.2 to present a detailed description. It is noted that both column and pan soil evaporation test are shown in one figure for convenience. However, they are carried out separately for different evaporation tests.

Figure 3.1 Pictures of the climate control apparatus. The left one shows the setup for conducting pan soil evaporation test while the right one is for the column soil evaporation test.

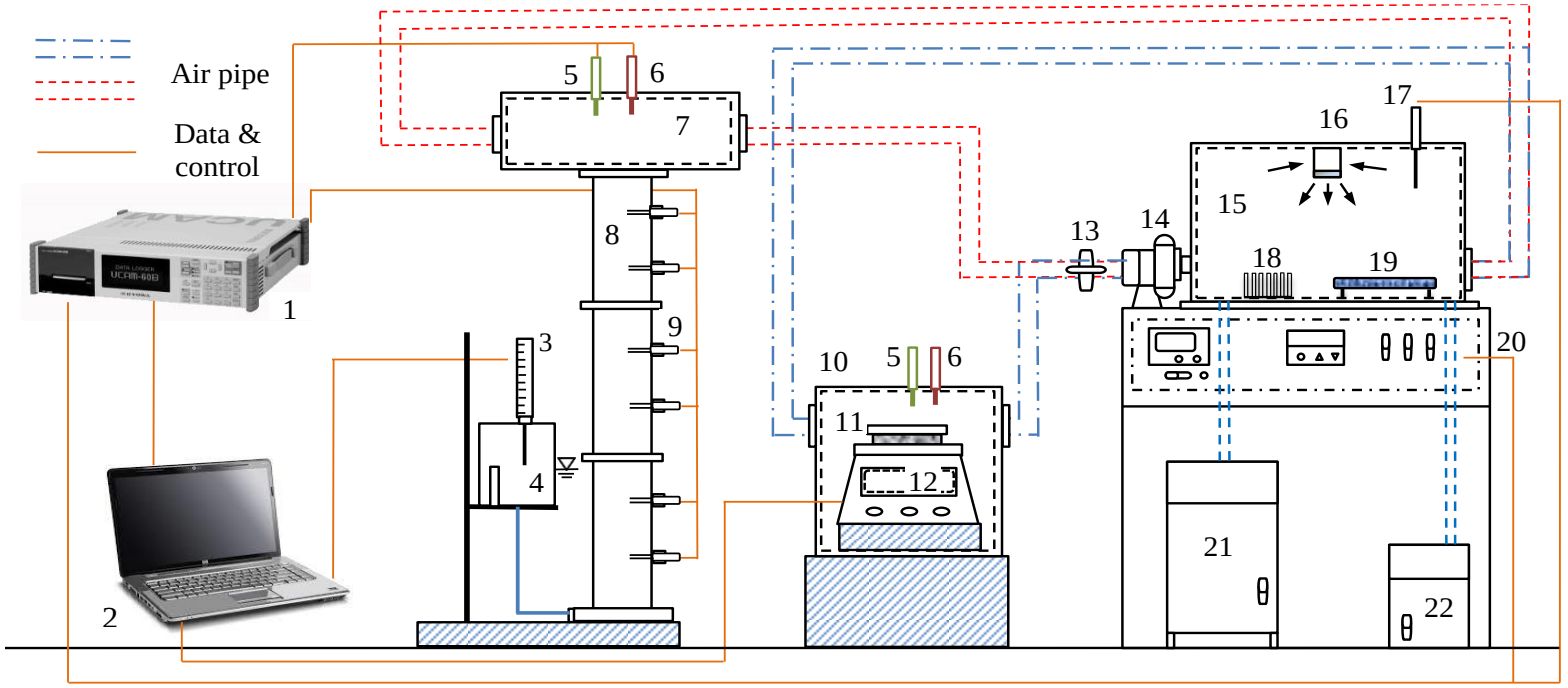

(a) Control and data acquisition (b) Column soil evaporation (c) Pan soil evaporation (d) Climate control part

No.	Accessory	Functions and remarks
1	Data logger	Monitor data and accepting command
2	Computer	With USB or RS232 connector
3	Burette	Sealed up and measure the volume of water supplied
4	Tank	Store water maintain water table
5	Wind speed sensor	Monitor the wind speed (accuracy: 0.1 m/s)
6	Thermo-hygrometer	Monitor the relative humidity and temperature
7	Evaporation chamber	Length: 40 cm, width: 30 cm and height: 15 cm
8	Soil column	Diameter: 10 cm, total height: 200 cm
9	Water content sensor	EC-5 soil moisture sensor
10	Evaporation chamber	Length and width: 40 cm, height: 50 cm
11	Evaporation pan	Thickness: 1cm, diameter: 10 cm

No.	Accessory	Functions and remarks
12	Scale	GX-32K, AND Co. Ltd, solution is 0.1g
13	Switch	Control the wind speed
14	Air blender	Ventilate air and supply wind speed
15	Environmental chamber	Diameter: 50 cm, height: 32 cm
16	Air blender	Rabble the air
17	Thermo-hygrometer	Monitor the relative humidity and temperature
18	Freezer	Cool down the air
19	Heater	Warm up the air
20	Control panel	Set and monitor climatic index
21	Dehumidifier	EFA5-100-A, decrease the relative humidity
22	Ultrasonic humidifier	WM-SCA1000, increase the relative humidity

Figure 3.2 Schematic illustration of climate control apparatus for investigating evaporation

This system mainly consists of three components:

(1) Climate control part: a set of devices to control the atmospheric conditions.

(2) The evaporation measuring part for column evaporation test or pan soil evaporation test.

(3) The control and data acquisition system.

The use of a radioactive flux is avoided in this apparatus so that this approach can eliminate or at least minimize the concern for the energy budget at the soil surface. The effect of the energy budget on the evaporation process is paramount in the field studies. However, it is deliberately set aside in this study thus the fundamental process of soil evaporation could be observed.

3.2.1 CLIMATE CONTROL PART

The environmental chamber is a circular cylinder that is made of transparent acrylic material with the thickness of 1.5cm, high of 320cm and diameter of 500cm. The resistive heater and freezer (E5CN, Omron Co. Ltd) controlling air temperature are automatically operated in an alternative mode, in other words, the resistive heater launches when actual temperature in the environmental chamber is lower than the set value; otherwise, the freezer is activated. The humidity is controlled by the dehumidifier (EFA5-100-A, IAG Co. Ltd) and ultrasonic humidifier (WM-SCA1000, Wet master Co. Ltd), both of which are also in alternative operation model. The air in the environmental chamber could be sufficiently agitated by the air blender, while the thermo-hygrometer installed at the top of chamber is used to monitor climatic indicators.

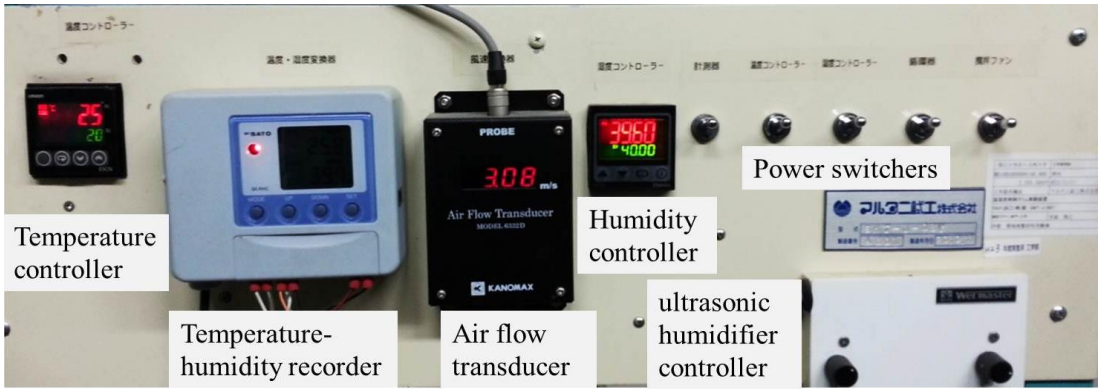

Figure 3.3 Photograph of devices fabricated on the control panel

The control panel is designed as a visualization form to set and monitor each index. The devices fabricated on the control panel is shown in Figure 3.3. A temperature controller displays the continuous temperature value and controls the activation of heater and freezer by setting the target value. The temperature-humidity recorder (SK-RHC, SATO Co. Ltd) displays the value measured by the thermo-hydrometer installed at the evaporation chamber. The airflow transducer (Model 6332, KANOMAX Japan, INC.) is used to monitor the instantaneous wind speed measured by the wind speed probe at evaporation chamber. The humidity controller shows the relative humidity value and control the activation of dehumidifier and ultrasonic humidifier. The out power of ultrasonic humidifier is manipulated the controller.

3.2.2 EVAPORATION TEST PART

Evaporation takes place in the cubic evaporation chamber that is connected to environmental chamber by two plastic pipes (Φ3.5 cm). The air blower is used to ventilate air in the pipe by a wind speed that is controlled by the switch at the forepart of the pipe. Humidity, temperature and wind speed in the evaporation chamber are measured by thermo-hygrometer (SK-RHC Sato Keiryoki Mfg. Co., Ltd) and wind speed sensor (Model 0962-00 Kanomax Japan, Inc) respectively. The measured climatic indexes are given as a feedback to control panel to operate the devices in environmental chamber.

For the pan soil evaporation test, the evaporation chamber is rectangular block with the size of length 40 cm, width 40 cm and height 50 cm. A scale (GX-32K, AND Co. Ltd, 0.1g solution) gives a continuous weight measurement of the evaporation pan (Φ10 cm, depth of 10mm), Styrofoam insulation is inserted between the scale and evaporation pan.

For the column soil evaporation test, the evaporation chamber is a relatively smaller with the size of length 40 cm, width 30 cm and height 15 cm. The specimen filled evaporation column are constructed using 10 cm diameter acrylic material having a wall thickness about 0.90 cm. The column height can be changed corresponding to the experiment aims. The water content sensors (EC-5, Decagon Devices) was inserted into the soil specimen to measure the instantaneous volumetric water content at different. A water tank supplying water to the column maintains the water table by overflow. At the top of tank, Burette is taken upside down with the

lower end placing just right at the water table. As a consequence, the amount of water supplied into the soil column can be monitored by the volume change of burette.

3.2.3 DATA ACQUISITION SYSTEM

Data acquisition systems, as the name implies, are processes used to collect information to document and analyze some phenomenon. A UCAM-60A data logger (Kyowa Co. Ltd) is used with sensors to document information relating to the process, which is an all-in-one measuring instrument. The data logger simultaneously input signals from various sensors-wind speed sensor, thermo-hydrometer and water moisture probe. Ethernet LAN interface is adopted for connecting the data logger to computer. The control software installed in the computer enables the computer to not only control the data logger but also perform data processing and display instantaneously. This software is written by the geotechnical research laboratory, which is based on Visual Basic Language. It is ensured that response time of the sensors is optimum and the data acquired from the sensors is displayed instantaneously.

The interval of system task is invoked by the timer-control at any interval (e.g. 30 s, 1 min, 2 min, 5 min, 10 min and 15 min), and then all the monitored data is stored into excel file.

3.3 FEATURES OF THE DEVELOPED APPARATUS

The success of experimental research relies on suitable experimental and appropriate experimental techniques. A good experiment system should consist of instruments of good workability, durability, and reliability of calibration.

This section will describe the function of the developed apparatus, which would also be the original characteristics that are differing from pervious devices.

3.3.1 FLEXIBLE CONFIGURE FOR SPECIMEN

Both evaluating the soil properties related to evaporation process and soil water content profile in certain depth during evaporation are essential for investigating soil evaporation problem, meanwhile, most pervious apparatus only could handle with one condition for the evaporation experiment for pan soil evaporation or column soil evaporation (Wilson et al., 1997; Yanful et al., 1997). The apparatus can meet the

multi requirement for pan soil evaporation and column soil evaporation.

As shown in Figure 3.2, two pipes are connected to the evaporation chamber No.7 or No.10. It is soil column evaporation test for No.7 chamber, while the pan soil evaporation chamber for No.10 chamber. The specimen in this apparatus is optional according to the experimental purpose. For the pan soil evaporation, the thin soil section is artificially formed on circular, 10 cm diameter, evaporation pan as shown in Figure 3.2. The thickness of the specimen is 1 cm that is considered to eliminate hydraulic gradient in the specimen, thus the water content in the specimen is homogeneous. And then the targeted atmosphere condition is applied on the specimen with monitoring the weight time to time. It is purposed to investigate the soil water dynamic during evaporation process for soil column evaporation test. The soil specimen is compacted into a column with certain dry density. The specially designed cylindrical column was fabricated from a 1.0 cm thick, an internal diameter of 10 cm and an alterable height (totally 200 cm). The No.7 chamber is fabricated on the soil column, and then the controlled atmosphere condition is applied.

3.3.2 ACCURACY INCREASED

Comparing with the pervious apparatus for investigating soil evaporation, the current apparatus shows higher accuracy, including the accuracy both in meteorological parameters and measured evaporation rate.

First for the aspects of atmosphere condition, most geotechnical researchers mainly focused on the soil properties, the variation was taken less attention. For example, the relative humidity in Wilson's experiment (Wilson et al., 1997) varies from 39% to 62% even for the same soil specimen. In Yanful's study (Yanful et al., 1997), although the experimental condition is controlled, the derivation of relative humidity was still large to nearly 20% in one day. All these variation would cause the error for the measured value. This apparatus can fully controlled the temperature, relative humidity, and the wind speed with lower index varying range. It supplies a relatively stable atmosphere condition for investigating evaporation property.

For the measured evaporation rate, the usual unit is "mm/d", however, this apparatus always provide the evaporation rate in "mm/h" attributing to the high solution of the scale (0.1 g). Therefore, this apparatus is able to measure the minimal change of evaporation rate. It almost increases the accuracy in 10 times. However, it should be noted that the wind speed has some disturbance for measuring weight loss

of specimen thus the evaporation rate.

3.3.3 AUTOMATIC CONTROL AND VISUALIZATION

Control program and logging system for data acquisition is cable of collecting the signals from sensors or the control panel. The system can be controlled in two different ways: via environment variables, which should be sufficient in most scenarios, and via the application level logging, which provides programmatic access to the logging system for manual use-cases. The control starts system from setting the value of atmosphere conditions (temperature, relative humidity). The software record the instantaneous and judging the ratio of measured value to set value. For the case that the ratio is greater than 1.0, the dehumidifier or freezer would be activated to work. For the case that it is lower than 1.0, the ultrasonic humidifier or the heater would be at work. The control system of auto-operation model ensures the constant environmental condition in the chamber.

Visualization of technology process on PC monitor, which displays the equipment operation together the instantaneous monitored data. The visualization ensures continuous production by providing all necessary and relevant information for each individual process step. Moreover, an instantaneous value would be available to be recorded between the intervals.

3.4 ACCURACY CALIBRATION

It is important to investigate the accuracy and the ability for controlling atmospheric conditions before conducting evaporation experiments. The calibration tests were carried out after the system was sealed and circulated unceasingly. It was conducted prior to the beginning of test program and after the completion of all the test programs. For the case of beginning of test program, there was not water or soil specimen placed in the environment chamber during calibration. The calibration method was that changing one index systematically with the other two indexes maintained, for example, relative humidity was evaluated the while maintaining the temperature and wind speed.

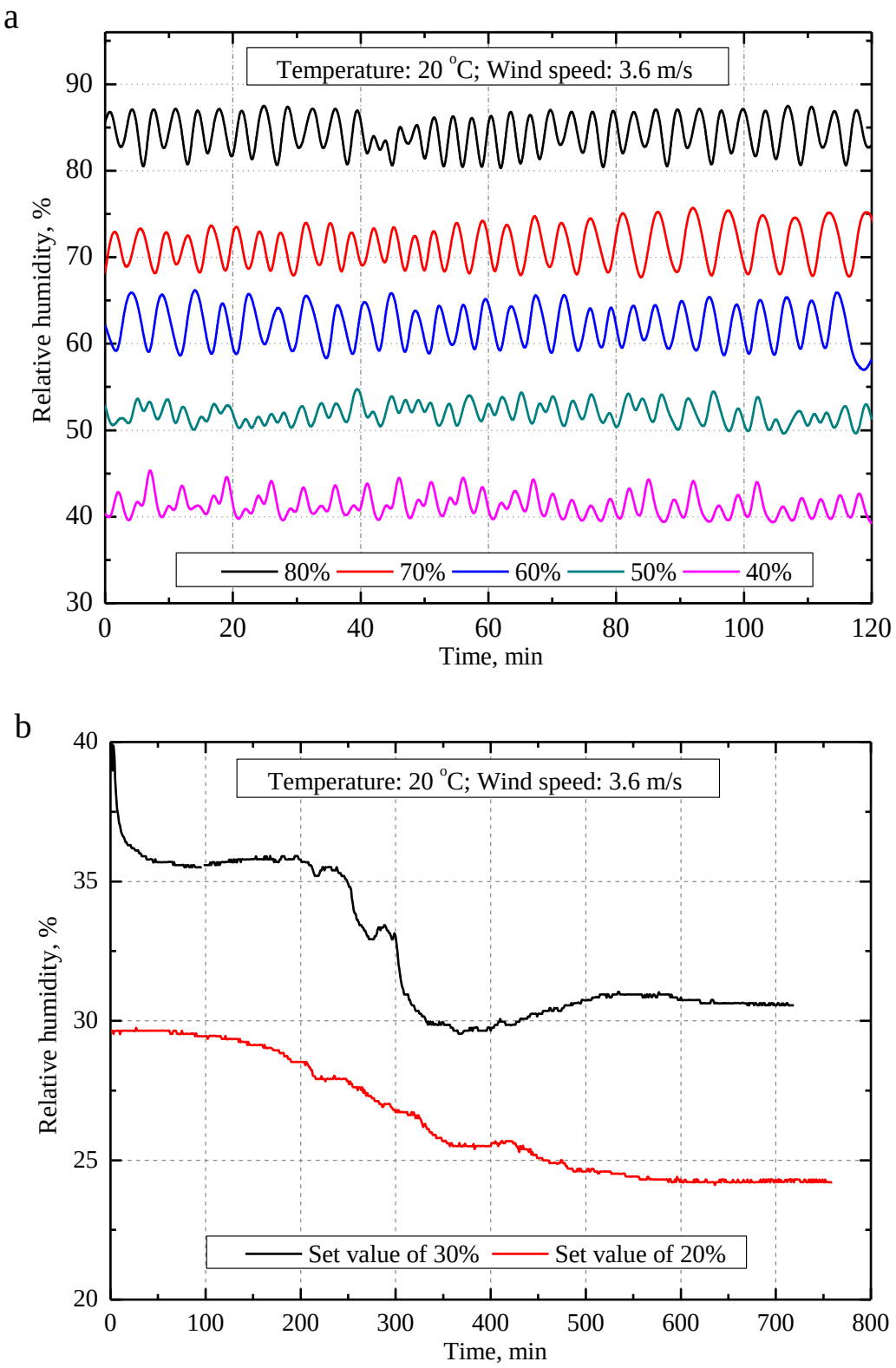

Figure 3.4 Transient change of relative humidity, (a) from 40% to 80% and (b) from 20% to 30%.

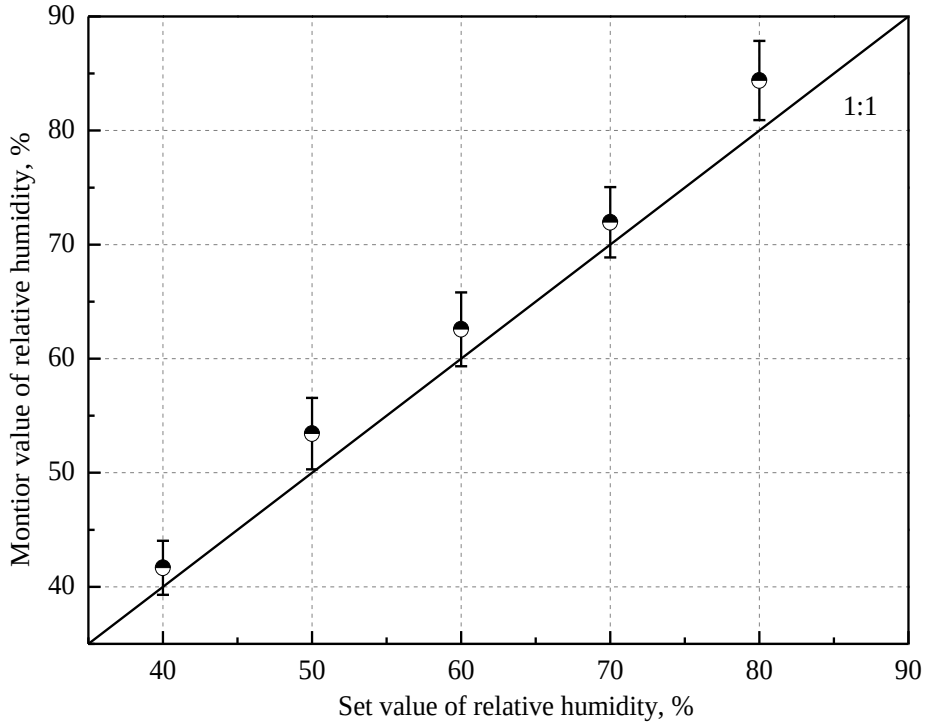

Figure 3.5 Standard deviations for relative humidity from 40% to 80%

The relative humidity was checked in seven groups from 20% to 80% with 10% interval. It was taken 2 hour for each case of 40%, 50%, 60%, 70% and 80% whose the variation was presented in Figure 3.4(a), while the duration was 12 hour for the case of 20% and 30% as shown in Figure 3.4(b). The standard deviations of the relative humidity for the values of 40%, 50%, 60%, 70% and 80% were plotted in the Figure 3.5. Figure 3.4 (a) shows that all the value fluctuates similar to the trigonometry function that produces an ever-repeating wave of peaks and valleys. The mean values of monitored result are greater than the set value in all cases. The amplitudes of relative humidity of 40% and 50% are a little smaller comparing to the other cases. Figure 3.5 shows that the range of fluctuation is about 6% while the mean value is about 2%-5% higher than the set relative humidity. These may attribute to the delay and vapor pressure loss during transfer in the pipe, in addition, the higher efficiency of humidifier than dehumidifier may also result in this condition. Figure 3.4(b) shows that it is time consuming to achieve the set value of 20% and 30%. It takes about 350 minutes for reducing the relative humidity from 40% to 30%, while 500 minutes for the process from 30% to 24%. Therefore, the 30% is the limiting value of relative humidity for this apparatus. It is concluded that

the apparatus can meet the requirement for the relative humidity from 40% to 80%.

For the calibration of wind speed, three set values of 1.4 m/s, 2.5 m/s and 3.6 m/s were evaluated in 24 hour. Figure 3.6 displays the transient variation of wind speed versus elapsed time, which shows it randomly fluctuated around the corresponding set value. Figure 3.7 shows the standard deviation of the corresponding wind speeds, it is indicated that there is close correlation between average value and set value, and wind speed value is discrete and fluctuates at a range of 0.5 m/s. The standard deviation of wind speed 2.5 m/s is greater than the other two cases. In one word, the wind speed controlled ability of this apparatus satisfies the demand of evaporation experiment.

In order to reveal the properties of airflow in the evaporation chamber, the vertical profile of the wind speed is necessary to evaluate. Since the position of specimen surface was 2 cm lower than the wind port, the airflow probe was placed 2 cm higher than the port. Assuming the wind speed profile is symmetrical from the port, the measured value can represent actual wind speed of specimen surface. The wind speed profiles were measured for the actual wind speeds of 0.9 m/s, 1.4 m/s, 2.5 m/s and 3.6 m/s as presented in Figure 3.8. It shows that the wind speed is greater for closer to the port, and the gap among these four conditions is very large. If the vertical distance is greater than 7 cm, the wind speed has no obvious difference.

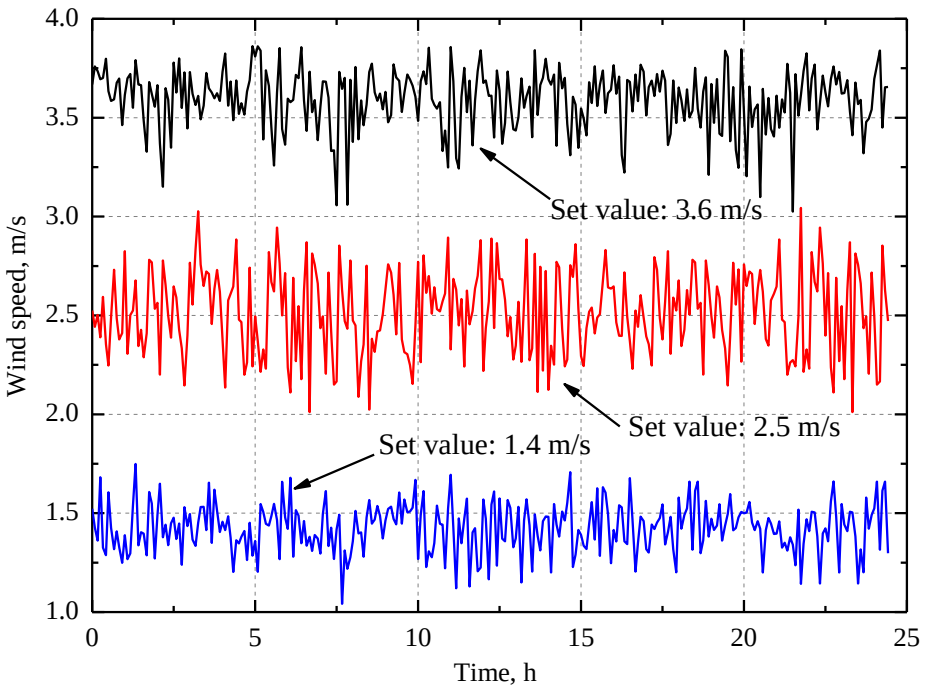

Figure 3.6 Wind speed variation for set values of 1.4, 2.5 and 3.6 m/s

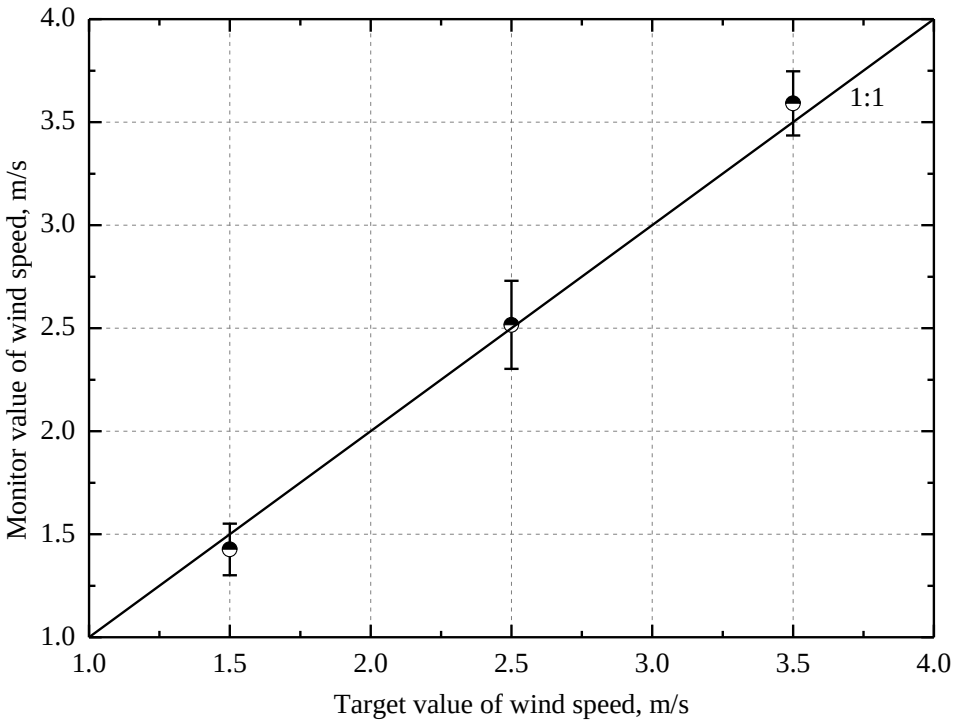

Figure 3.7 Standard deviations for different setting values of wind speeds

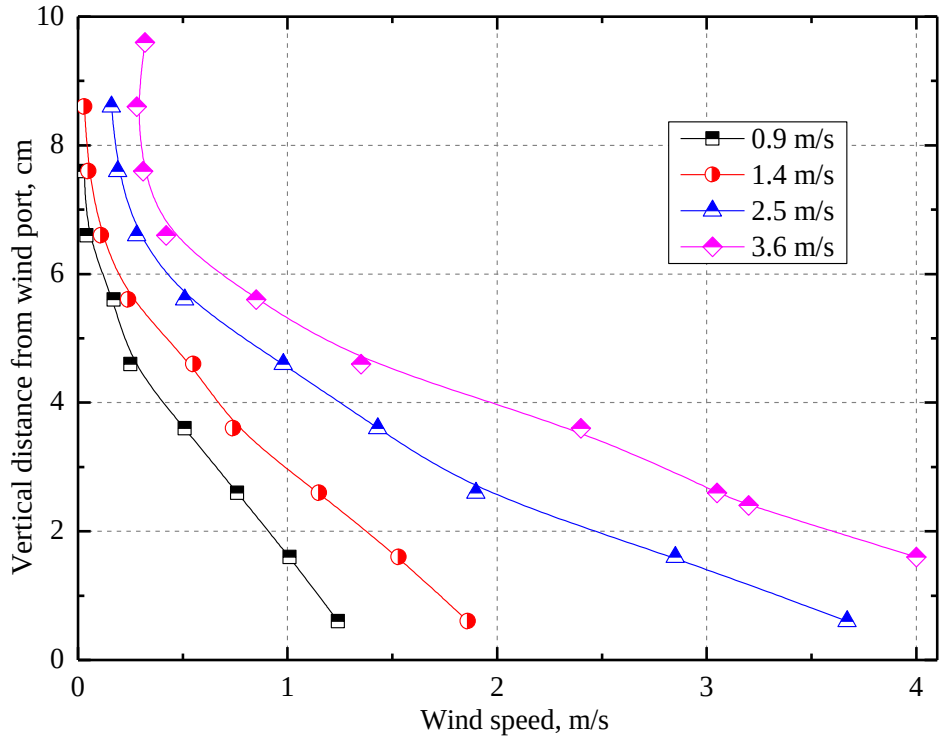

Figure 3.8 The vertical profile of wind speed

The temperature calibration was carried out for the set values of 50 °C, 40 °C, 30 °C, 20 °C and 10 °C. It lasted 20 hour for each case. The mean temperature of laboratory was around 20 °C. During the calibration, the relative humidity and wind speed were maintained at 40% and 3.6 m/s, respectively. The transient temperature variation is shown in Figure 3.9 while the corresponding standard deviation for different temperatures is shown in Figure 3.10. These two Figures demonstrate that the temperature is almost constant with a variation of 2 °C in average, thus the standard deviations is very small. However, due to the heat loss during circulation and temperature gradient between inside system and outside environment, the temperature in the evaporation chamber only maintained at the range of 20 °C to 30 °C, which cannot satisfy the design requirement. The efficiency of controlling temperature needs to be further improved. It is concluded that the apparatus can produce good performance only when set temperature value is close to the laboratory temperature, for example the condition of 20 °C as shown in Figure 3.10.

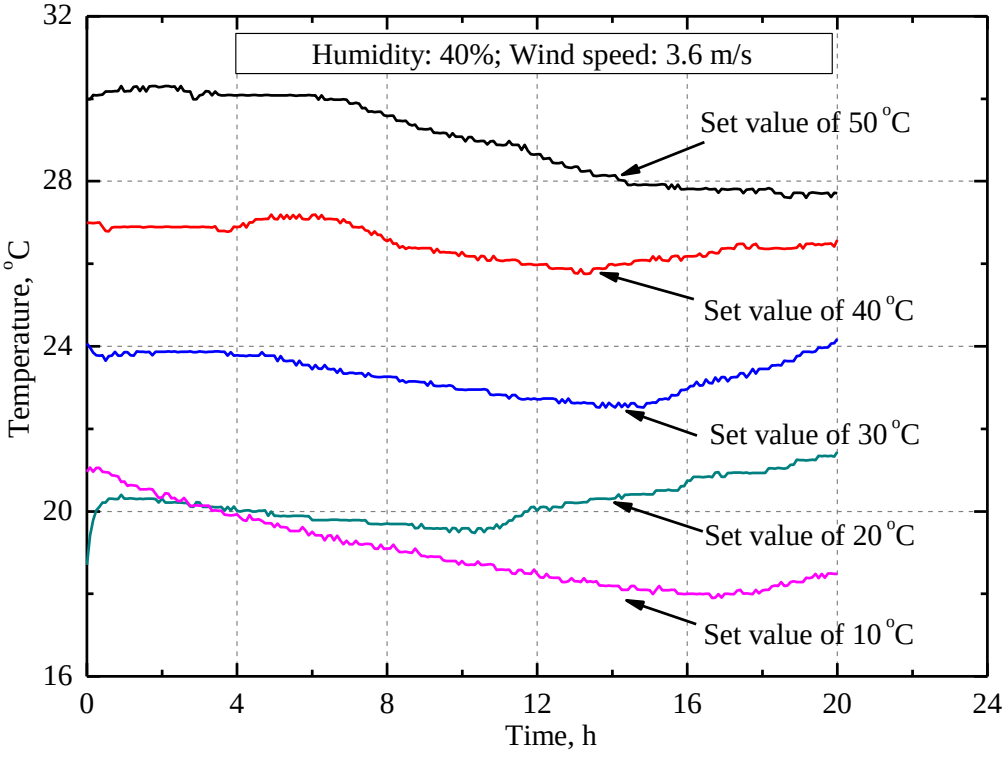

Figure 3.9 Temperature variation for different set values from 10 °C to 50 °C

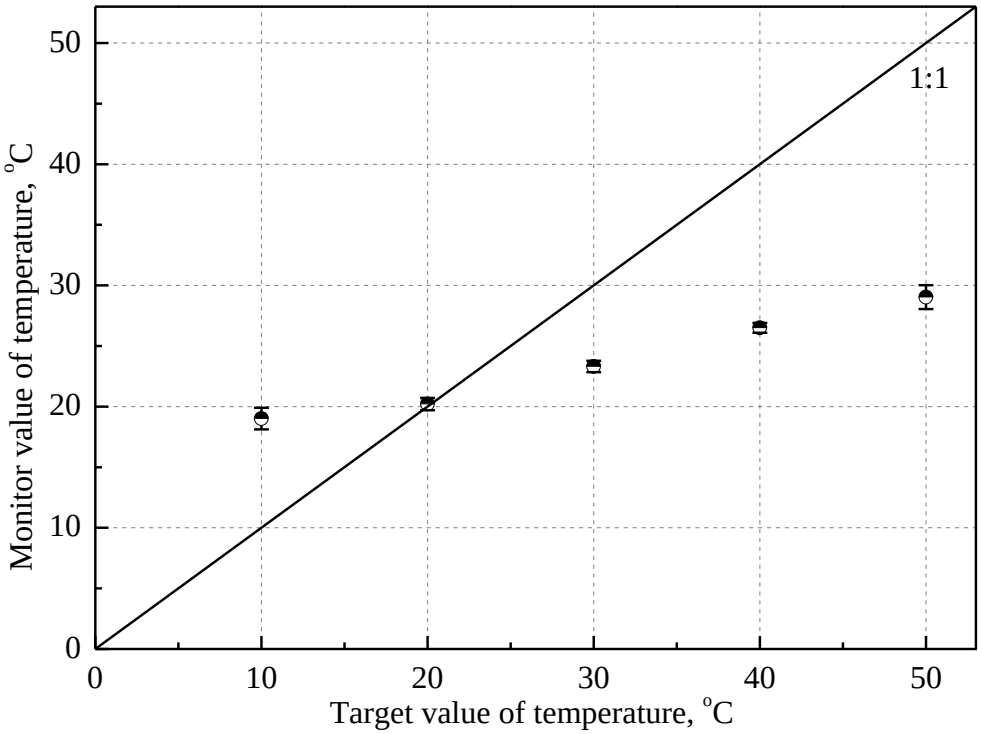

Figure 3.10 Standard deviations for temperature at different values

3.5 SUMMARY

This chapter mainly focuses on the apparatus development. A climate control apparatus is comprehensively introduced from the aspects of instrumentation of the apparatus, features and accuracy calibration. The apparatus can be described in generally as follows,

(1) The apparatus is composed of climate control part, evaporation part and data acquisition system.

(2) The features of this apparatus are flexible configure for specimen, increased accuracy, and automatic control and visualization. The first one means that it is able to handle both the pan soil evaporation and column soil evaporation for different purpose. The increased accuracy indicates that the apparatus maintains the atmosphere conditions with little variation, also the solution evaporation rate is high to 0.1 mm/h. The automatic control and visualization means the control program and logging system for data acquisition is not only cable of collecting the signals, but also displays the operation and instantaneous data on the PC monitor.

(3) The calibration tests shows that the apparatus is capable to favorably control wind speed and relative humidity with ranges of 0 to 3.6 m/s and 30% to 80%, respectively, and the control rang for temperature is limited from 20 to 30 ℃, which needs further more improvement.

REFERENCE

Aluwihare, S. and Watanabe, K. (2003): Measurement of evaporation on bare soil and estimating surface resistance. Journal of Environment Engineering. 129(12), 1157-1168.

Teng, J.D., Yasufuku, N., Liu, Q., Omine, K. (2012): A climate control apparatus and its application to evaluate evaporation process. Proceedings of 8th International Symposium on Lowland Technology, P.161-166, Bali, Indonesia, Sep. 11-13, 2012.

Wilson, G.W., Fredlund, D.G., and Barbour, S.L. (1997): The effect of soil suction on evaporartive fluxes from soil surfaces. Canadian Geotechnical Journal, 34, 145-155.

Yanful, E.K., and Choo, L.P. (1997): Measurement of evaporative fluxes from candidate cover soils. Canadian Geotechnical Journal, 34, 447-459.

CHAPTER 4

METHODOLOGY FOR DETERMING SOIL EVAPORATION

4.1 INTRODUCTION

Surface evaporation is one of the main process in the soil-atmosphere interaction, this process is not only a function of soil physical parameters such as moisture, vapor pressure and temperature gradient, matric forces, pore diameter, etc., but also a function of air turbulence at the soil-atmosphere interface. Therefore, prediction of drying rates from soil surface remains a challenge. Although specific descriptions have been proposed for various applications, their applicability seems to be limited because they are mostly based on measurements under limited conditions of soils, for example, the soils of a specific thickness or type (Komatsu, 2003). Therefore, it is important to develop a unified description and a robust parameterization of evaporation from soil surface, which can be applied to soil of arbitrary types in a systematic way.

In contrast with the complexity of defining soil surface evaporation (E_a), a standard description for the evaporation from water surface (E_p) has been established as reviewed in section 2.4 and item 2.5.3, the effect of environmental temperature, humidity, and wind speed can be well described. Therefore, one feasible way is to determine the relationship between E_p and E_a. The establishment of such a relationship requires independent analysis of atmospheric conditions and soil properties.

The purpose of this chapter is to elucidate the soil evaporation phenomenon, parameterize soil evaporation and finally the experimental evaluation. A rational model should take account of as many as all relevant factors. Therefore, in the first section the factors affecting the soil evaporation are finally analyzed and clarified

based on the laboratory tests. Secondly, the theoretical development of the ratio of E_a to E_p is presented from two aspects, and finally, the parameterization of soil evaporation is clear expressed, and also this expression is verified by the experimental results.

4.2 EVALUATION OF THE EFFECT FACTORS OF SOIL EVAPORATION

Evaporation from soil surface occurs when the molecules in a liquid state absorb enough heat energy to vaporize into a gas. Since it is highly interacted between soil and atmosphere, many factors have influences on the soil evaporation process as generally reviewed in section 2.2. For parameterizing the soil evaporation, it is necessary to conduct research on related factors of soil evaporation to investigate its influence separately. This section will be extended for describing from the aspects of atmospheric variables and soil properties.

4.2.1 INFLUENCE OF METEOROLOGICAL VARIABLES

1. The influence of temperature

A kind of fine sand named K-7 sand was selected as the materials for evaporation tests as well as the water drying test. K-7 is a standard silica sand in Japan, a summary of the soil properties is presented in Table 4.1. The soil was packed into a circular pan with a diameter of 8.8 cm and height of 2 cm. Then the specimen was wetted to saturation using a fine uniform mist of distilled water with appropriate amount. Wilson et al. (1997) also adopted this procedure. For the purpose of comparison, the parallel test was conducted for these two cases; the specimen was shown in Figure 4.1. Then two specimens were put into the oven where the constant temperature was maintained. Three cases of temperature 30 °C, 40 °C and 50 °C were conducted separately, the relative humidity under these three conditions are about 63.0%, 46.3% and 26.4%, respectively. A scale (solution of 0.01g) was used to measure the continuous weight of specimen with time interval of about 2 hour. The monitored data can produce the value of evaporation rate and mean soil water content.

The mean water content and evaporation rate versus elapsed time are displayed in Figure 4.2 and Figure 4.3, respectively. Figure 4.2 shows that the drying curves for soil samples in parallel is almost same, which indicates the evaporation tests has good reproducibility. At the beginning of drying, the mean water content shows liner

relationship with the elapsed time. Then mean water content changes to slowly decrease and finally reach a residual stage where the water content is nearly zero. During the drying period, the evaporation rate clearly shows three stages as presented in Figure 4.3, they are constant rate stage, falling rate stage and slow rate stage that are defined in Figure 2.1. At the end of soil drying, the evaporation rate is nearly zero.

Table 4.1 Summary of the properties of soil specimens

Specimen	Specific gravity (g/cm^3)	Bulk density (g/cm^3)	Sand (%)	Silt (%)	Clay (%)	Uniformity coefficient	Curvature coefficient	Median diameter (mm)
K-7 sand	2.67	1.45	85.8	14.2	0	3.57	1.20	0.214
Fly ash	2.26	1.17	0	100	0	1.93	1.17	0.025
K-3 sand	2.67	1.33	100	0	0	1.21	0.69	0.606

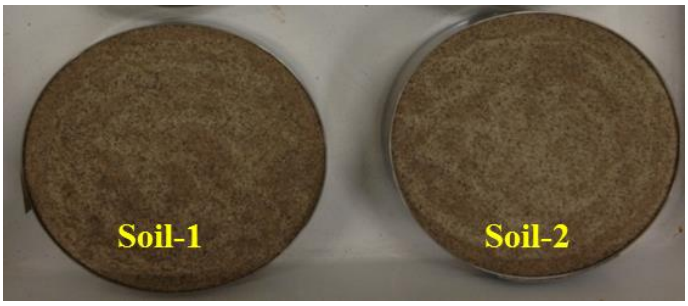

Figure 4.1 Photograph of the specimen for oven dry test

As shown in Figure 4.2, the drying curve shifts to the left, the slope of the line gradually increases. Actually, the value of slope reflects the change of soil water state of specimen. The higher atmosphere temperature results in the faster reduction of mean water content and shorter time for reaching the residual stage. The time for the specimens reach residual stages are about 138 h, 45 h and 28 h corresponding to the temperatures of 30 °C, 40 °C and 50 °C, respectively. In other words, for the temperature increases from 30 °C to 50 °C, the time would shorten 4% in average for temperature increasing 1 °C. From the evaporation curve in Figure 4.3, it shows that the initial evaporation rate changes from 0.08 mm/h to 0.37 mm/h for the temperature increases from 30 °C to 50 °C. The duration of the initial constant stage becomes smaller with the temperature increasing.

Since the high temperature increases the thermal motion of water molecule that is the kinetic energy, more water molecules have the potential to escape from the friction of the liquid surface. On the other hands, the higher temperature results in lower rate of water retention ability and water velocity. In addition, Derjagiun et al. (1986) stated that the bound water in soil pore would also transform into free water due to the increasing temperature. All these factors mentioned above benefits the vaporing of liquid water, transport speed of water molecule. These also explain the phoneme that higher temperature leads to shorter drying time and higher initial evaporation rate. In addition, the lower relative humidity caused by higher temperature somehow accelerates the evaporation from soil surface.

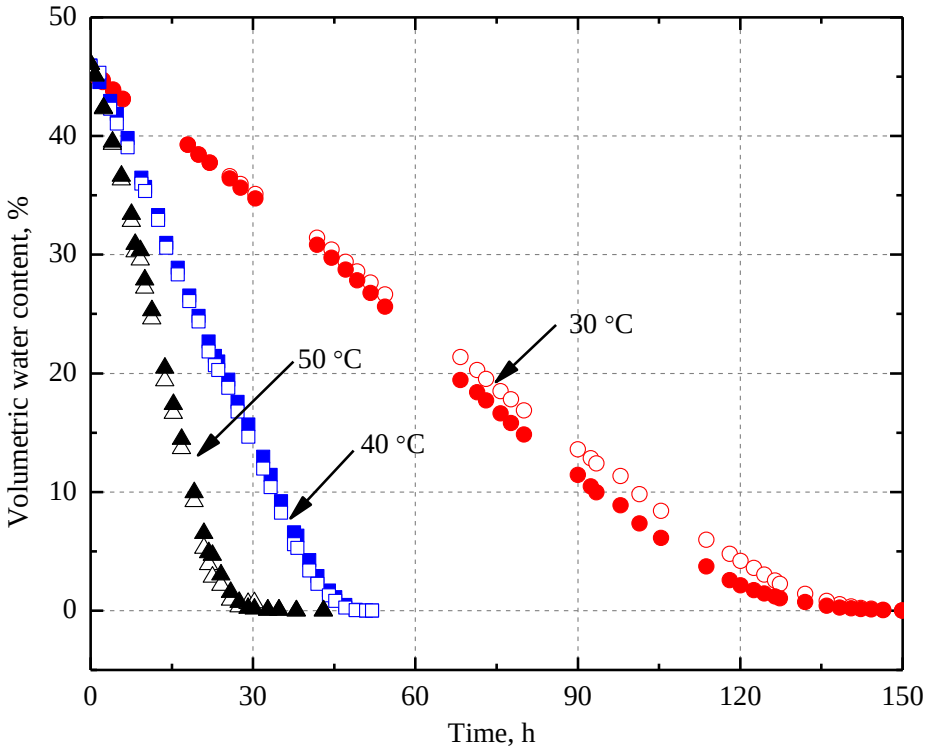

Figure 4.2 The change of average water content of samples at different temperature

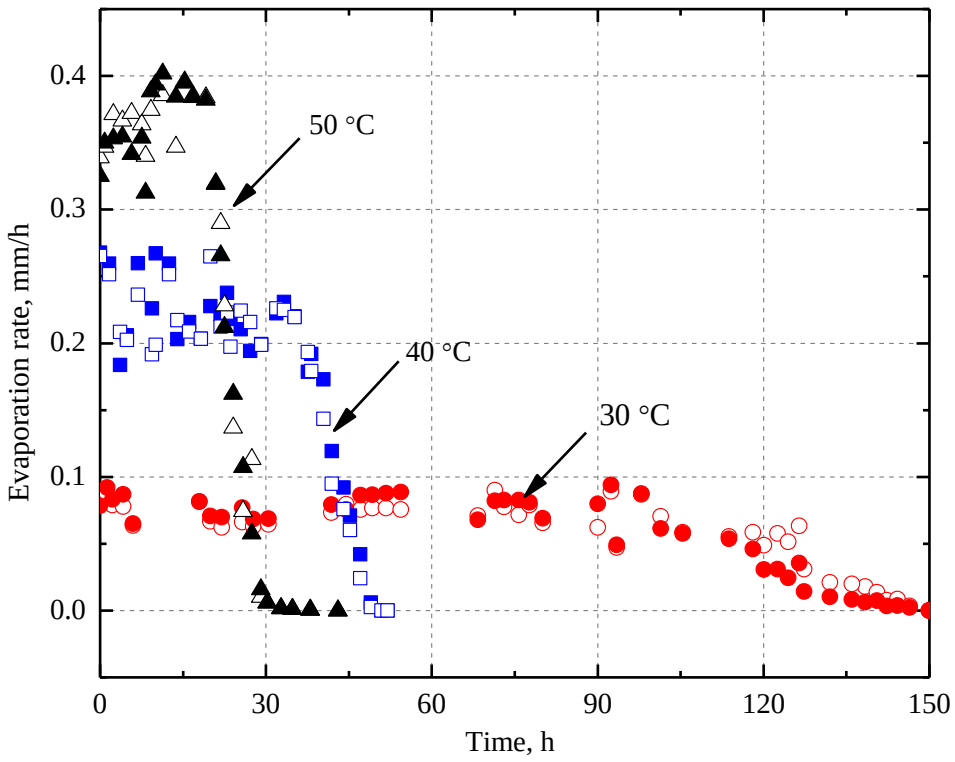

Figure 4.3 The change of evaporation rate of samples at different temperatures

2. The influence of wind speed

To investigate the influence of wind speed on the evaporation rate, the experiment work was performed by using the developed climate control apparatus. The K-7 sand was firstly packed into the evaporation pan (Φ10cm, 1cm thickness), and then the specimen was wetted to saturation by specific amount of water. The pan soil was placed in the evaporation chamber as shown in Figure 3.2. Twelve different conditions were applied for each soil specimen as listed in Table 4.2. For all conditions, temperature was maintained at 25 °C (±1.0 °C); the relative humidity was controlled at three degrees of 40% (±2.37%), 60% (±3.24%), and 80% (±3.47%); wind speed was controlled at four degrees of 0.5 m/s (±0.09), 1.4 m/s (±0.13), 2.5 m/s (±0.21), and 3.6 m/s (±0.16). In addition, the evaporation pan that contained distilled water was firstly tested to measure the potential evaporation rate of each condition; the result is summarized in Table 4.2.

Table 4.2 Experimental conditions

Items	C1	C2	C3	C4	C5	C6	C7	C8	C9	C10	C11	C12
Temperature (℃)	25	25	25	25	25	25	25	25	25	25	25	25
Relative humidity (%)	40	40	40	40	60	60	60	60	80	80	80	80
Wind speed (m/s)	0.5	1.4	2.5	3.6	0.5	1.4	2.5	3.6	0.5	1.4	2.5	3.6
Potential evaporation (mm/h)	0.18	0.25	0.33	0.39	0.11	0.21	0.27	0.35	0.10	0.13	0.16	0.18

The evaporation rates under different groups are displayed in Figure 4.4 versus the elapsed time, the experiment data is presented in the groups depended on the degree of relative humidity, and thus the effect of wind speed can be easily observed. The result shows that higher wind speed always results in higher initial constant evaporation rate, earlier time for the evaporation rate reducing and shorter period for the evaporation process. Take the result in Figure 4.4 (a) for example, the initial constant evaporation rates are 0.18 mm/h, 0.25 mm/h, 0.33 mm/h and 0.39 mm/h corresponding to the wind speed of 0.5 m/s, 1.4 m/s, 2.5 m/s and 3.6 m/s, respectively. The inflection times when the evaporation rate starts to decrease are 21.0 h, 17.5 h, 11.0 h and 8.0h, respectively. Moreover, it takes about the 26.5 h, 23.5 h, 18 h and 13 h respectively for the soil specimen to get completely dry. It is noted that the slopes of the evaporation rates during falling rate stage are almost same.

We present the values of constant evaporation rate in Figure 4.5 versus the horizontal axis of wind speed. The result show that evaporation rate increases in all cases with an increase in wind speed. Evaporation rate is increased about 2 times by increasing wind speed from 0.5 m/s to 3.6 m/s. However, the average gradients of the line vary with the relative humidity. Since the evaporation is a diffusion process involving movement of vapor in response to concentration gradient, any force or disturbance causing mass movement of air would influence the rate of vaporization. Wind current moving across soil surface is going to carry away these newly evaporated water molecules, allowing more water to evaporate into that atmosphere space. The wind current will carry away more water molecules when the speed of that wind is higher, thus more evaporation in a shorter period. Moreover, fluctuation of wind at soil surface, while not necessarily causing a large amount of air to be removed from the soil, can speed up gaseous movement because of greater mixing of gases within the soil due to pressure changes. Hanks (1958) pointed out that the vapor conductivity of water vapor is increase with increased wind speed, and

changing the wind characteristics of period and amplitude of fluctuations would influence vapor transfer.

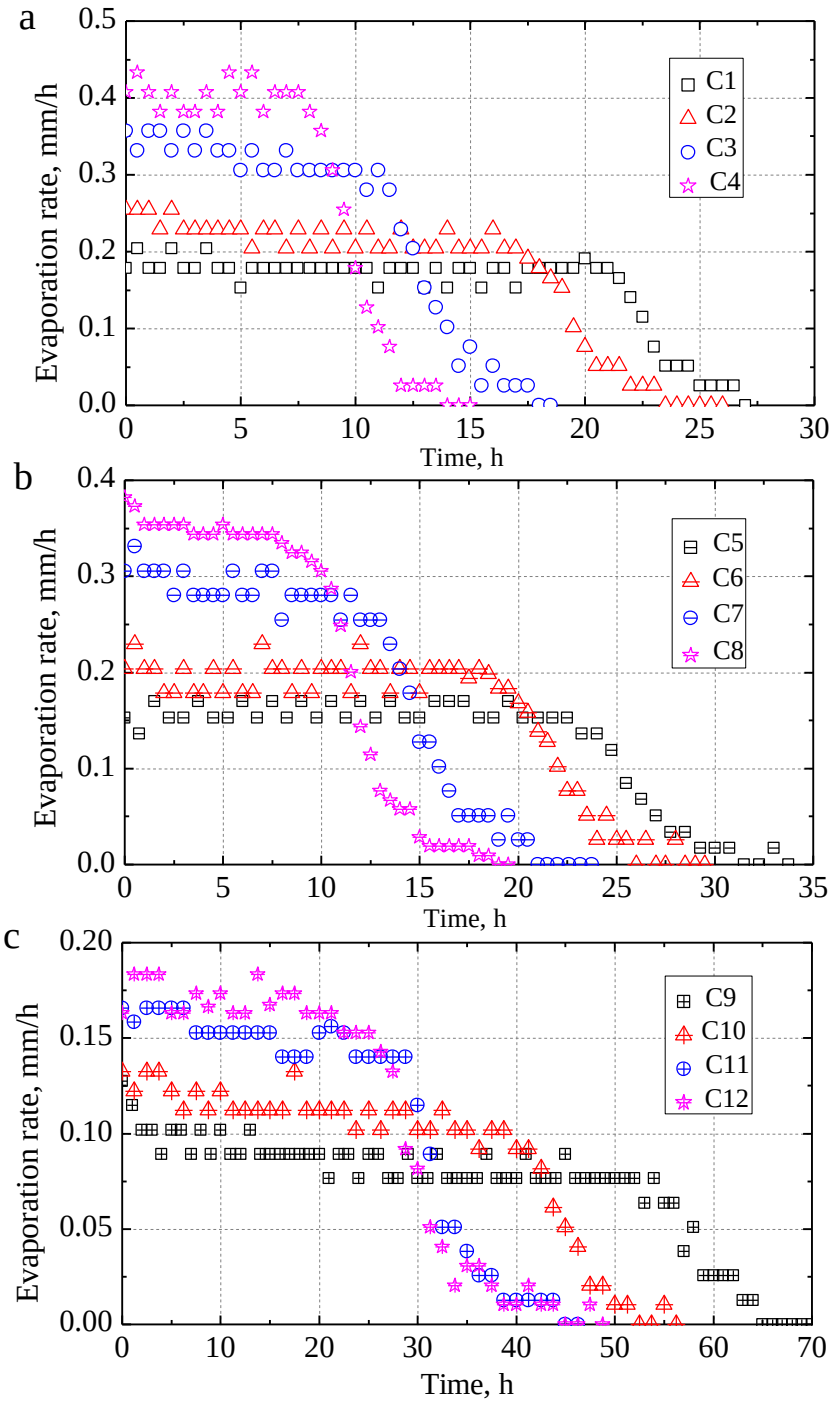

Figure 4.4 The evaporation rate versus elapsed time for the relative humidity of (a) 40%, (b) 60%, and (c) 80%, respectively

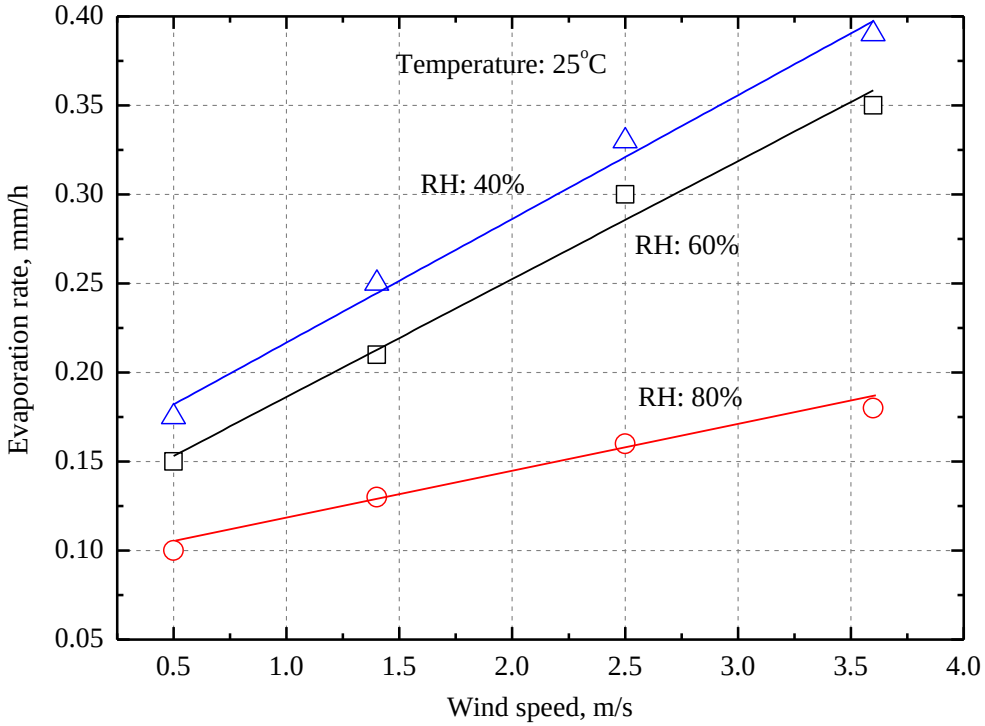

Figure 4.5 Relationship between constant evaporation rate and wind speed

3. The influence of relative humidity

The experiment result presented in Figure 4.4 and Figure 4.5 can also be applied to investigate influence of relative humidity on evaporation rate by transforming into another form. The evaporation rates versus drying time are presented in Figure 4.6 that are in groups of wind speeds. The result show that the greater relative humidity would produce smaller initial constant evaporation rate, and longer time would be consumed for specimens dry out. It is observed that the evaporation curves for relative humidity at 40% and 60% are close in all cases. The evaporation curves at relative humidity of 80% show a long-period of constant rate stage although its rate is relatively lower, they show clear residual rate stage comparing to the cases of relative humidity at 40% and 60%. The relationship between constant evaporation rate and relative humidity is presented in Figure 4.7. The evaporation rate at relative humidity 100% is assumed to be zero. The evaporation rate in all cases slowly and then sharply decreases with the inflection point at about 60%. That phenomena can be explained that the water delivered in soil cannot meets the evaporative demand, at that time the evaporation rate would not controlled by the hydraulic properties of soil.

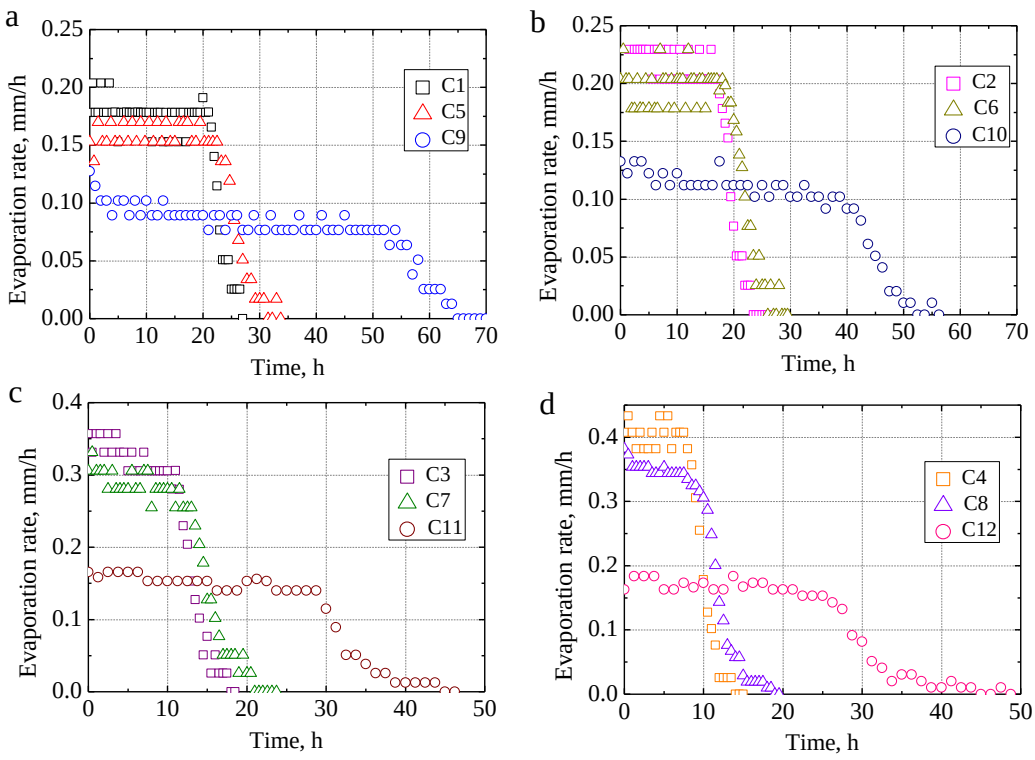

Figure 4.6 The evaporation rate versus elapsed time for the wind speed of (a) 0.5 m/s, (b) 1.4 m/s, (c) 2.5 m/s and (d) 3.6 m/s, respectively

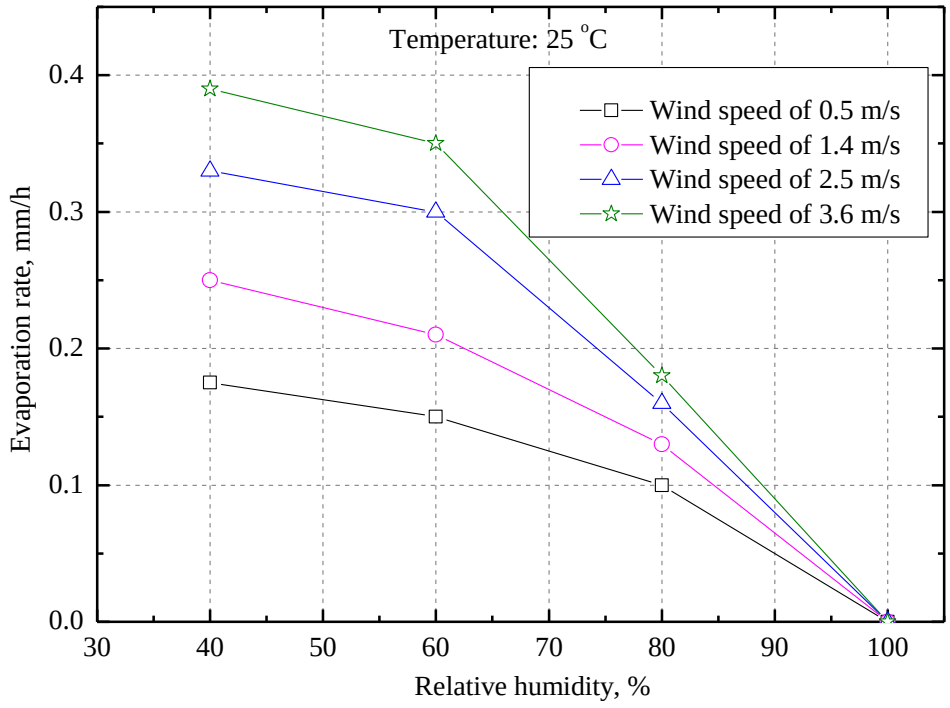

Figure 4.7 Relationship between constant evaporation rate and relative humidity

4.2.2 INFLUENCE OF SOIL PROPERTIES

1. The influence of soil density

The dry density is always considered as a basic index of soil state, and it has effect on hydraulic and mechanical properties. In order to understand the effect of soil density on evaporation properties, a series of laboratory tests were executed. The K-7 sand was selected as the material. By connecting a soil column upon the evaporation pan, the samples were compacted into the soil column; the soil specimen with different dry density can be performed procedure according to the procedures stipulated by Japanese Geotechnical Society (JGS). Then the soil column was moved away, and the surface of evaporation pan was flattened. Three cases of dry density were controlled, which are 1.41 g/cm^3, 1.49 g/cm^3 and 1.58 g/cm^3. The densities of 1.41 g/cm^3 and 1.58 g/cm^3 reflect the most loose and dense state of K-7 sand, respectively. Then specific amount of distilled water was supplied to saturate the soil specimen. The C8 climate condition in Table 4.2 was the standard condition and applied to the soil specimen. For all the cases, the evaporation tests were carried out in parallel.

Figure 4.8 shows the variation of evaporation rate at different soil densities. The evaporation curves show similar tendency, the densest soil firstly reaches the end of constant rate stage, then medium-dense soil, lastly the loosest soil. These would be caused by the different amount of water in soil void. Moreover, the smaller dry density would result in greater initial volumetric water content. Checking the relationship between evaporation rate versus instantaneous water content as displayed in Figure 4.8(b), the critical water content is almost same where the evaporation rate starts to decline, they are at around 10% for the three density cases. This result indicates that the soil density has no obvious influence on the evaporation process, which may due to the soil density has little changing of the soil water hydraulic property.

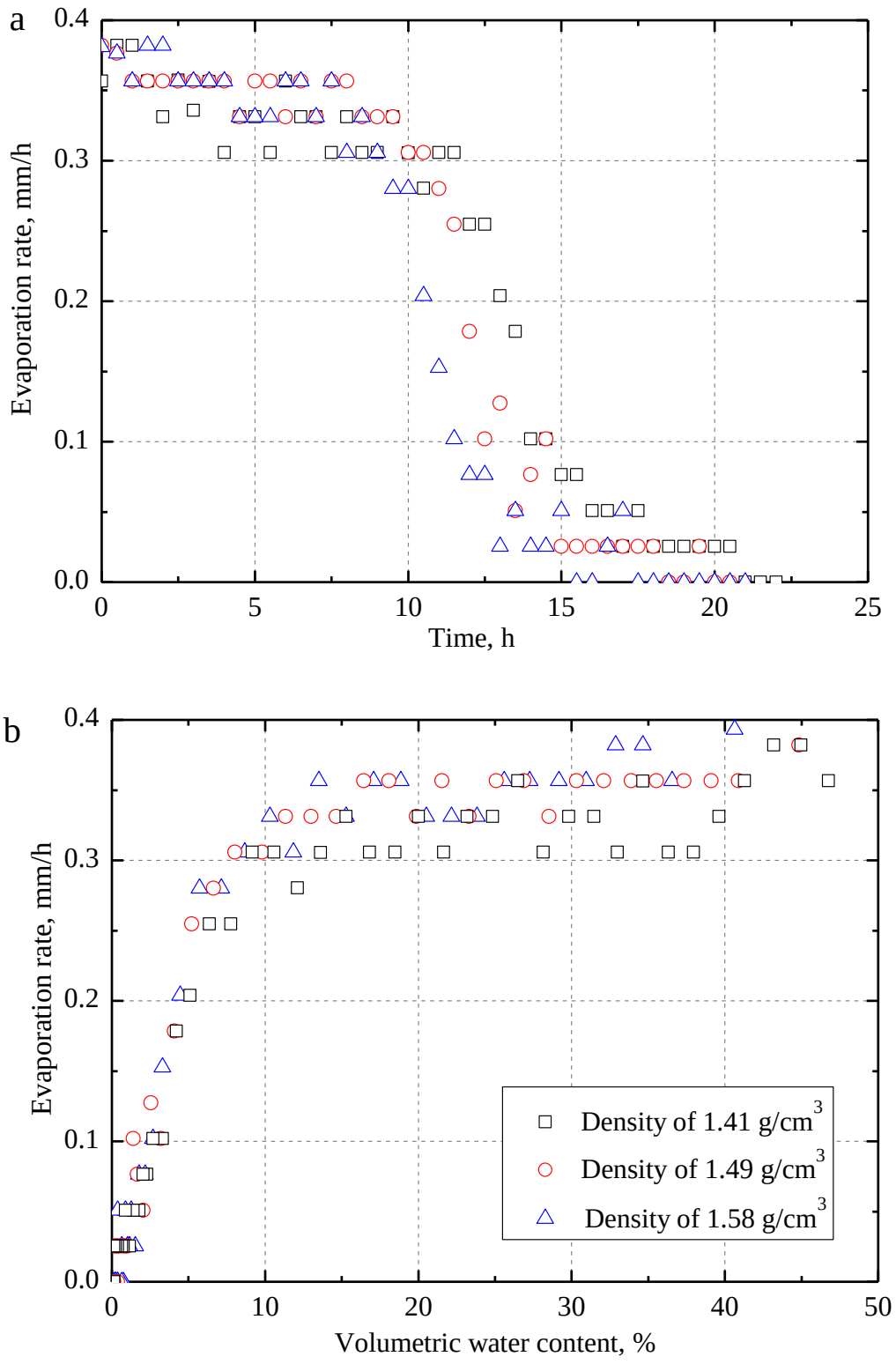

Figure 4.8 Influence of dry density of soil on evaporation rate, (a) evaporation rate versus elapsed time, and (b) evaporation versus soil water content

2. The influence of soil particle size

Three different soil specimens K-3 sand, K-7 sand, and fly ash were selected as the materials of evaporation tests. K-3 and K-7 are coarse and fine silica sand, respectively. Fly ash is a kind of silt soil from the Association of Powder Process Industry and Engineering, Japan. The photograph of these three kinds of soils is presented in Figure 4.9, while the soil properties are summarized in Table 4.1. The particle size distributions of these three soils are shown in Figure 4.10. For the K-3 and K-7 sand cases, the material was firstly packed into the evaporation pan (Φ10 cm, 1 cm thickness), and then the specimen was wetted to saturation using a fine uniform mist of distilled water with appropriate amount. For the case of fly ash, the specimen was saturated by capillary rise method, and then filled into the pan to measure the initial water content of evaporation test. 12 different climate conditions in Table 4.2 were applied to each soil specimen time to time. The mass of soil specimen was continuously monitored every 5 minutes with a solution of 0.1 g until evaporating to completely air-dry state, thus the instantaneous value of evaporation rate and water content could be determined.

Figure 4.11 shows the evaporation rate of these three kinds of soils under C8 condition. The evaporation rate decreases firstly for fly ash, followed by K-7 sand, and finally the K-3 sand, the corresponding time are 7.0 h 8.5 h and 13 h, respectively. It may attribute to the different initial water content for three kinds of soils, it takes longer time to dry out for the specimen with greater initial water content. Evaporation rates of K-7 sand and fly ash show similar tendency that it gradually reduces in stage 2 and then continues at a slow rate. While for K-3 sand, it sharply reduces with no obvious stage 3. It indicates that the restriction to vapor diffusion in soil varies with different soil textures. The result of Figure 4.11(b) shows that the critical water content varies for different soil type, the smaller soil particle size always result in greater critical water content.

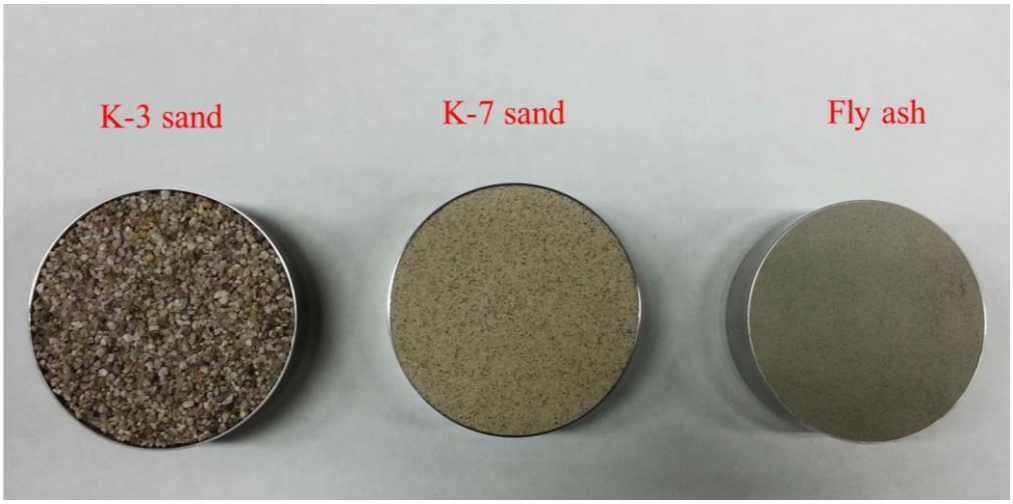

Figure 4.9 Photograph of K-7 sand, K-3 sand and Fly ash

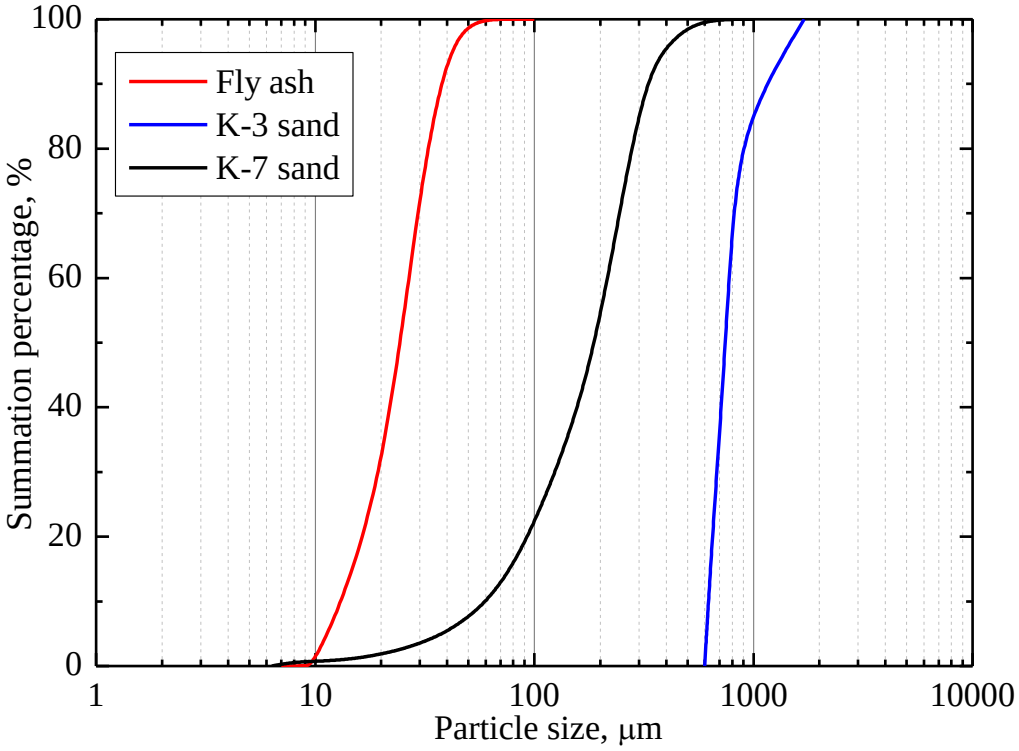

Figure 4.10 Particle size distribution of K-7 sand, K-3 sand and Fly ash

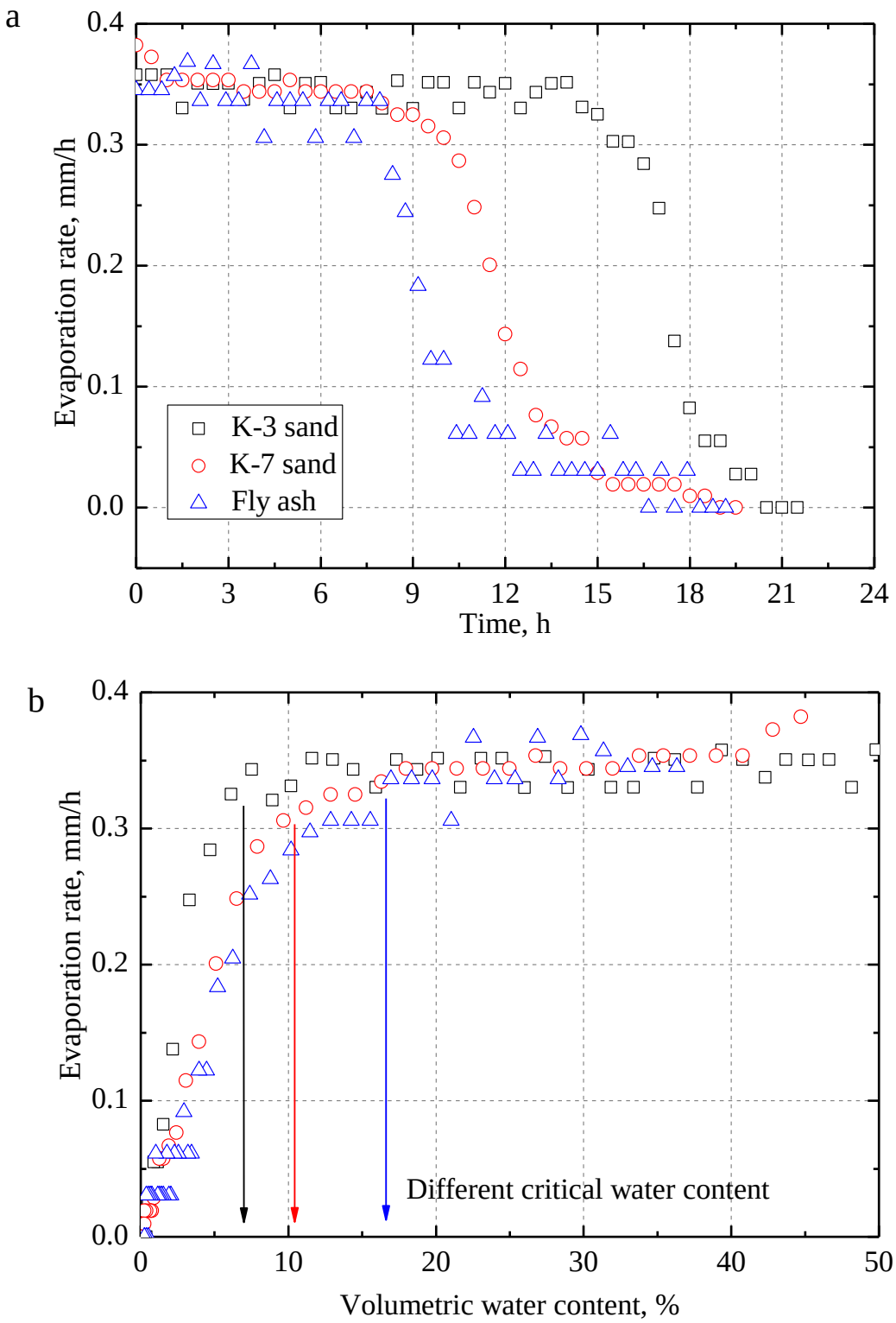

Figure 4.11 Evaporation rate of K-3, K-7 and fly ash under C8 condition versus (a) elapsed time, and (b) soil water content

4.3 THEORETICAL DEVELOPMENT FOR CALCULATING ACTUAL EVAPORATION

In geotechnical field, the potential evaporation (E_p) has been traditionally used to estimate evaporation or evapotranspiration for several decades (Wilson et al., 1997). It can be explicitly determined by absolute meteorological indexes (Penman, 1948). However, it is the actual evaporation (E_a) from soil surface, which is required for design of near ground surface structures. The E_a is generally lower than the potential evaporation except for the beginning of drying process when the soil is nearly saturated and E_a is considered to be nearly equal to E_p. In addition, E_a has not been rationally demonstrated yet due to complex interaction between atmosphere conditions and soil properties.

Figure 4.12 shows the flowchart to determine actual evaporation, the potential evaporation is completely computed from the meteorological variables, while the actual evaporation rate can be evaluated either from calculating the actual vapor pressure of soil surface, soil surface resistance, or the relative evaporation rate. Several literatures in different categories are also shown in Figure 4.12. For the first approach, one equation derived by Philip and de Vries (1957) from thermodynamic laws is usually applied to calculate the actual vapor pressure of soil surface.

$$h_r = \exp(\frac{\psi g}{RT_s}) \tag{4.1}$$

Where, h_r represents the relative humidity at soil surface, ψ is the soil water potential at the soil surface, g is the acceleration of gravity and R is the gas constant for water vapor. The relationship between the h_r and ψ is shown in Figure 4.13. Although this equation connects the soil water property with atmosphere character, and provides an easy way for numerical simulation, this scheme may be invalid, especially when the upper layer is dry. That is to say, the relative humidity in adjacent to the water in soil pore, cannot represent the soil surface humidity (Kondo et al., 1990). At most 1500 kPa is necessary to extract water out of soil from agriculture view, it is obviously not representative when soil is dry. Moreover, result calculated by Philip's formula trends to oscillate between wet and dry soil-moisture regimes because of the sharp gradient of the function.

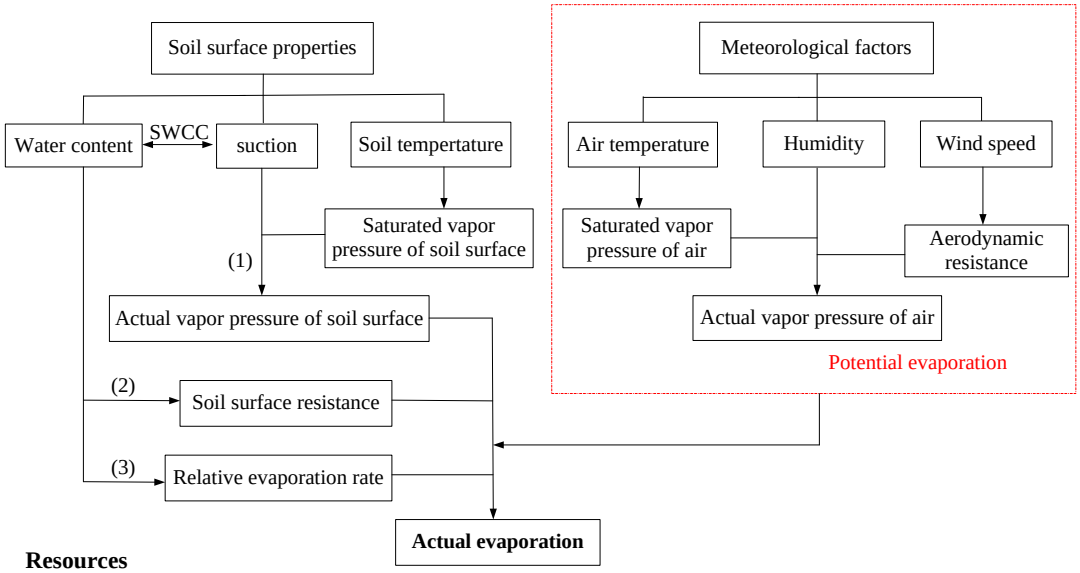

Resources

(1) Staple (1974); Wilson et al. (1997); Konukcu (2007); Fredlund et al. (2010); Fredlund et al. (2011)

(2) Monteith (1981); Camillo and Gurney (1986); van de Griend and Owe (1994); Daamen and Simmonds (1996); Aluwihare and Watanabe (2003)

(3) Barton (1979); Kondo et al. (1990); Mahfouf and Noilhan (1991); Lee and Pielke (1992); Chanzy and Bruckler (1993); Komatsu (2003); Merlin et al. (2011)

Figure 4.12 Flowchart to estimate actual evaporation

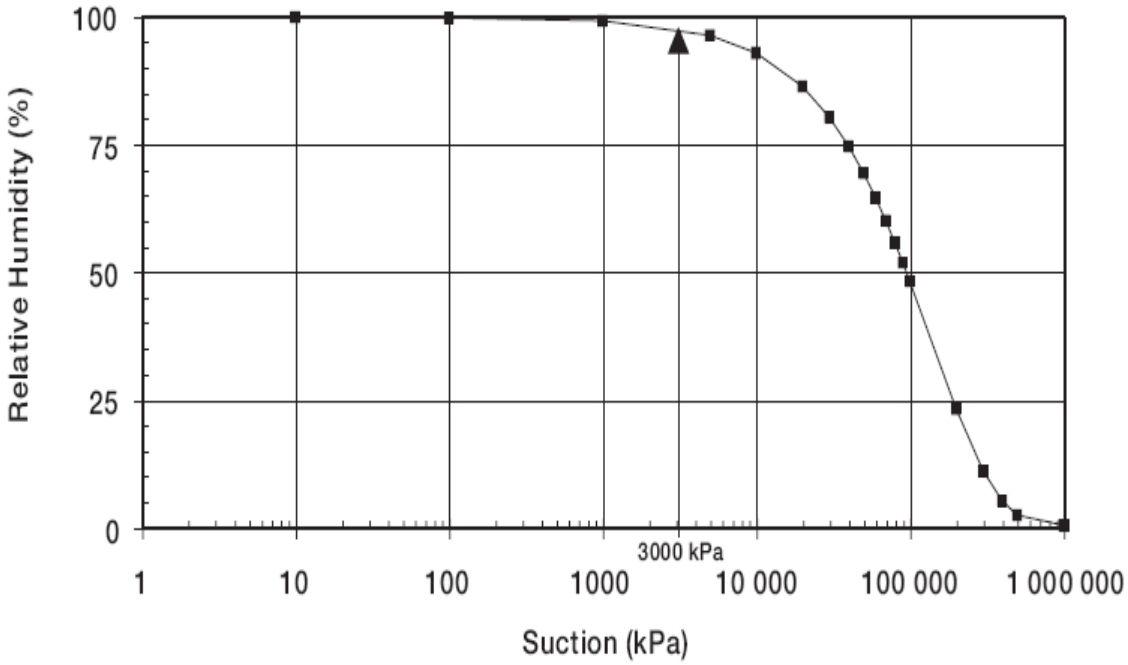

Figure 4.13 Relative humidity of soil surface versus total suction calculated on the basis of Eq.(4.1) (after Wilson et al. 1997)

There are already many previous studies dealing with the use of soil surface water content θ to predict E_a, where θ is related to the relative evaporation ratio of E_a/E_p (Chanzy and Bruckler, 1993). For one approach, E_a/E_p is formulated by a surface resistance r_s that represents the restriction for the diffusion of vapor in soil pore. Many empirical expressions between r_s and θ are available and most studies have documented difficulties with the uniqueness of the resistance formulation (Monteith, 1981; Camillo and Gurney, 1986; van de Griend and Owe, 1994; Daamen and Simmonds, 1996; Aluwihare and Watanabe, 2003). However, every expression has applicable condition; that is to say, it would induce inconsistencies when generalizing r_s to different soil types or different atmosphere conditions (Merlin et al., 2011). Another method is directly expressing E_a/E_p as only a function of soil water content (Barton, 1979; Mahfouf and Noilhan, 1991; Lee and Pielke, 1992), in which the influence of climatic conditions on E_a/E_p was always neglected. Nevertheless, researchers recently found that the E_a and E_p were not affected by the wind speed in the same proportion, thus the relative evaporation ratio is also related to wind speed (Kondo et al., 1990; Chanzy and Bruckler, 1993; Yamanaka, 1997; Komatsu, 2003). This conclusion coincides with the results of Shokri et al. (2008) and Shahraeeni et al. (2012) that evaporation was investigated from pore scale. Although all researchers agree with the dependence of relative evaporation ratio to atmosphere conditions, no clear consensus exists to express E_a/E_p appropriately since no single variable or soil property appears to control ideally (Merlin et al., 2011). Therefore, general relationships applied for a wide range of soil and atmosphere conditions are still lacking.

This section will analyze the relevant variables for determining the evaporation rate. Two approaches are presented to parameterize evaporation from unsaturated soil. The theoretical formulation from aerodynamic view and molecular physics view would be developed.

4.3.1 AERODYNAMIC APPROACH

Evaporation from water surface, E_p is represented by the simple form for mass transfer, as follows

$$E_p = \rho_a \frac{q^*(T_w) - q_a}{r_a} \tag{4.1}$$

where ρ_a is density of air (kg/m^3), q^* is the saturated specific humidity as a function of temperature (kPa/kPa), T_w is temperature of water surface (K). q_a is the specific humidity at a reference level in atmosphere (kPa/kPa); r_a is the aerodynamic resistance to vapor transfer (s/m), it is normally expressed as a function of wind speed. The calculation of the aerodynamic resistance, r_a assumes a reference crop height of 0.12 m and a standardized height for wind speed, temperature, and humidity measurement of 2 m above the surface, and follows a logarithmic wind speed profile. Several equations exist to estimate aerodynamic resistance, as referred to Monteith (1973), Viney (1991), Liu (2007) and so on.

It is supposed that the evaporation from soil surface consists of two processes (Figure 4.14). In process I, water vapor transports by molecular diffusion from evaporating surface to soil surface. Here, the evaporating surface is defined as the physical boundary between continuous state and inconsecutive state of free water in soil pore. In process II, water vapor transfers from soil surface to the atmosphere by laminar or turbulent flow.

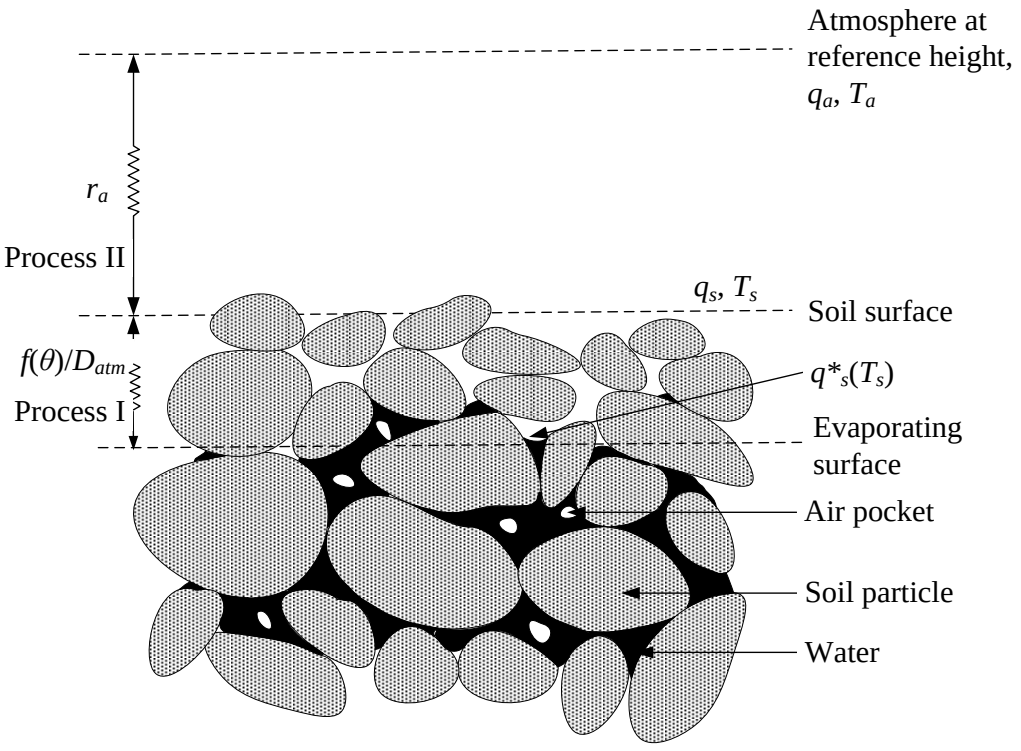

Figure 4.14 Schematic illustration of the resistance to vapor diffusion from soil pores to atmosphere

The vapor diffusion in process I is assumed to be controlled only by molecular diffusion. The expression can be referred to Kondo (1990), as follows

$$E_a = \rho_a \frac{q^*(T_s) - q_s}{f(\theta) / D_{atm}} \tag{4.2}$$

where $q^*(T_s)$ is the saturated specific humidity at the evaporating surface with the soil temperature of T_s. q_s is the specific humidity of air at the soil surface (kPa/kPa); $f(\theta)/D_{atm}$ represents the resistance to vapor diffusing from the interior of soil pore to the surface. $f(\theta)$ is a function of soil water content that indicates the soil water state, it represents an undetermined term, D_{atm} is the molecular diffusivity of vapor in air (m^2/s).

The fluxes of two processes are equal due to conservation of mass, the vapor flux in the process II can be represented by

$$E_a = \rho_a \frac{q_s - q_a}{r_a} \tag{4.3}$$

Combining Eqs. (4.2) and (4.3) and eliminating q_s, the E_a can be expressed as

$$E_a = \rho_a \frac{q^*(T_s) - q_a}{r_a + \frac{f(\theta)}{D_{atm}}} \tag{4.4}$$

With not considering the temperature influence and assuming that T_w equals to T_s, then the relative evaporation ratio can be calculated by Eqs. (4.1) and (4.4), as follows

$$\frac{E_a}{E_p} = \frac{1}{1 + \frac{f(\theta)}{D_{atm} r_a}} \tag{4.5}$$

Since the D_{atm} is a constant for certain air temperature, we rewrite the Eq. (4.5) by neglecting the influence of temperature:

$$\frac{E_a}{E_p} = \frac{1}{1 + F(\theta, r_a)} \tag{4.6}$$

in which, $F(\theta, r_a)$ represents an undetermined function and may be established empirically, these formulas show that the relative evaporation ratio is depends on the soil water content θ and aerodynamic resistance r_a.

4.3.2 MOLECULAR PHYSICS APPROACH

Figure 4.15 shows coupling between evaporative surface and ambient air;

pore-scale evaporation takes place from discontinuous menisci on the surface supplied by capillary connected pathways underneath. Advection-diffusion process in the boundary layer (BL) transports vapor and controls demand above menisci at surface.

Figure 4.16 shows the partially wetted surface, the void of soil is sets of parallel pipes with radius of r, the spacing of them is $2l$, the extension of the wet patches shall be small compared to the thickness of the viscous sublayer so that the shape of their surface are is of minor importance. The vapor pressure at the gas-liquid interface is e^*. The vapor pressure is e_l from the center of the wet patches with distance l, the external vapor pressure is e_a.

We assume that the thickness of the viscous sublayer δ is always much larger than the mean free path of the gas molecules Λ, which is a realistic assumption for normal (or higher) pressure, The radius of the wet patches r, however, as well as their distance $2l$ may be larger or smaller than Λ. Therefore, Stefan diffusion applies within the δ-region, while Knudsen diffusion and Stefan diffusion in series apply to the l-r region. Eventually diffusion in the l-r region and in the δ-region occurs in series. Schlunder (1988) and Chen (2002) obtained the vapor pressure ratio (e^*-e_l)/(e_l- e_a) the following expression

$$\frac{e^*-e_l}{e_l-e_a}=\varsigma=\frac{1}{2}\frac{\Lambda}{\delta}\frac{r}{\Lambda}\frac{1}{s_1}\left(\frac{2\Lambda}{r}+\frac{1}{1+\Lambda/r}-\sqrt{\frac{4s_1}{\pi}}\right) \tag{4.7}$$

Where the s_1 is the relative wetted surface area

$$s_1=\frac{\pi}{4}\left(\frac{r}{l}\right)^2 \tag{4.8}$$

Since the drying rate from a fully wetted surface E_p is proportional to the vapor pressure difference e^*-e_l, the relative evaporation rate E_a/E_p is given by

$$\frac{E_a}{E_p}=\frac{1}{1+\varsigma} \tag{4.9}$$

Here, the ς equals to $F(\theta, r_a)$ in Eq. (4.6). Obviously, the relative evaporation rate E_a/E_p depends on three independent variables

$$\frac{E_a}{E_p}=f\left(\frac{\Lambda}{\delta},\frac{r}{\Lambda},s_1\right) \tag{4.10}$$

Where

$$\frac{\Lambda}{\delta}=\frac{\text{length of mean free path}}{\text{thickness of viscous sublayer}}$$

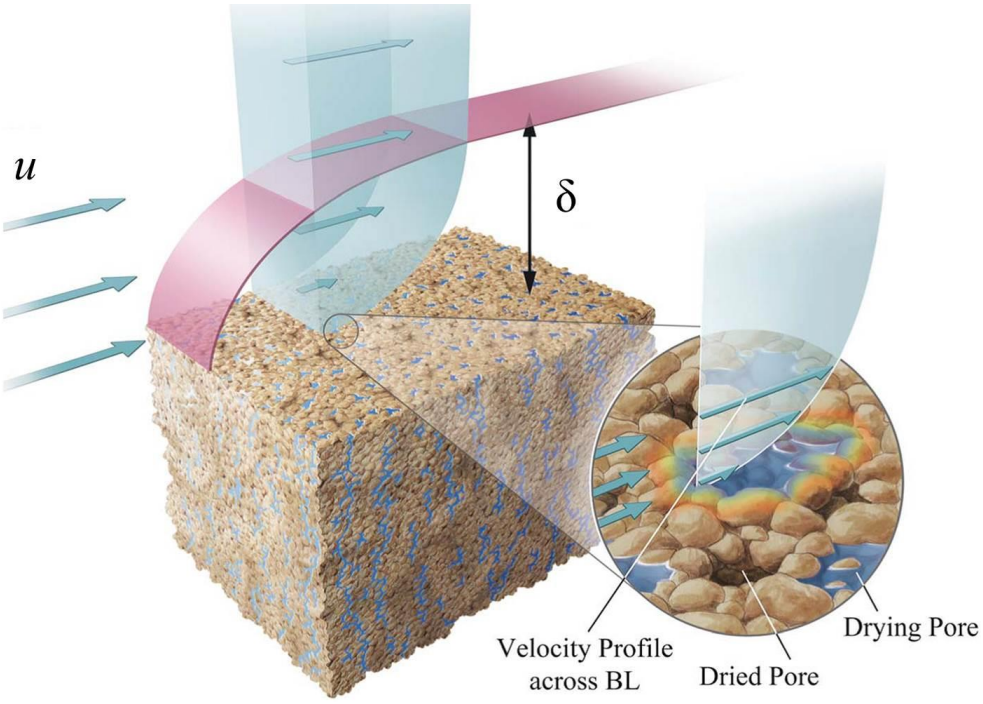

Figure 4.15 Coupling between evaporative surface and ambient air with velocity *u*, the boundary layer (BL) has a thickness of *δ* (after Shahraeeni et al., 2012)

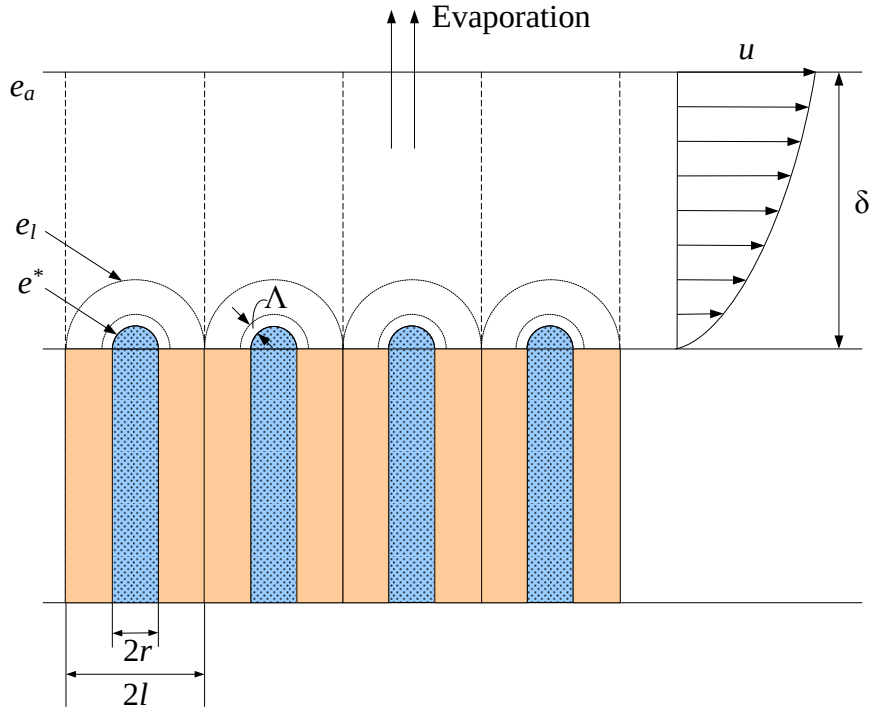

Figure 4.16 Modeling of a partially wetted surface from which evaporation takes place into a gas stream. *δ* is thickness of the viscous sublayer, *r* is radius of the wet patches, *l* is distance of the wet patches

$$\frac{r}{\Lambda} = \frac{\text{radius of wet patches}}{\text{length of mean free path}}$$

$$s_1 = \text{relative wetted surface area}$$

At normal pressure and temperature, the magnitude of the mean free path Λ is in the order of 10^{-7} m, while the thickness of the viscous sublayer δ is about 10^{-3} m. For the evaporation from soil surface, the radius of wet patches is greater than the length of mean free patch; hence, the Eq. (4.7) has an asymptotic solution:

$$\lim_{\Lambda/r \to 0} \varsigma = \frac{2}{\pi} \frac{r}{\delta} \sqrt{\frac{\pi}{4s_1}} \left(\sqrt{\frac{\pi}{4s_1}} - 1 \right) \tag{4.11}$$

Eq. (4.11) indicates that E_a/E_p is related to the wind speed (related to the thickness of the viscous sublayer δ), soil type (related to r) and the soil water content (related to s_1).

Although Eqs. (4.9) and (4.11) give the theoretical formulation of E_a/E_p, its value is still impossible to be determined because δ and r cannot be directly measured. We include a variable the critical water content θ_c, which indicates the end of constant rate stage. Thus E_a equals to E_p when the volumetric water content is greater than θ_c. For the case of θ smaller than θ_c, we should evaluate the relationship among θ_c and soil type and wind speed.

4.4 PARAMETERIZATION OF SOIL EVAPORATION

4.4.1 RELATIONSHIP BETWEEN CRITICAL WATER CONTENT AND SOIL TEXTURE

Based on the evaporation tests described in section 4.2.2 that three kinds of soil were evaporated to dry under 12 different conditions. The empirical formulation between θ_c and soil type and wind speed aims to be determined based on the experiment result. It should be noted that the evaporation pan that contained distilled water was tested to measure the E_p before measuring the E_a under each condition.

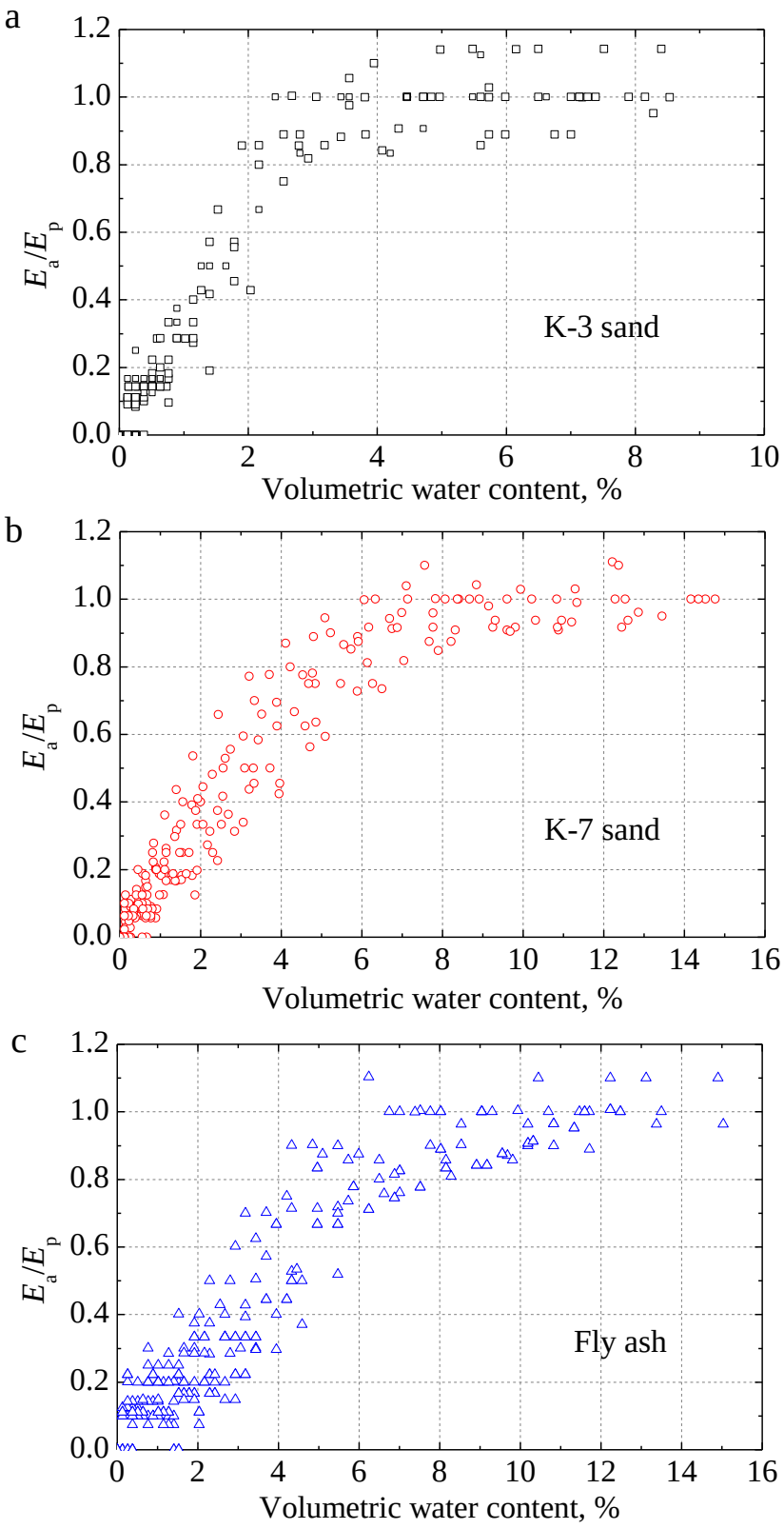

Figure 4.17 The relative evaporation rate versus volumetric water content for (a) K-3 sand, (b) K-7 sand and (c) Fly ash

The scatter diagram of E_a/E_p versus volumetric water content under the 12 climatic conditions for each soil is shown in Figure 4.17. Since the value of E_a/E_p is close to 1.0 at stage 1, it is mainly shown for stage 2 and stage 3 aiming to distinguish the critical water content at each condition. The three stages of the bare soil evaporation appear in these figures: Stage 1, as the soil is wet, The E_a/E_p is equals to 1; for Stage 2, in which the soil surface become dry, E_a is a rapidly decreasing propotion of E_p; finially for Stage 3 in which the soil is dry, E_a/E_p is very low and approaching zero. E_a/E_p starts to decline at different water content for various soil type, it is the critical value that from 2.5% to 6%, 6% to 10% and 6% to 12% for K-3 sand, K-7 sand and fly ash, respectively. It appears that finer soil usually results in higher critical water content. Such a soil effect is mainly due to the hydraulic properties and the retention curve of the soil, only when the proper variable is chosen to access these soil parameter, prediction of the relationship between E_a/E_p and soil texture appears to feasible. Moreover, the knowledge of water content seems to be insufficient. For instance, if we consider the water content at 4% of K-7 sand (Figure 4.17(b)), E_a/E_p changes from 0.4 to 0.9 that corresponds to roughly half range. Similar result can be observed for the other two specimens. This means that the surface water content is unable to describe accurately the decrease in the E_a/E_p ratio within a significant range of values. Result emphasizes the need for additional variables besides water content and soil texture to improve the expression.

4.4.2 Relationship between critical water content and aerodynamic resistance

From the theoretical derivation, Eqs. (4.6) and (4.11) show the formula of E_a/E_p with an undetermined function that is dependent on aerodynamic resistance r_a, it leads the authors to experimentally investigate the expression. Komatsu (2003) pointed out that wind speed can only be characterized in the wind tunnel, while aerodynamic resistance r_a shows relatively small fluctuation comparing to the wind speed, which is almost solely determined by wind speed. This suggests that r_a can robustly parameterize evaporation rate even in a fluctuating environment. It has advantage for taking this change in analysis the influent of wind speed. In this study, aerodynamic resistance was determined from the measured value of E_p.

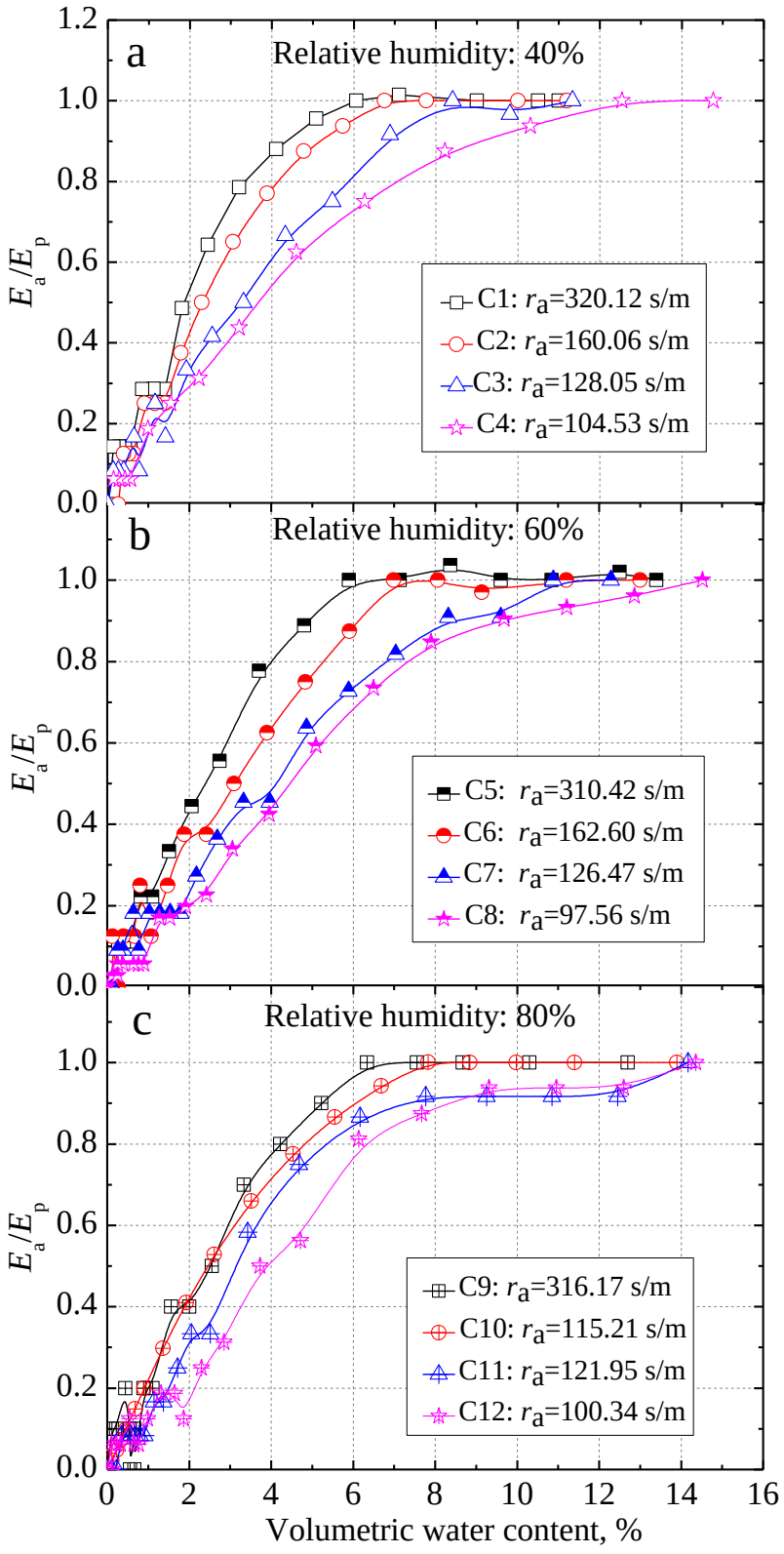

Figure 4.18 The relative evaporation rate versus volumetric water content for K-7 sand at the conditions of (a) C1-C4; (b) C5-C8 and (c) C9-C12

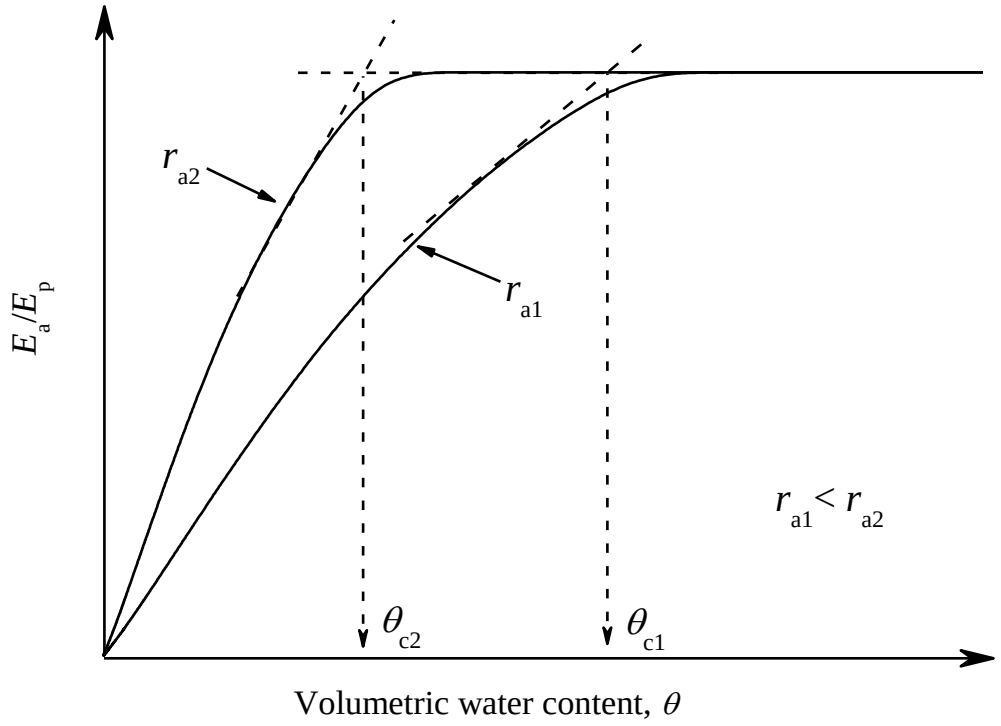

Figure 4.19 Schematic illustration of aerodynamic resistance influence on relative evaporation rate

The result of K-7 under C1-C4, C5-C8 and C9-C12 conditions is presented in Figure 4.18. The results verify the theoretical deduction that greater r_a results in higher E_a/E_p at stage 2 and 3, but the influence of r_a on E_a/E_p is weak at stage 1 where evaporation is mainly controlled by soil water content. In other words, it indicates that an increase in r_a always induces a decrease in E_p while E_a does not vary or decreases at stage 2 and 3. This is also the reason why the methods relating E_a/E_p directly to water content cannot give accurate simulation result.

For the sake of clear description of evaporating curve, the authors define a critical water content θ_c where E_a/E_p starts to decline from 1.0. And Figure 4.19 schematically demonstrates the influence of r_a on critical water content θ_c. θ_{c1} and θ_{c2} present the threshold between stage 1 and stage 2 corresponding to evaporating curves at r_{a1} and r_{a2} condition. It suggests that higher aerodynamic resistance results in lower critical water content. In other words, the wins speed controls the shift of the evaporative curve. This is reasonable because the non-uniformity of vertical distribution of water is larger when the wind speed is higher. An increase in wind speed or a decrease in aerodynamic resistance always induces an increase in E_p,

while E_a does not vary or decrease in the drier case. Thus the wind speed may affect the E_a/E_p significantly.

4.4.3 FORMULATION TO DETERMINE SOIL EVAPORATION

The above experiment result and analysis indicates that it is essential to formulate E_a/E_p considering the influence of soil texture and aerodynamic resistance. Since E_a/E_p has different feature at stage 1 from that at stage 2 and 3, it is feasible to clearly define the critical water content and adopt a piecewise function to describe the evaporation curve. For stage 1, E_a/E_p is nearly 1.0 that is uninfluenced by water content and r_a, hence the $F(\theta,r_a)$ in Eq.(4.6) is considered to be 0. For simulating the evaporating curves at stage 2 and 3, a simple empirical formula of $F(\theta,r_a)$ is proposed as

$$F(\theta, r_a) = \frac{\theta_c}{\theta} - \sqrt{\frac{\theta_c}{\theta}} \tag{4.12}$$

Where the θ_c is the critical water content, it would be related the wind speed and soil texture. To evaluate the performance of proposed formula in simulating evaporative curve in stage 2 and 3, the θ_c is clearly assigned from experiment data for each condition. As the $F(\theta,r_a)$ can also be definitely determined from Eq. (4.6) based on the measured value of E_a/E_p. Figure 4.20 shows the comparison between the estimated values of $F(\theta,r_a)$ by Eq.(4.12) versus that determined from Eq. (4.6). Good agreement is found for the values determined from two approaches in the cases of K-3, K-7 and fly ash. It is observed that the value tends to disperse for the value of $F(\theta,r_a)$ at about 10, where the relative evaporation ratio is already very low and the effect of error should be neglected. Therefore, it is rational to adopt the empirical formula of Eq. (4.12) to fit the evaporation curve at stage 2 and 3.

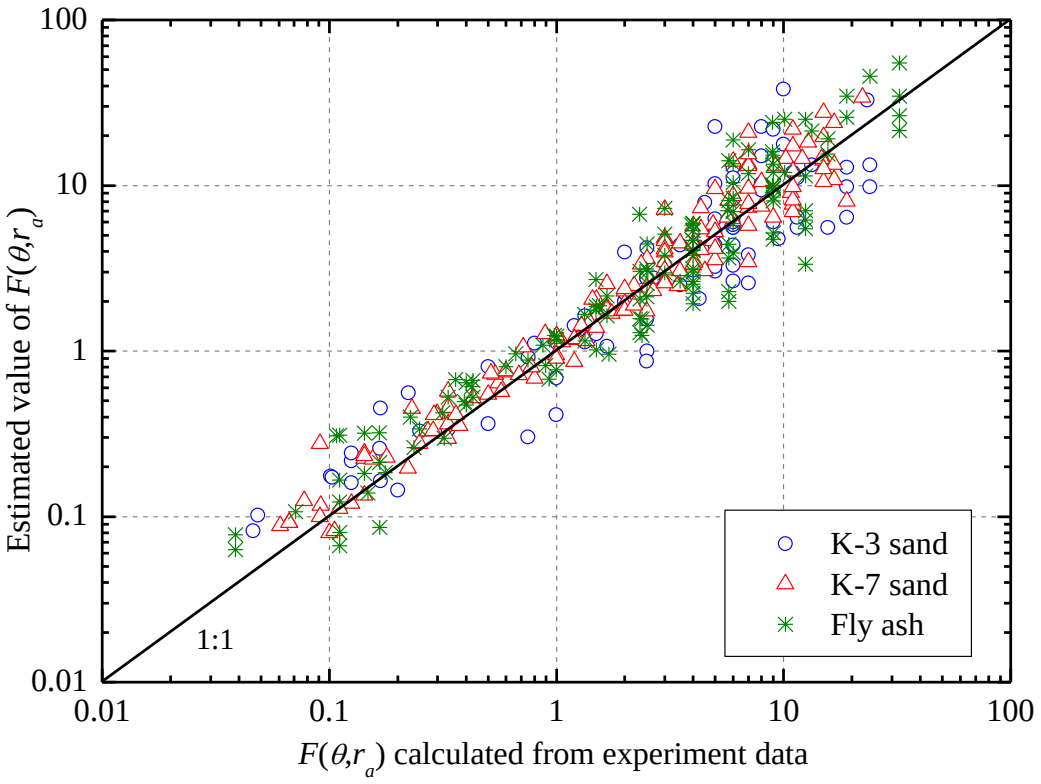

Figure 4.20 Scatter diagrams of estimated $F(\theta,r_a)$versus the value calculated from experiment data for K-3 sand, K-7 sand and fly ash

Here, a new parameter m defined as the ratio of critical water content to volumetric water content is introduced, as following,

$$m = \frac{\theta_c}{\theta} \tag{4.13}$$

The equation for predicting relative evaporation ratio can be expressed by combining the Eqs. (4.6), (4.12) and (4.13):

$$\frac{E_a}{E_p} = \begin{cases} 1 & m < 1 \\ \dfrac{1}{1+m-\sqrt{m}} & m \le 1 \end{cases} \tag{4.14}$$

Based on the former analysis, the parameterization of soil evaporation would be expressed if the relationship among θ_c soil texture and aerodynamic resistance is formulated. Here we adopt the field capacity (θ_{fc}) to eliminate the dependence on the soil texture, which is referred to Lee and Pielke (1992) and Milly (1992). The value of θ_{fc} for each soil type is modified from Lee and Pielke (1992) as listed in Table 4.3, which is defined as either a soil water potential of -33 kPa or a hydraulic

conductivity of 0.1 mm/d.To investigate the relationship between θ_c and r_a, the value of θ_c/θ_{fc} of three soil samples is plotted versus $1/r_a$ in Figure 4.21 together with the result from some literatures. It is found that θ_c/θ_{fc} among different soil types linearly depends on $1/r_a$, and the empirical relation is expressed as

$$\frac{\theta_c}{\theta_{fc}} = \frac{49.83}{r_a} + 0.30 \tag{4.15}$$

This equation is obtained from all kinds of soils including coarse sand, fine sand, silt, loam and clay. It seeks to be the basis of systematic calculation of evaporation from various soil textures under different atmosphere conditions.

Table 4.3The value of field capacity for several soils

Soil type	θ_{fc}
Coarse sand	0.065
Fine sand	0.123
Sandy loam	0.195
loam	0.240
Silt	0.152
Sandy clay	0.310
Silty clay	0.370
Clay	0.367

Modified from Lee and Pielke (1992)

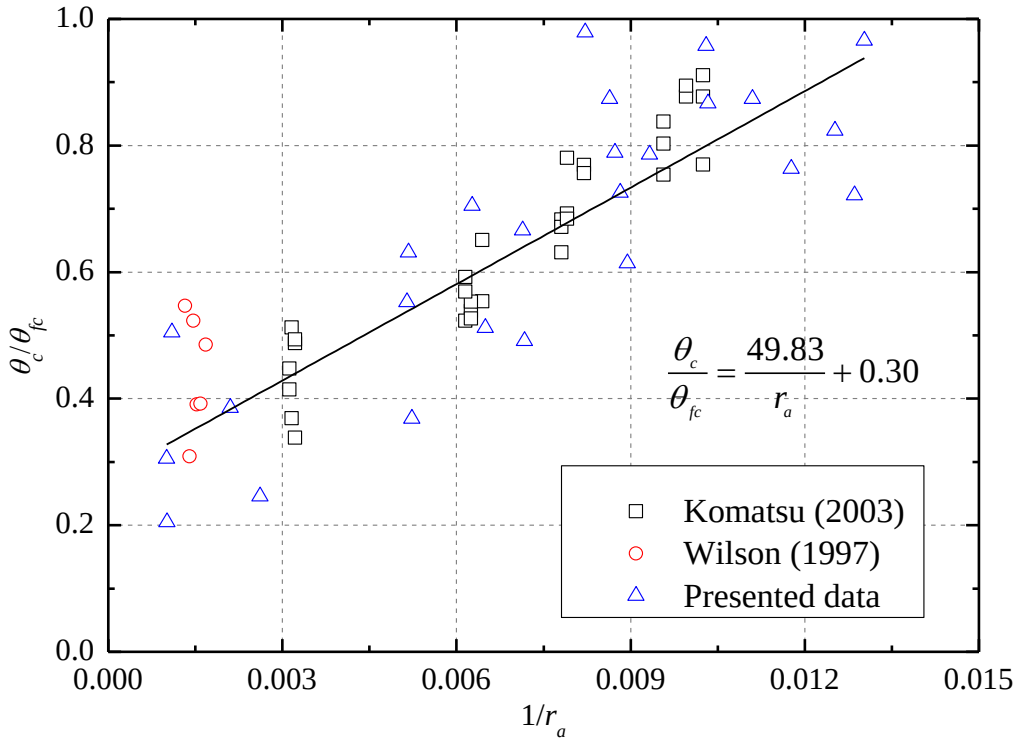

Figure 4.21 Relationship between critical water content and aerodynamic resistance

Combining Eqs. (4.13) and (4.15), and eliminating θ_c, m can be determined as

$$m = (\frac{49.83}{r_a} + 0.30)\frac{\theta_{fc}}{\theta} \tag{4.16}$$

Therefore, the value of E_a/E_p can be formulated by Eqs. (4.14) and (4.16). This model needs three input parameters: θ can be measured from the top 1cm soil, r_a can be determined by the monitored wind speed, and θ_{fc} is a constant value for specified soil texture. Since no fitting parameter exists in the model that varies with soil texture, it is easy to apply. Figure 4.22 shows the value of E_a/E_p for the three kinds of soils under C5-C8 conditions, respectively, each symbol denotes an experimental value, and the solid lines express Eqs. (4.14) and (4.16). The simulation result agrees well with the observations expect for the fly ash at the extremely dry condition the value of E_a/E_p already becomes very small for the stage 3, thus the error could be neglected. Above all, the present model can capture the critical point and reasonably express the slope of evaporating curve.

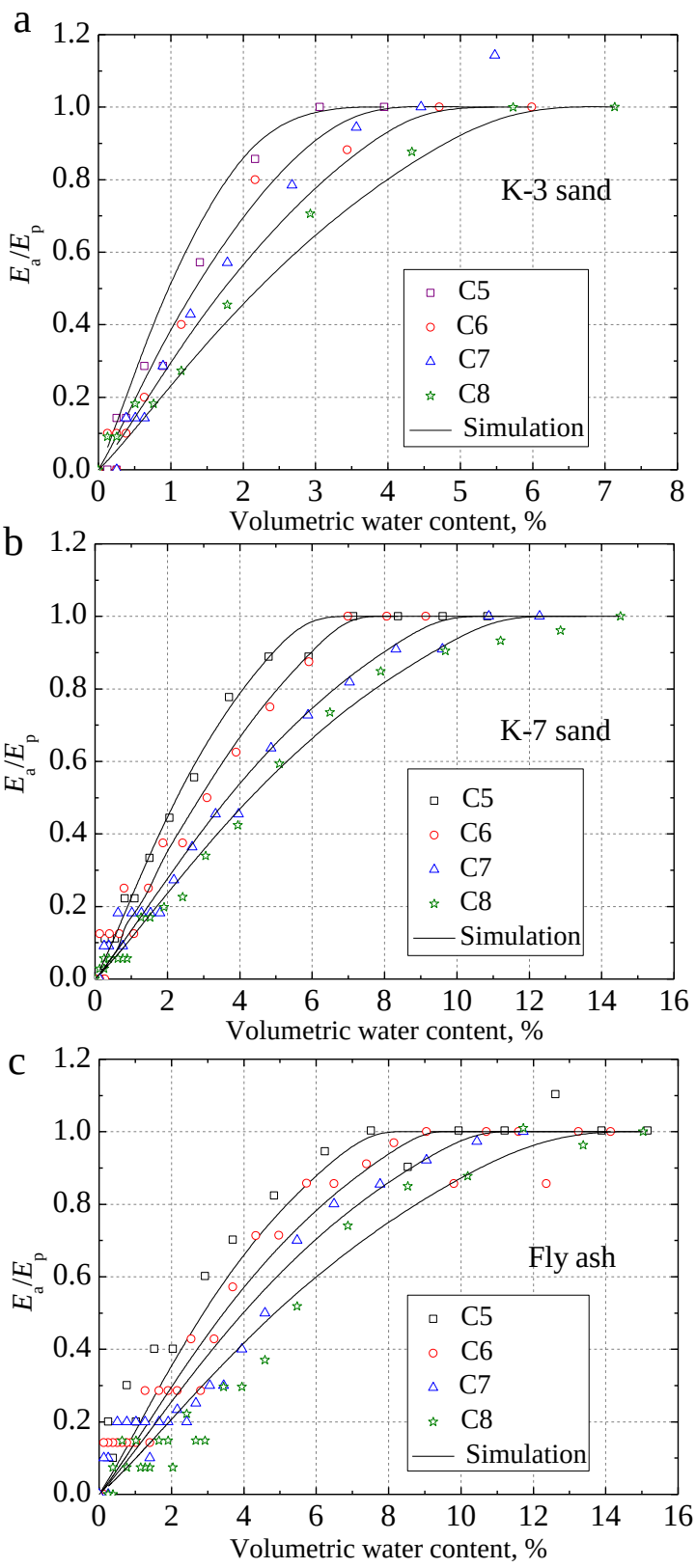

Figure 4.22 Comparison between estimated relative evaporation rate and observation value for (a) K-3 sand, (b) K-7 sand and (c) fly ash

It should note that this paper discusses only the properties of soil surface that control evaporation process, and the thin soil specimen in the evaporation test is regarded as element section without considering the hydraulic conductivity in soil. For the analysis of evaporation from soil with enough thickness, it's essential to simulate the flow processes below soil surface, at this condition, the proposed model in this paper is recommended to formulate the boundary of soil-atmosphere interaction.

4.5 SUMMARY

This chapter mainly focuses on the methodology for determining soil surface evaporation. The influence factors of soil evaporation were separately evaluated by the evaporation test, then the theoretical formulation of the actual evaporation rate is derived from the approaches of aerodynamic approach and molecular physics approach, finally the parameterization of the soil evaporation is proposed with its verification from experimental result. The conclusions can be drawn as follows,

(1) Higher atmosphere temperature results in the faster reduction of mean water content and shorter time for reaching the residual stage, time would shorten 4% in average for temperature increasing 1 °C. Evaporation rate always linearly increases causing by an increase in wind speed, However, average gradients of the increase is related to relative humidity. It would not be a linear relationship between evaporation rate and relative humidity, an inflection point properly exists at about 60%.

(2) Soil structure (dry density) has little influence on the evaporation rate, while particle size of soil affects the diffusion of vapor in soil and thus the evaporation process, soil with larger particle size can lasts longer time for stage 1.

(3) Theoretical derivation of E_a/E_p from aerodynamic approach and molecular physics approach shows that the water content alone cannot be identified as the unique independent variable to control the evaporation from all soil surfaces. Additional parameters for soil texture and wind speed must be taken into consideration as well. However, an undetermined function $F(\theta,r_a)$ exists in aerodynamic approach, and viscous sublayer thickness δ and soil pore size r in molecular physics approach are not easily determined.

(4) A parameterizing method of evaporation is presented by defining a critical water content θ_c and setting up the formulation of θ_c for different soil textures and wind speeds. Three easily measured indexes is needed in this model: the moisture of

top 1cm soil, aerodynamic resistance (wind speed), and field capacity as a constant for specified soil texture. Although this parameterization is empirical form, its accuracy for estimating evaporation is evaluated that it agrees well with the experimental data for different soil types.

(5) Future studies should concentrate on verifying the proposed formulation for various soil textures and climate conditions. Moreover, the transport of multiphase below soil surface is essential for predicting the surface soil water content.

REFERENCE

Aluwihare, S. and Watanabe, K. (2003): Measurement of evaporation on bare soil and estimating surface resistance. Journal of Environment Engineering, 129(12), 1157-1168.

Barton, I., J. (1979): A parameterization of the evaporation from nonsaturated surfaces. Journal of Applied Meteorology, 18, 43-47.

Camillo, P. J., and Curney, R. J. (1986): A resistance parameter for bare soil evaporation models. Soil Science, 141, 95-105.

Chanzy, A. and Bruckler, L. (1993): Significance of soil surfaces moisture with respect to daily bare soil evaporation. Water Resources Research, 29(4), 1113-1125.

Chen, X.D. (2002): On the characteristic drying rate approach to correlating experimental results of the drying of moist porous materials, The Canadian Journal of Chemical Engineering. 80, 984-90.

Daamen, C.C., and Simmonds, L.P. (1996): Measurement of evaporation from bare soil and its estimation using surface resistance. Water Resources Research, 32, 1393-1402.

Derjagiun, B.V., Kasasev, V.V., Khromova, E.N. (1986): Thermal expansion of water in fine pores. Journal of Colloid and Interface Science, 106, 586-587.

Fredlund, D. G., Vu, H. Q., Stianson, J. (2010): Engineering protocols for the assessment of the net moisture flux at the ground surface, Geotechnical Engineering Journal of the SEAGS&AGSSEA, 4(4), 1-11.

Fredlund, M.D., Zhang, J.M., Tran, D., and Fredlund, D.G. (2010): Coupling heat and moisture flow for the computation of actual evaporation. Procedings of 2011 Pan-Am CGS Geotechnical Conference.

Hanks, R.J., and Woodruff, N.P. (1958): Influence of wind on water vapor transfer

through soil, gravel, and straw mulches. Reprinted from Soil Science, 86(3), 160-164.

Komatsu, T. S. (2003): Towards a robust phenomenological expression of evaporation efficiency for unsaturated soil surfaces. Journal of Applied Meteorology, 42, 1330-1334.

Kondo, J., Saigusa, N., and Sato, T. (1990): A parameterization of evaporation from bare soil surface. Journal of Applied Meteorology, 29,385-389.

Konukcu, F. (2007):Modification of the Penman method for computing bare soil evaporation. Hodrological Processes, 21, 3627-3634.

Lee, T. J., and Pielke R. A. (1992): Estimating the soil surface specific humidity. Journal of Applied Meteorology, 31, 480-484.

Liu, S.M., Lu, L., Mao, D., and Jia, L. (2007): Evaluating parameterizations of aerodynamic resistance to heat transfer using field measurements. Hydrology Earth System Science, 11, 769-783.

Mahfouf, J.F., and Noilhan J. (1991): Comparative study of various formulations of evaporation from bare soil using in situ data. Journal of Applied Meteorology, 30, 1354-1365.

Merlin, O., Bitar, A. A., Rivalland, V., Beziat, P., Ceschia, E. and Dedieu, G. (2011): An analytical model of evaporation efficiency for unsaturated soil surfaces with an arbitrary thickness. Journal of Applied Meteorology and Climatology, 30, 1354-1365.

Monteith, J. L. (1973): Principles of Environmental Physics, Arnold, Paris.

Monteith, J. L. (1981): Evaporation and surface temperature. Quarterly Journal of the Royal Meteorological Society, 107, 1-27.

Milly, P. C.D. (1992): Potential evaporation and soil moisture in general circulation models. Journal of Climate, 5(3), 209-226.

Penman, H. L. (1948): Natural evaporation from open water, bare soil and grass. Proceeding of the Royal Society of London, 193, 120-145.

Philip, J. R., de Vries, D. A. (1957): Moisture movement in porous material under temperature gradients, Transactions of the American Geophysical Union, 38,222-232.

Schlunder, E.U. (1988): On the mechanism of the constant drying rate period and its relevance to diffusion controlled catalytic gas phase reactions. Chemical Engineering Science, 43(10), 2685-2688.

Shahraeeni, E., Lehmann, P., and Or, D. (2012): Coupling of evaporative fluxes from

drying porous surfaces with air boundary layer: Characteristics of evaporation from discrete pores. Water Resources Research, 48, W09525, doi:10.1029/2012WR011857.

Shokri, N., Lehmann, P., Vontobel, P., and Or, D. (2008): Drying front and water content dynamics during evaporation from sand delineated by neutron radiography. Water Resources Research, 44, W06418, doi:10.1029/2007WR006385.

Staple, W.J. (1974): Modified Penman equation to provide the upper boundary condition in computing evaporation from soil. Soil Science Society of America Proceedings 38, 837- 839.

Van de Griend, A. and Owe, M. (1994): Bare soil surface resistance to evaporation by vapor diffusion under semiarid conditions. Water Resource Research, 30(2), 181-188.

Viney, N. R.(1991): An empirical expression for aerodynamic resistance in the unstable boundary layer, Boundary-Layer Meteorology., 56, 381–393.

Wilson, G. W., Fredlund, D. G., and Barbour, S. L. (1997): The effect of soil suction on evaporative fluxes from soil surfaces. Canadian Geotechnical Journal, 34, 145-155.

Yamanaka, T., Takeda, A. and Sugita, F. (1997): A modified surface-resistance approach for representing bare-soil evaporation: wind tunnel experiments under various atmospheric conditions. Water Resources Research, 33(9), 2117-2128.

CHAPTER 5

ANALYTICAL EVALUATION OF WATER CONTENT DISTRIBUTION DURING EVAPORAITON

5.1 INTRODUCTION

The phenomenon of evaporation in natural unsaturated soils is an important element in the hydrologic cycle. Time and space variability of evaporation variables such as water content, given certain soil properties, soil-water physical relationship; boundary conditions; and initial conditions are necessary in many applications, especially for the assessment of soil water practices in arid and semi-arid region (Serrano, 1998). On the other hands, evaporation and water redistribution in soil can exist simultaneously and detract from each other, thus the soil-atmosphere is a heavily coupled system. Efficient modeling of this soil-atmosphere interaction in unsaturated zone remains a significant challenge is the disciplines of hydrology, meteorology and environmental engineering.

The space and time evolution of the soil water content in an unsaturated medium is described by the Richards' equation (Richard, 1931). This equation is highly nonlinear because of the dependence of both hydraulic conductivity and the matric suction on soil water content. Therefore, several numerical routines have been developed to solve the Richards' equation with numerical schemes. However, numerical simulation usually requires sophisticated algorithms to overcome convergence and mass conservation problems (Yuan and Lu, 2005). It is well recognized that analytical of differential equations describing physical problems provide general insights and concisely identify the relationship among the variables of the studied problems, allowing rational approximations and simplification,

Therefore, although numerical methods are powerful in solving complex nonlinear problems, analytical solutions maintain their utility and can also provide a useful check to numerical procedures.

In this chapter, analytical solution is developed for one-dimensional evaporation process. Based on some assumptions and linearization of Richards' equation, the analytical model are set up for two evaporation problems, including the evaporation process without water table which the soil domain is considered as infinite, evaporation process with water table. Then the column experiments are conducted to verify the proposed model. Finally, the parameter study is carried out to understand the influence of hydraulic properties and atmosphere condition on evaporation mechanism and hen on the soil water distribution in underground system.

5.2 ANALYTICAL SOLUTION OF RICHARDS' EQUATION

5.2.1 BASIC ASSUMPTION

The following assumptions are made in order to derive the equations which describe soil water dynamic during evaporation:

(1) Water movement in liquid form during evaporation happens under isothermal conditions.

(2) The soil is homogenous, thus the flow of liquid water in soil is due to the gradient of matric suction or water content, the osmotic pressure is neglected.

(3) Gardner's (1959) analysis showed good agreement between prediction based on flow equations that neglected the vapor transport mechanism and laboratory measurements of drying column, which provides the support for the assumption that vapor transmission of water through the soil profile is not considered into.

(4) Hysteresis in the relations between the matric suction and the soil water content is not taken into account.

5.2.2 RICHARDS' EQUATION

The Richards' equation is a general partial differential equation describing water flow in unsaturated, non-swelling soils with the matric suction as the single dependent variable (Ghotbi, 2011). There are generally three main forms of Richards' equation presented in the literature namely the mixed formulation, the h-based formulation and the θ-based formulation, where h is the hydraulic water head in

water phase and θ is the volumetric water content.

The partial differential equation governing the one dimensional movement of water in the vertical direction in an unsaturated soil maybe derived by invoking Darcy's law and the continuity equation as follows

$$q = -k\frac{\partial(h-z)}{\partial z} = -k(\frac{\partial h}{\partial z} - 1) \tag{5.1}$$

$$\frac{\partial \theta}{\partial t} = -\frac{\partial q}{\partial z} \tag{5.2}$$

where k is the hydraulic conductivity; q is volumetric liquid water flux and t is time, z is vertical coordinate pointing downward. The mixed form of Richards' equation is obtained by substituting Eqs. (5.1) and (5.2):

$$\frac{\partial \theta}{\partial t} = \frac{\partial}{\partial z}[k(\frac{\partial h}{\partial z} - 1)] \tag{5.3}$$

the two independent variable in Eq. (5.3) are soil water content (θ) and the pore water pressure head (h). Instead of employing constitutive relations for describing the interdependence of the two afore mentioned parameters, it is possible to eliminate either θ or h by adopting the concept of specific water capacity (Hillel, 1971), defined as the derivative of the soil water retention curve:

$$C(\theta) = \frac{d\theta}{dh} \tag{5.4}$$

The h-based formulation of Richards' equation is thus obtained by replacing Eq. (5.4) in Eq. (5.3):

$$C(\theta) \times \frac{\partial h}{\partial t} = \frac{\partial}{\partial z}(k\frac{\partial h}{\partial z}) - \frac{\partial k}{\partial z} \tag{5.5}$$

Introducing a new term D, pore water diffusivity defines as the ratio of the hydraulic conductivity to the differential water capacity, the θ-based form of Richards' equation may be obtained, D can be written as

$$D = \frac{k}{C(\theta)} = k\frac{dh}{d\theta} \tag{5.6}$$

It should be noted that both D and k are highly dependent on water content. Combing Eq. (5.6) with Eq. (5.3) gives Richards' equation as:

$$\frac{\partial \theta}{\partial t} = \frac{\partial}{\partial z}(D\frac{\partial \theta}{\partial z}) - \frac{\partial k}{\partial z} \tag{5.7}$$

In employing the diffusivity concept, and all other relationships derived from it, it must be noted that liquid water moves in soils by mass flow and not by diffusion.

Diffusivity is used in the present work to facilitate the analysis of water flow in unsaturated soil. Yanful and Mousavi (2003) pointed out the advantages of adopting the diffusivity concept that it decreases the number of variables form two (θ and h, Eq. (5.3)) to one (θ) in the diffusion equation (Eq. (5.7)). Another advantage is the smaller range of diffusivity relative to that of hydraulic conductivity, also measuring water content and its gradient, and relating it to volume fluxes, is often easier in practice than measuring suction and its gradient.

In order to linearize the above differential equation, the hydraulic conductivity model (Gardner, 1958) and the dependence of the water content on the pressure head (Chen et al., 2001) is assumed as the following constitutive relations:

$$k(\psi) = k_s e^{-\alpha\psi} \tag{5.8a}$$

$$\theta(\psi) = \theta_r + (\theta_s - \theta_r) e^{-\alpha\psi} \tag{5.8b}$$

where the k_s is the saturated hydraulic conductivity, α is a soil pore-size distribution parameter, ψ is soil water suction (ψ = -h), θ_s and θ_r are saturated and residual water content, respectively. By substituting Eqs. (5.8a) and (5.8b) into Eq. (5.6), the expression of D yields:

$$D = \frac{k_s}{\alpha(\theta_s - \theta_r)} \tag{5.9}$$

here, normalized soil water content Θ is defined as

$$\Theta = \frac{\theta - \theta_r}{\theta_s - \theta_r} \tag{5.10}$$

Substituting the Eqs. (5.8), (5.9) and (5.10) into Eq.(5.7), Eq. (5.11) is achieved

$$\frac{\partial\Theta}{\partial t} = \frac{\partial}{\partial z}\left(D\frac{\partial\Theta}{\partial z}\right) - D\alpha\frac{\partial\Theta}{\partial z} \tag{5.11}$$

5.2.3 ONE DIMENSIONAL EVAPORATION PROBLEM WITHOUT WATER TABLE

In natural condition, the infiltration or evaporation problem is always handled without considering water table if the water table is deep enough and has little influence on the overlaying soil. In this case, the problem will be examined the case of a homogeneous half-space domain. To solve Eq. (5.11), an initial condition and one time dependent boundary condition have to be assigned.

In analytical solution, the initial condition is always the soil water content

profile while the boundary conditions can be the soil water content at the surface or the surface fluxes. However, it is relatively difficult to model the whole two stages of evaporative flux. Thus, in this case, the soil water content is selected as the boundary condition. The following initial and boundary conditions are chosen when the surface water content varies with the time for arbitrary water content profile:

$$\Theta(z,0) = f(z) \tag{5.12a}$$

$$\Theta(0,t) = g(t) \tag{5.12b}$$

where the $f(z)$ and $g(t)$ represent arbitrary functions for the vertical water content profile and the change of surface water content, respectively. Following solutions of Carslaw and Jaeger (1959) and Menziani et al. (2005, 2007), the space and time evolution of the soil water content is given by the sum of two solutions:

$$\Theta(z,t) = \Theta_1(z,t) + \Theta_2(z,t) \tag{5.13}$$

where $\Theta_1(z,t)$ represents the solution of Eq. (5.11) with the initial condition (5.12a) and a null boundary condition, while $\Theta_2(z,t)$ represents the solution of Eq. (5.11) with a null initial condition and the boundary condition (5.12b). That is:

$$\Theta_1(z,t) = \frac{e^{\frac{2\alpha z - D\alpha^2 t}{4}}}{\sqrt{\pi}\sqrt{4Dt}} \int_0^\infty f(z')\, e^{\frac{-\alpha z'}{2}} [e^{-(\frac{z-z'}{\sqrt{4Dt}})^2} - e^{-(\frac{z+z'}{\sqrt{4Dt}})^2}]\, dz' \tag{5.14a}$$

$$\Theta_2(z,t) = \frac{1}{2\sqrt{\pi}} \int_0^t g(t')\, e^{\frac{-[D\alpha(t-t')-z]^2}{4D(t-t')}} \frac{zD}{[D(t-t')]^{3/2}}\, dt' \tag{5.14b}$$

Since the $f(z)$ and $g(t)$ are arbitrary functions of depth z and time t, respectively, various soil water redistribution can be produced by selecting appropriate functions for $f(z)$ and $g(t)$. However, it is noted that the integrals in the aforementioned equations can be difficult to be solved analytically. In this section, a specific condition that the evaporation occurs in homogenous saturated soil is chosen to analyze, and the change of water content at soil surface is assumed to decrease exponentially with time (Menziani et al., 2005 and 2007). The initial and boundary conditions are formulated in Eq. (5.15),

$$\Theta(z,0) = 1, \text{ and } \Theta(0,t) = e^{-\beta t} \tag{5.15}$$

where, β is a positive constant with the unit of one over time, and it could be written as $\beta = 4Db^2$ (Menziani et al., 2005), where b is a fitting parameter. According to the value of b, the solution has two different expressions because of the presence of a square root with a radicand. Therefore, the closed-form solution of Eq. (5.11)

corresponding to the above conditions can be expressed as:

for $b \le \alpha/4$,

$$\Theta(z,t) = \frac{1}{2}[\text{erfc}(\frac{D\alpha t - z}{2\sqrt{Dt}}) - e^{\alpha z}\,\text{erfc}(\frac{D\alpha t + z}{2\sqrt{Dt}})] + \frac{1}{2}e^{(\frac{\alpha z}{2} - 4b^2 Dt)}[e^{2zc}\,\text{erfc}(\frac{z}{2\sqrt{Dt}} + 2c\sqrt{Dt}) + e^{-2zc}\,\text{erfc}(\frac{z}{2\sqrt{Dt}} - 2c\sqrt{Dt})] \tag{5.16}$$

where $c = \sqrt{(\frac{\alpha}{4})^2 - b^2}$; erfc(x) is error function, $\text{erfc}(x) = \frac{2}{\sqrt{\pi}}\int_0^x e^{-t^2} dt$.

for $b > \alpha/4$,

$$\Theta(z,t) = \frac{1}{2}[\text{erfc}(\frac{D\alpha t - z}{2\sqrt{Dt}}) - e^{\alpha z}\,\text{erfc}(\frac{D\alpha t + z}{2\sqrt{Dt}})] + e^{-\frac{(z - Dt\alpha)^2}{4Dt}} R\{\text{W}(2\sqrt{(b^2 - \frac{\alpha^2}{16})Dt} + i\frac{z}{2\sqrt{Dt}})\} \tag{5.17}$$

where $W(x+iy) \equiv W(z) = e^{-z^2}\,\text{erfc}(-iz)$ is an error function of complex variable whose real and imaginary parts are reported in the Appendix II, Table I, p.485 (Carslaw and Jaeger, 1959) and in Table 7.9, p.326 (Abramowitz and Stegun, 1965).

Consider the surface flux $E(t)$ can be given by (neglecting gravity)

$$-E(t) = -D\left.\frac{\partial \theta}{\partial z}\right|_{z=0} \tag{5.18}$$

As it is quite complicated and difficult to analytically calculate the derivative of error function of complex variable, this study only reports the surface flux solution in the case of $b \le \alpha/4$. Substituting Eqs. (5.8), (5.9), (5.10) and (5.16) into Eq. (5.18), it yields

$$E(t) = D(\theta_s - \theta_r)e^{-4b^2 Dt}[\frac{\alpha}{2} - 2c\,\text{erf}(2c\sqrt{Dt}) - \frac{\alpha}{2}\text{erfc}(\frac{\alpha}{2}\sqrt{Dt})] \tag{5.19}$$

For the case that complicated forms of $f(z)$ and $g(t)$ are chosen, the solutions for Eq.(5.11) and (5.19) have to be expressed as integral solutions and numerical integration. This solutions obtained here were for specific condition that the soil is evaporated from initially saturated.

5.2.4 ONE DIMENSIONAL EVAPORATION PROBLEM WITH WATER TABLE

In this section, we will examine the case of soil water dynamic during evaporation bounded by a pair of parallel planes, usually the soil surface z = 0 and

the depth of water table or lower boundary $z = L$. Figure 5.1 shows the schematic of hypothetical water content distribution in unsaturated soil. Since a flux boundary condition can be experimentally available, $q_1(t)$ the prescribed surface flux at the upper boundary condition. The lower boundary condition is presented by the prescribed water content θ_s at water table. The analytical solution in this case would be derived in this section.

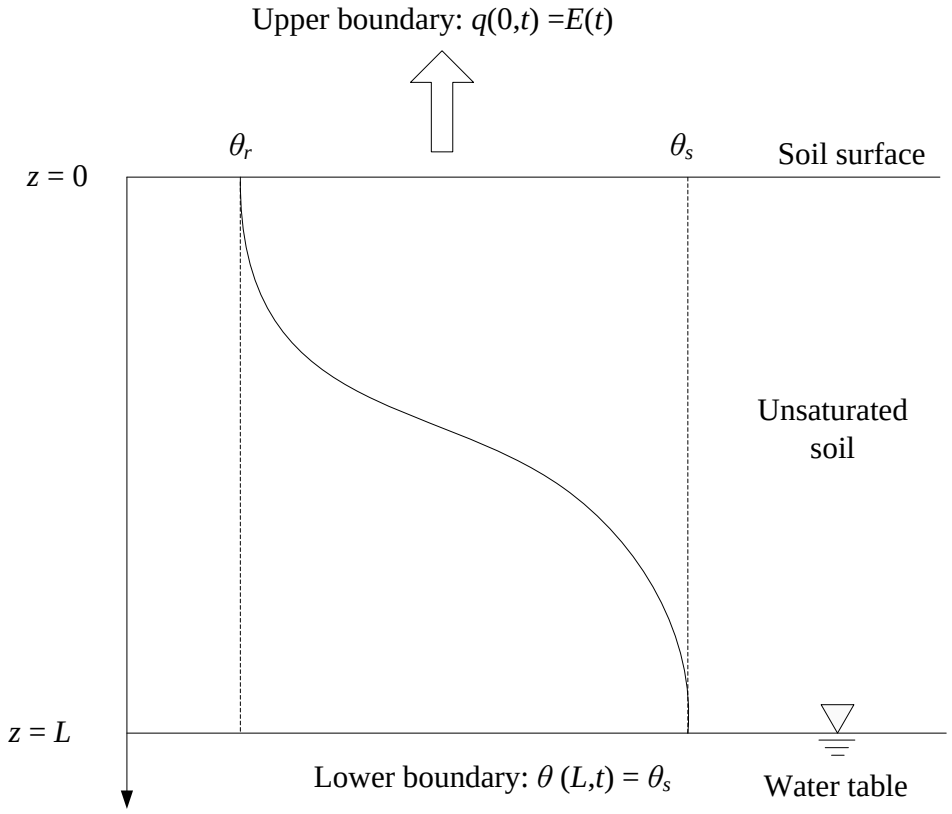

Figure 5.1 Schematic of hypothetical water content distribution in unsaturated soil. θ_s is the water content at saturated, θ_r is the residual water content, $E(t)$ is time-dependent varying surface fluxes.

Processes may also occur in which the gradient of the gravitational head is negligible compared to the strong matric suction gradient (Yanful and Mousavi, 2003; Menziani et al., 2005), also, the analytical solution for Richards' equation with two arbitrary boundary conditions seems impossible to solve out due to the difficult forms of integrals or series. Even if the solution has clear formulations, it is somehow divorced from the mechanism of boundary condition (Srivastava and Jim Yeh, 1991; Nachabe et al., 1995; Basha, 2000; Chen et al., 2001&2003; Nasseri et al.,

2012). Because of these mentioned above, the fundamental differential equation of flow without gravity in unsaturated porous media is formulated as follows

$$\frac{\partial \Theta}{\partial t} = \frac{\partial}{\partial z}(D\frac{\partial \Theta}{\partial z}) \tag{5.20}$$

Since the soil evaporation process is assumed to starts from saturation, the upper boundary at the ground surface is subjected to a evaporation, which is a time dependent function, the water content at lower boundary is prescribed as θ_s. Thus, the initial and boundary condition can be expressed as

$$\Theta(z,0) = 1 \tag{5.21a}$$

$$\Theta(L,t) = 1 \tag{5.21b}$$

$$q(0,t) = E(t) = D\frac{\partial \theta}{\partial z}\bigg|_{z=0} \tag{5.21c}$$

Some results for the cases in which the surface flux has different forms can be obtained by Laplace transformation (Carslaw and Jaeger, 1959; Richard, 2007).

(1) The surface flux is constant value that is expressed as *E*(*t*) = *E*.

To easily get the solution for Eq. (5.20), we include a new parameter *y* to replace the *z*, *y* is defined as

$$y = L - z \tag{5.22}$$

Substituting Eq. (5.22) into Eqs. (5.20) and (5.21), after taking Laplace transform of Eq. (5.20) and denoting the transform of Θ by $\overline{\Theta}$, we can write

$$D\frac{\partial^2 \overline{\Theta}}{\partial y^2} - s\overline{\Theta} + 1 = 0 \tag{5.23}$$

The corresponding boundary conditions (Eq. (5.21b) and Eq. (5.21c)) are

$$\overline{\Theta}(0) = \frac{1}{s} \tag{5.24a}$$

$$D\frac{\partial \overline{\Theta}}{\partial y}\bigg|_{y=L} = \frac{E}{s} \tag{5.24b}$$

The solution of these is

$$\overline{\Theta}(y) = \frac{1}{s} + \frac{e\,\mathrm{sech}(\frac{L\sqrt{s}}{\sqrt{D}})\sinh(\frac{y\sqrt{s}}{\sqrt{D}})}{\sqrt{D}s^{\frac{3}{2}}} \tag{5.25}$$

Taking inversion theorem of Laplace transformation for Eq. (5.25), it results in

$$\Theta(y,t)=\frac{2E(Dt)^{\frac{1}{2}}}{D}\sum_{n=0}^{\infty}(-1)^n\{\text{ierfc}\frac{(2n+1)L-y}{2(Dt)^{\frac{1}{2}}}-\text{ierfc}\frac{(2n+1)L+y}{2(Dt)^{\frac{1}{2}}}\} \tag{5.26}$$

Taking the variable substitution that Eq. (5.22) into Eq. (5.26), the final solution can be obtained as follows

$$\Theta(z,t)=1-\frac{2E(Dt)^{\frac{1}{2}}}{D}\sum_{n=0}^{\infty}(-1)^n\{\text{ierfc}\frac{2nL+z}{2(Dt)^{\frac{1}{2}}}-\text{ierfc}\frac{2(n+1)L-z}{2(Dt)^{\frac{1}{2}}}\} \tag{5.27}$$

(2) The surface flux is a prescribed function of time

Result for this case may be written down by Duhamel's theorem. Here, the surface flux is specified as Eq. (5.28), the corresponding analytical solution is generalized as Eq. (5.29) by the same procedure with the development of Eq. (5.27).

$$E(t)=Et^{\frac{1}{2}m} \tag{5.28}$$

where m = -1, 0, 1, …

$$\Theta(z,t)=1-\frac{(2)^{m+1}Et^{\frac{1}{2}(m+1)}\Gamma(\frac{1}{2}m+1)}{\sqrt{D}}\sum_{n=0}^{\infty}(-1)^n\{\text{i}^{m+1}\text{erfc}\frac{2nL+z}{2(Dt)^{\frac{1}{2}}}-\text{i}^{m+1}\text{erfc}\frac{2(n+1)L-z}{2(Dt)^{\frac{1}{2}}}\} \tag{5.29}$$

From the analysis in Chapter 4, we know that the constant rate stage (Stage 1) of evaporation will continue until surface water content reaches the critical value θ_c. Then, the falling rate stage (Stage 2 and 3) would be prevailing. Therefore, the transition between Stage 1 and Stage 2 of the evaporative cycle may be determined by investigating the value of water content at the surface of soil over time. For the falling rate stage, Ritchie (1972) proposed a linear relationship with zero intercept between cumulative evaporation (E_c) and the square root of time ($t^{1/2}$). Shokri and Or (2011) also verified this deduction by evaporation tests for different soil sizes. The value of the slope of this relationship (λ) is needed. Bonsu (1997) observed that λ is correlated to soil texture but the correlation was statistically insignificant. Yunusa et al. (1994), Brutsaert and Chen (1995), and Suleiman and Ritchie (2003) among others have reported experimental values of λ for different soils. Thus, the cumulative evaporation (E_c) is given by

$$E_c=\frac{1}{2}\lambda t^{\frac{1}{2}} \tag{5.30}$$

and the evaporation rate $E(t)$ can be obtained from derivation of Eq. (5.30)

$$E(t) = \frac{1}{2}\lambda t^{-\frac{1}{2}} \tag{5.31}$$

where λ is the soil water desorption, it is constant for a given soil.

Comparing the formulations of Eqs. (5.28) and (5.31), we know that *m* equalling to -1 is suitable for modelling the evaporation during falling rate stage. And thus, the Eq. (5.29) can be written as

$$\Theta(z,t) = 1 - \frac{\lambda\Gamma(-\frac{1}{2})}{\sqrt{D}} \sum_{n=0}^{\infty} (-1)^n \{\text{erfc}\frac{2nL+z}{2(Dt)^{\frac{1}{2}}} - \text{erfc}\frac{2(n+1)L-z}{2(Dt)^{\frac{1}{2}}}\} \tag{5.32}$$

this formula is the final equation to model the soil water distribution during falling rate stage. It should be noted that, the unit of λ usually is $cm/d^{1/2}$, which should be unified when calculating the soil water distribution.

5.3 COLUMN EVAPORATION TEST

The column evaporation test was the final stage of the laboratory test program carried out. The evaporation test for the thin soil sections represented soil desiccation under special conditions. The soil sections were made extremely thin in order to minimize the effects of transfer mechanisms with the soil matrix. Moisture recharge to the evaporating surface was not available from underlying wetter soil.

The objective of the column evaporation test is to measure evaporation from a soil column with sufficient thickness such that flow mechanisms within the soil, thus to verify the proposed analytical model. In this study, the column evaporation test were conducted in two cases, in the first case, the atmosphere condition were controlled in several groups, while the water table is the key parameter in the second case.

5.3.1 CLIMATE CONDITIONS CONTROLLED CASE

Laboratory evaporation tests have been conducted to investigate soil water dynamic during evaporation. In this test, the same column soil specimen was controlled to subject to different environmental conditions. These tests were performed by the newly developed climate control apparatus, which is described in Chapter 3 in detail. The use of a radiative flux is avoided in the column evaporation test. The effect of the energy budget on the evaporation process is paramount in the field studies. However, it was deliberately set aside in this study so that the

fundamental process of soil evaporation could be observed.

The K-7 sand was adopted as the most suitable material for the laboratory column evaporation test. To complement the properties of K-7 sand, hydraulic parameters are shown in Table 5.1. This material offered several advantages over the fly ash and K-3. K-7 sand has the medium porosity and therefore was expected to desaturation quickly under a specific evaporative flux. In addition, the K-7 sand has a low "bubbling pressure" and a steep moisture retention curve. Hence, it was expected that a distinct drying front would develop as evaporation progressed. Finally, the selection of K-7 sand minimized the effect of volume change of as desiccation occurred. The sample was packed into a cylinder with diameter 10 cm and height 20 cm. The water content probes (time-domain reflectometry (TDR), EC-5 water moisture sensor) were inserted into the cylinder at the depths of 1 cm, 5 cm, 10 cm, 15 cm and 20 cm, respectively. To saturate the soil samples after packing and assembling the soil column, a plastic tube was connected to the bottom side hole of the column and then connected to a constant-head water tank. Distilled water was applied to the soil specimen from the bottom of the column. The saturation procedure was terminated when slight ponding occurred on the top of the soil column. At this time the volumetric water content was measured by the TDR probes to confirm the achieved degree of saturation. The saturation process took 3-4 h in average for the specimens.

Table 5.1 Summary of the properties of soil sample

Specimen	θ_r	θ_s	k_s (m/s)	α (m^{-1})
K-7 sand	0.01	0.41	3.9×10^{-6}	4.80

Table 5.2 Experimental conditions, the number in parenthesis is the mean error for each item

Condition No.	Relative humidity (%)	Wind speed (m/s)	Temperature (°C)	Duration (h)
Case 1	60 (±3.2)	2.0 (±0.2)	25 (±1.0)	574
Case 2	40 (±2.3)	2.0 (±0.2)	25 (±1.0)	343
Case 3	40 (±3.2)	1.0 (±0.1)	25 (±1.0)	868

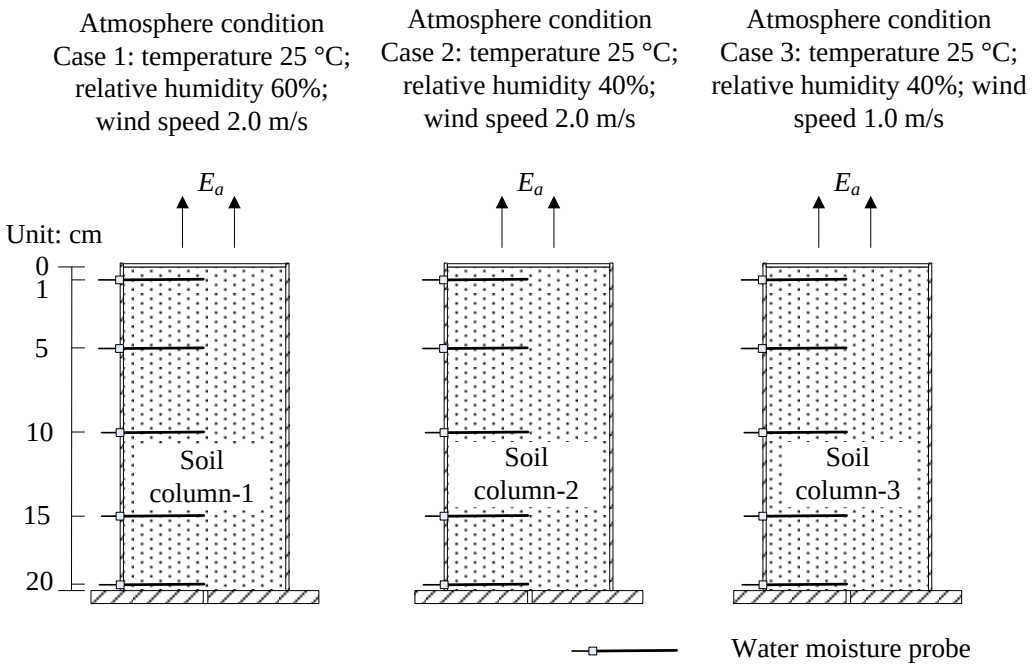

Figure 5.2 Schematic of evaporation column showing the size of soil specimen and positions of sensors

Then soil columns were then subjected to three different environmental conditions time to time that were controlled as shown in Table 5.2. Figure 5.2 is the schematic representation of the evaporation column, showing the thickness of the soil specimen, the location of the TDR probes. The potential evaporation rate for each case was measured throughout the experiment by means of a free water surface of the same dimensions taken in advance; they are 0.31 mm/h, 0.36 mm/h and 0.22 mm/h for case 1, 2, and 3, respectively. The soil column was supported on scale to give a continuous measurement of their mass and, therefore, their change in mass. The actual rate of soil evaporation was determined on the basis of change in mass for each column which was automatically recorded at 15 minutes intervals. The water content profile along the column were also measured at same interval. The duration of the whole experiment was 77 days.

5.3.2 WATER TABLE CONTROLLED CASE

Figure 5.3 shows the picture of the setup of column evaporation test with constant water table. The evaporation tests in this group were also performed based on the climate control apparatus. The distinguish is that the evaporation chamber

(length 42 cm; width 22 cm; height 17 cm) was installed up on the soil column. The temperature, relative humidity, wind speed were maintained comprehensively at about 30 °C, 40% and 3.6 m/s, respectively.

Figure 5.3 Picture of the setup of column evaporation test with constant water table

Figure 5.4 show a detail of the soil column and water supply system. The sand filled evaporation column were constructed using 10 cm diameter polypropylene transparent cylinder having a wall thickness of 10.5 mm. The dry soil was packed into the column with both knocking the column sides and compacting from soil top to achieve a maximum dry density. The soil evaporation columns measured in two cases, Case A: 150 cm and Case B: 200 cm in height. For Case A, eight TDR probes were installed along the center axis of column. A water tank containing enough water supplied the water to the bottom of column. Water table was maintained at the height of 100 cm that is 50 cm up of the bottom as presented in Figure 5.4. A tube was used to connect the tank with a burette, at the top of which a switch is to control sealing during water supply. The low side of tube was set just right at the water surface, thus,

the amount of water supplied to the soil column equals to that of the water flowed down from the burette to the tank, and the volume change of water in burette can be monitored by a camera in specific time interval. For Case B, eleven TDR probes were inserted to measure the instantaneous volumetric water content, the height profile of the probe is marked in Figure 5.4. The water supply system were adopted to maintain the water table at 150 cm that of 50 cm from the bottom, whose mechanism was same to Case A.

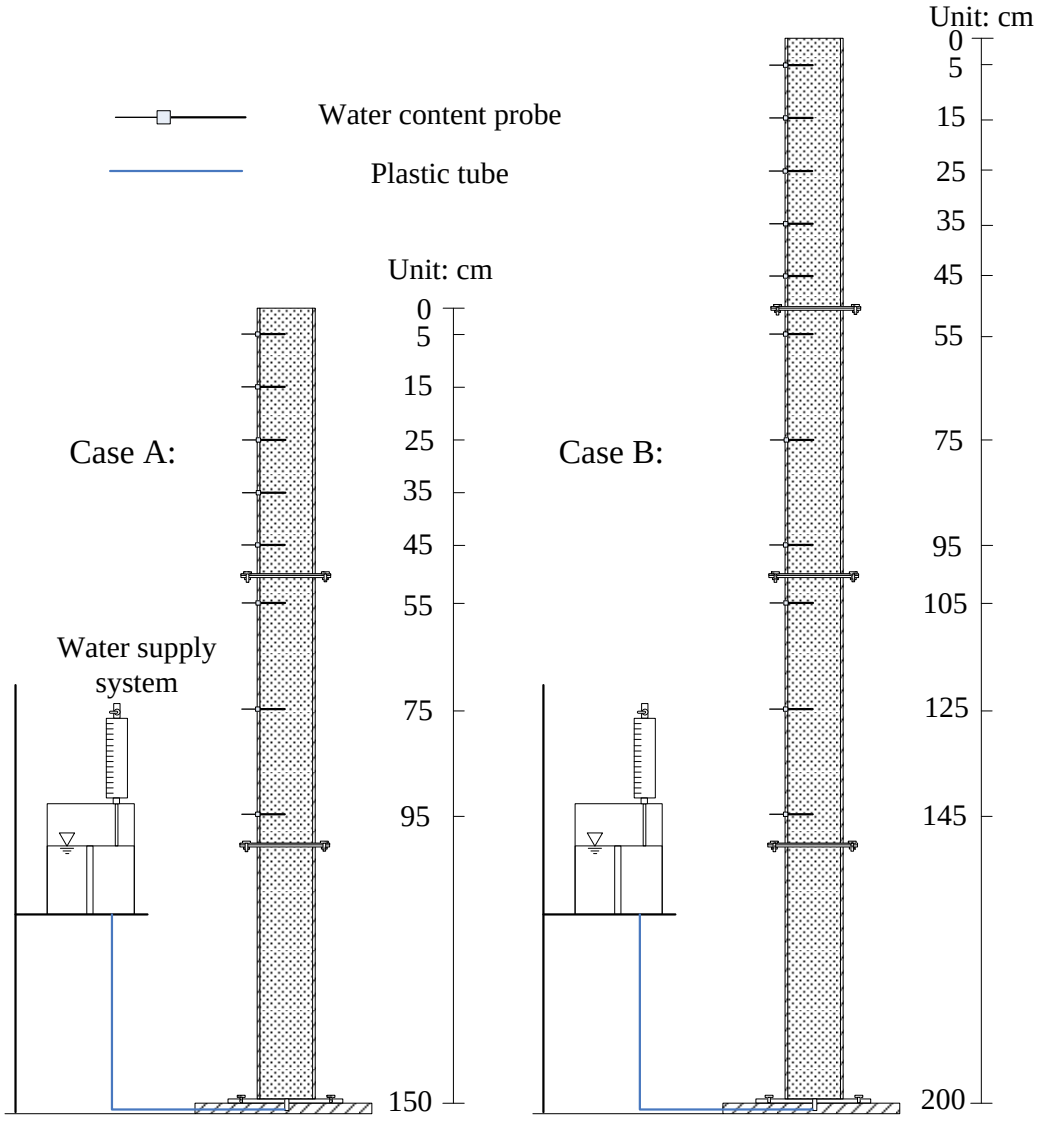

Figure 5.4 Schematic diagram of column soil evaporation test with constant water table

Before the evaporation tests start, the soil column was wetted to saturation by capillary rise method that enough water was supplied from the bottom. The periods

of saturation for a Case A and Case B are 7 days and 10 days respectively. The interval of 15 minutes was set to measure the continuous water content and the instantaneous atmosphere indexes. The evaporation for Case A continued from 31st January 2013 to 20th march, 2013, it is about 50 days. The period for Case B was from 8st April 2013 to 16th June 2013, about 70 days. Since the soil column in Case B has greater height, it takes longer time to evaluate the evaporation in soil.

5.4 RESULT ANALYSIS AND MODEL VALIDATION

5.4.1 EVAPORATION WITHOUT WATER TABLE

Figure 5.5 illustrates the variations of soil water content at the top 1cm versus the elapsed time for the three cases. It indicates that it takes shorter time for soil surface to get dry under higher potential evaporation rate condition. Because the water content gradient is not clearly performed yet at the first 24 h, the water supply is considered not being activated, which results in the normalized water content Θ sharply reducing at the beginning. Then, the value of Θ gradually decreases with no obvious inflection point observed, which is somehow distinct from the transformation of first stage and falling-rate stage in the evaporation curve. When its value is lower than about 0.2, the value of Θ smoothly changes and can last for a long period coincidently corresponding to the residual falling-rate stage. It is deduced that the transformation of surface water content is relatively easier to be simulated than that of evaporative fluxes. The experimental data is also modeled by exponential function following the Eq. (5.15), which indicates a relatively satisfying agreement. The values of fitting parameter b for case 1, 2 and 3 can be calculated from that of β, which are 0.413, 0.489, and 0.370, respectively.

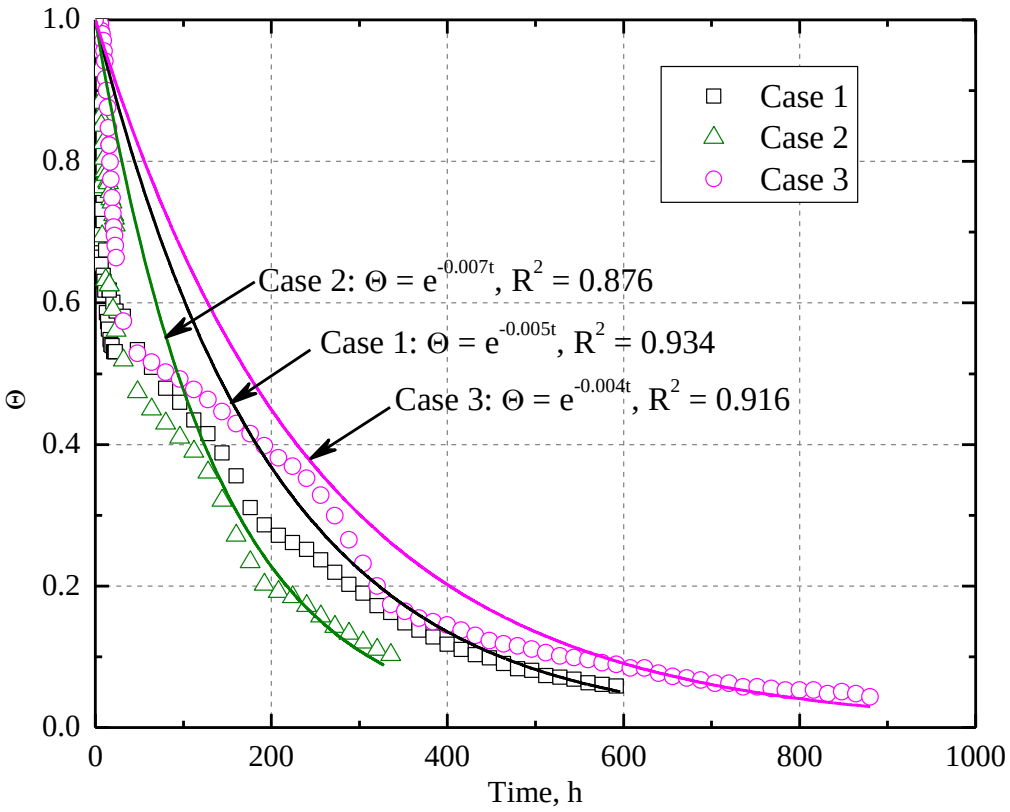

Figure 5.5 Measured and simulated soil water content at the depth of 1cm versus the elapsed time. The solid line represents simulated results, and the symbols are measured ones.

In order to evaluate the application of aforementioned theory, the water content distributions computed at the required time are displayed in Figure 5.6 to compare with the experiment result. The experiment data marked as scatters show that the surface water content (top 5 cm) is much lower than that of deeper soil at the beginning stage of evaporation process, and the water content gradually changes to be uniform for the latter stage. It can be observed in all three figures that, the higher drying rate results in lower water content profile at any given time, although a lower drying rate is maintained for a longer time. The computed result shown as solid line in Figure 5.6 are obtained using Eq. (5.16) since all the three cases coincide with the condition of $b \leq \alpha/4$. Good agreements between theory and experiments suggest that the theory proposed in this paper can competently simulate the water content redistribution during evaporation process. However, the nearly straight solid line simulated by this model also indicates that it cannot fit the variation of water content at soil surface very well, which may be due to the limitation of the soil depth and the

simplified assumption for surface water content versus elapsed time.

Figure 5.7 shows the resulting analytical evaporation rates compared to those obtained from experiments under the three cases. The experimental results show two distinct evaporation stages for each case, the constant rate stage last about 90 h, 60 h and 180 h for case 1, 2, and 3, respectively. Then it comes to the falling rate stage and finally a residual falling-rate stage starts from the 250h, 200h, and 370h, respectively. Figure 5.7 also shows that the evaporation rates computed from Eq. (5.19) sharply increase from initial zero at the beginning of 25 h, and then they decrease similar to the negative exponential function curve. After all, the comparisons of the results suggest that the analytical solution is capable of capturing trends of the evaporation curve. After all, the comparisons of the results suggest that the analytical solution is capable of capturing trends of the evaporation curve.

The cumulative evaporation is also obtained by integrating the analytical evaporation rate as presented in Figure 5.8, in which solid line representing analytical result compares with experimental symbols. It could be observed that the value of analytical cumulative evaporation is quite close to the experimental measurements at the first stage mentioned above, and then the gap starts to be greater at near the residual falling stage. The accumulated differences between analytical and experimental result are satisfied, about 4.4 mm, 10.9 mm and 6.0 mm respectively for the 3 cases. In addition, it shows that the water content distributions analytically predicted are lower than the measured data at nearly end stage of 500 h, 340 h, and 800 h, respectively, which is in consistent with Figure 5.6. The reason may be that the exponential function of the hydraulic conductivity and the water content on the pressure head somehow overestimates the value of hydraulic conductivity and the diffusivity.

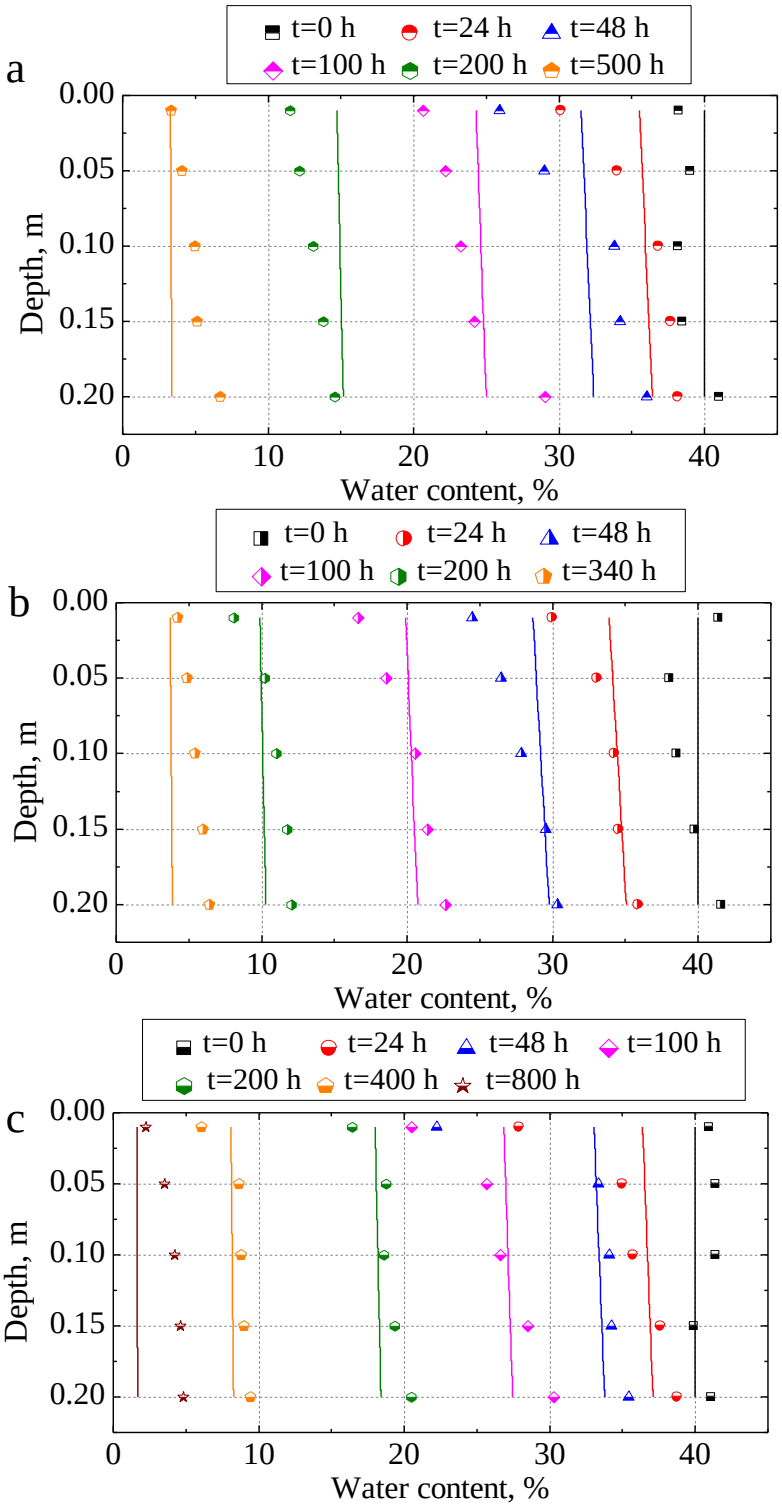

Figure 5.6 Measured and computed water content profile for (a) case 1, (b) case 2 and (c) case 3. Symbols present the experimental profile while the solid lines are theoretical trends

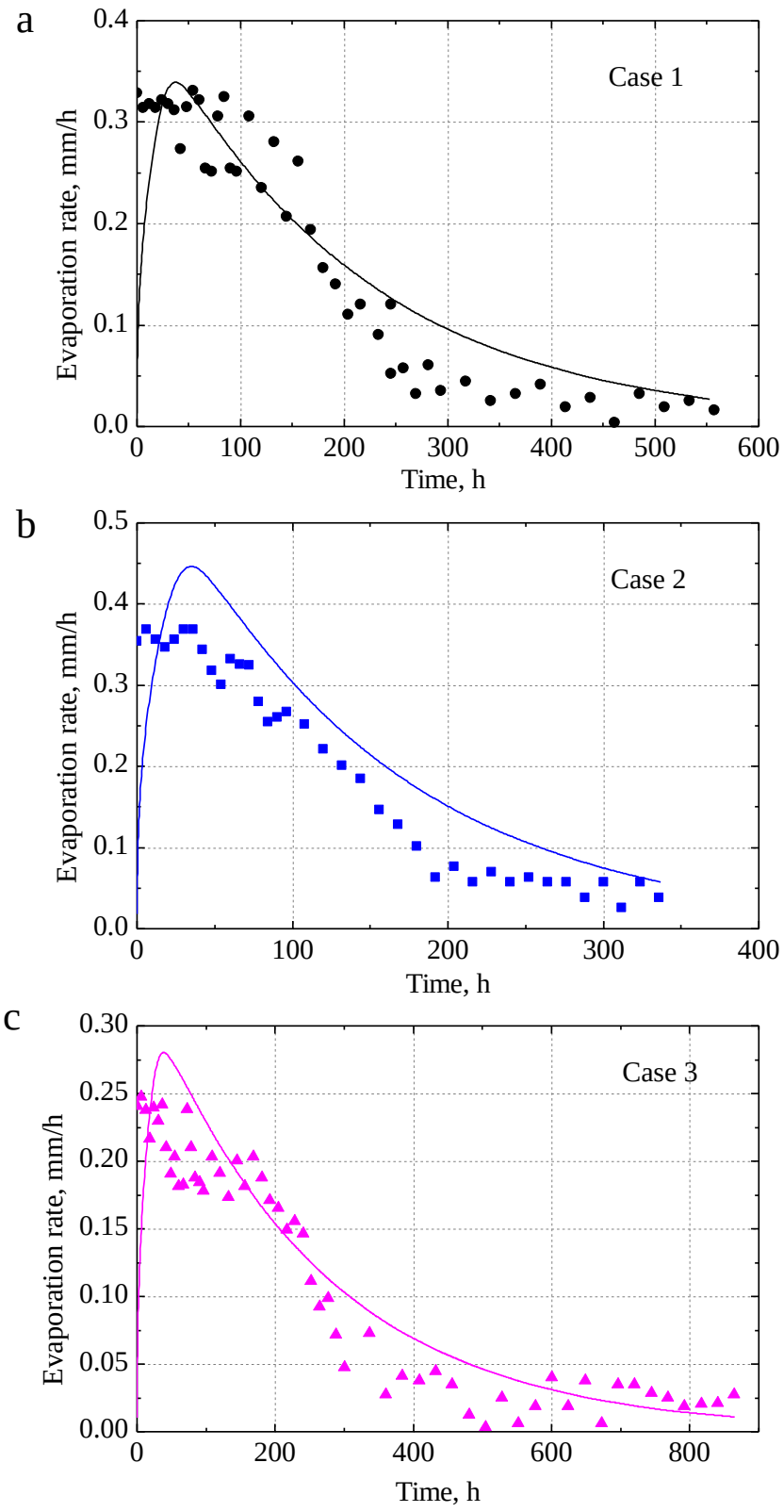

Figure 5.7 Measured and computed evaporative rate for (a) case 1, (b) case 2, and (c) case 3

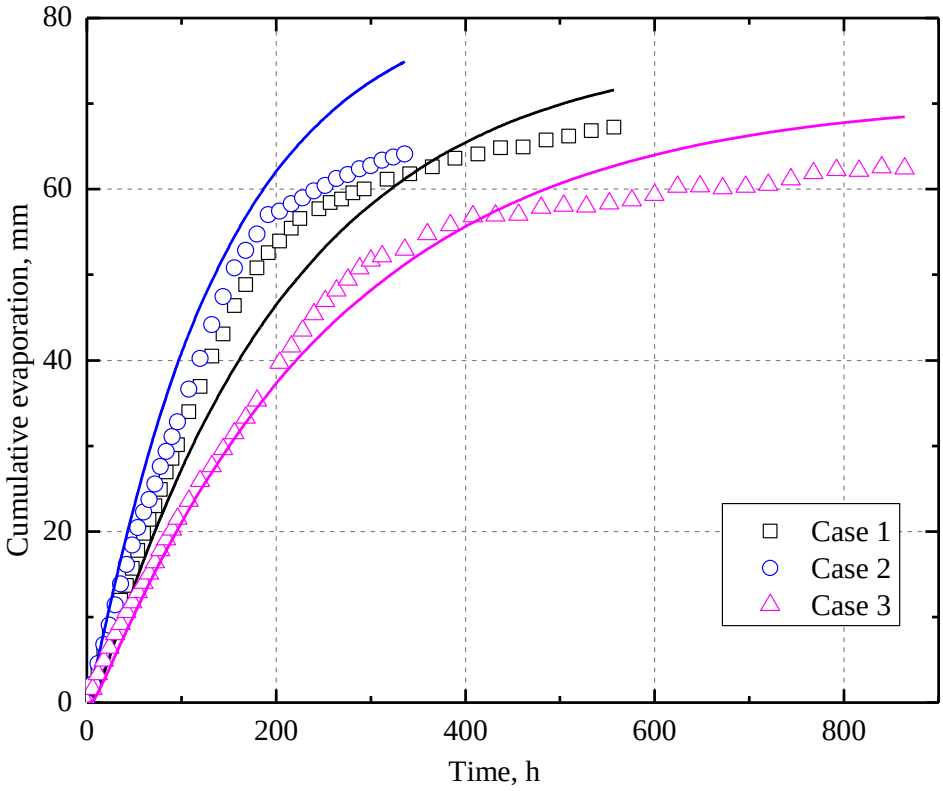

Figure 5.8 Measurement and computed cumulative evaporation versus elapsed time for the three cases

5.4.2 EVAPORATION WITH WATER TABLE

The result obtained for the column soil evaporation with water table at 1m is reported in Figure 5.9. It shows, for the K-7 sand, the water content distribution computed at the required times and depths. The black line on the right corresponds to the uniform soil volumetric water content distribution at the starting time, which is the initial condition. The quoted at the times (h) in the figure are drawn to the left after the constant evaporation occurs. The water content profile as presented in solid line is calculated from Eq. (5.27). The figure shows that the simulated water content coincides with the measured one. And from the time greater than 200 h, the soil water content changes little. In other words, the soil water dynamic reaches equilibrium state, when the soil evaporation and the water supply from the boundary are nearly same. The finial soil water distribution is shows like a line. The soil water content at top 50 cm has a relatively greater range for variation than the lower part. It should be noted that, during the evaporation process, the water content changes with

small amplitude. Even for the surface soil, it only reduces from 40% to about 35%, it may due to the rate of evaporation is much more lower than the hydraulic conductivity of soil.

To investigate the soil water variation time to time during the evaporation process, the measured and simulated water content at the depths of 0.05 m, 0.15m, 0.25m, 0.35m, and 0.45m are plotted separately in Figure 5.10. It shows that the water content quickly reduces at about the first 150 h, and then the values do not changes much until the end of test, which is at about 1200 h. It can be concluded that the water supply was not activated until the obvious water gradient being performed. As shown in Figure 5.10, small difference between symbols and lines can be appreciated, which indicates the proposed model is competent for simulating soil water dynamic during evaporation process. A "jump" of water content at the depths of 0.25 m and 0.35 m exists just between the two stages, it may be due to the partially extended water content gradient during the evaporation process. For the depth of 0.45 m, the water content changes little from 40% to about 37%, which shows a gap between the simulation and measured instantaneous water content.

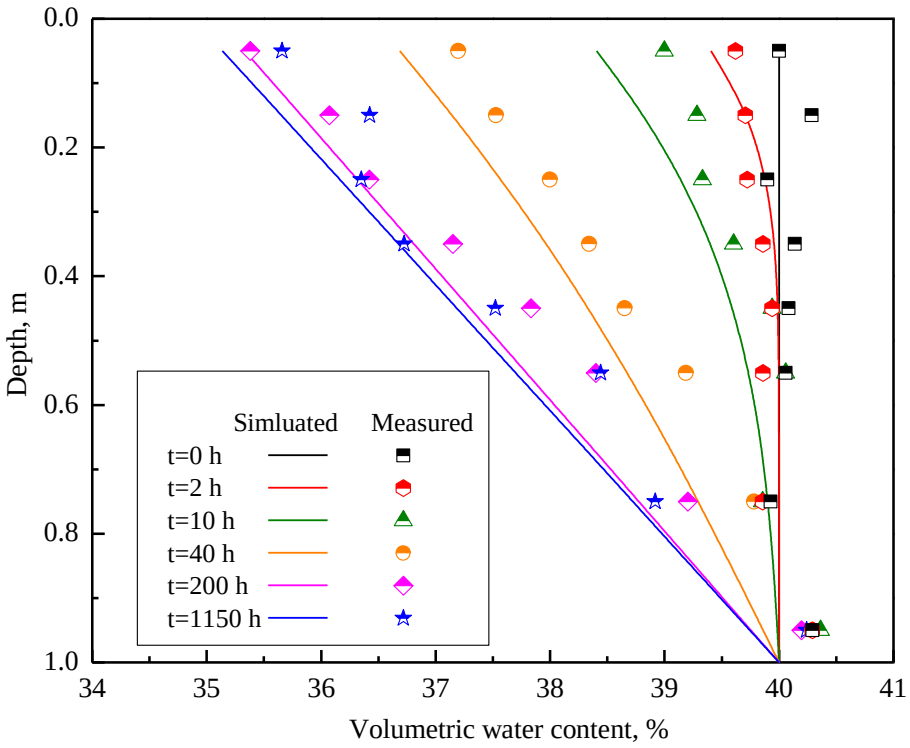

Figure 5.9 Measured and simulated water content profile with water table of 1 m

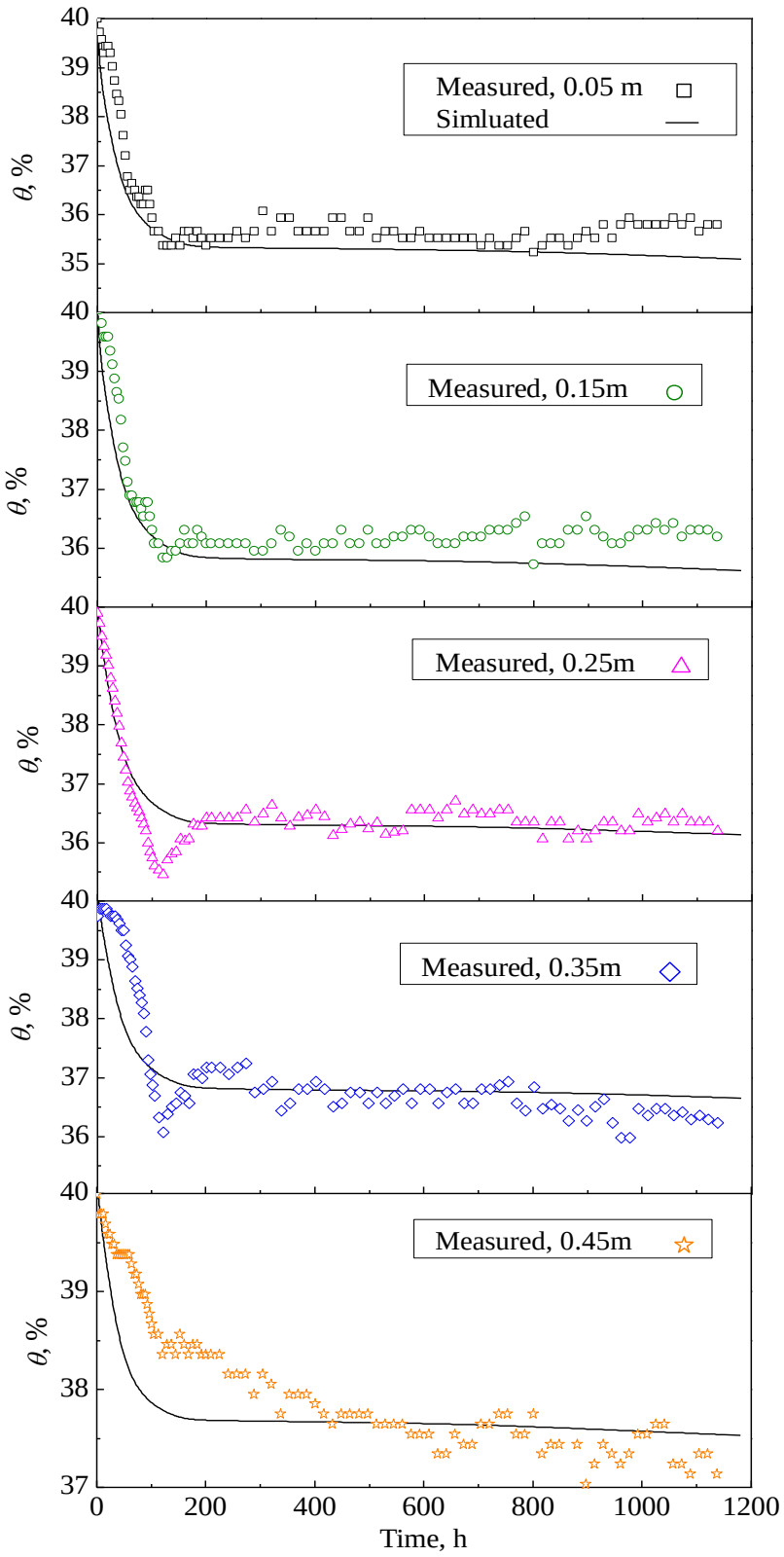

Figure 5.10 Measured and simulated soil water content at different depths versus elapsed time when the water table is 1 m

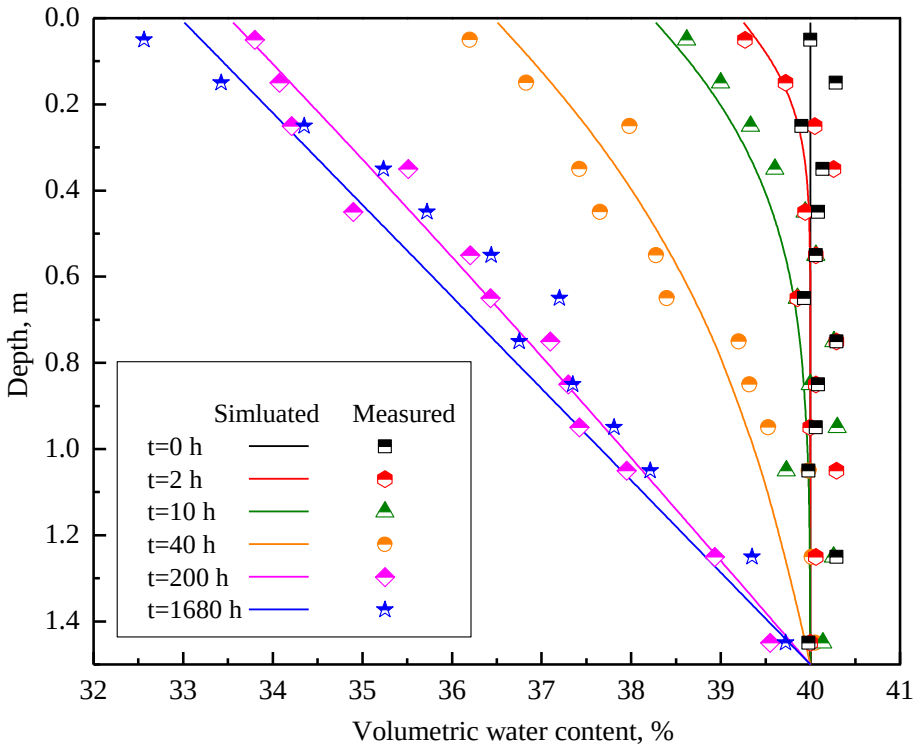

Figure 5.11 Measured and simulated water content profile with water table of 1.5 m

The second application of the proposed model is analyzed with the soil water column evaporation test with 1.5 m water table. A uniformly saturated soil water content is also assumed as initial condition. In Figure 5.11, the black line corresponds to the initial volumetric water content. The vertical water content distribution at the quoted time are displayed in different colors. The symbols represent the measured value by soil water probe at different depths. Both analytical solution and measured value are adopted at the times: 2 h, 10 h, 40 h, 200 h, and the finial state 1680 h. The results shows that the proposed analytical solution can simulate the soil water content distribution in satisfied accuracy. As the time goes on, the evaporative flux implies a decrease in surface moisture firstly, and then the decreasing extends to the deeper soil time to time. A small gap between water content profiles at 200 h and 1680 h indicates that the equilibrium state is achieved after 200 h. Comparing to the result presented in Figure 5.9, greater reduction of soil water content is observed, it is due to the deeper water table that results in longer time for water supply.

To investigate the instantaneous soil water content, the measured water content at the depths of 0.05 m, 0.65 m, and 1.05 m are selected and plotted in Figure 5.12, where the simulation by analytical solution is shown as solid line. It clearly shows

that the soil water reduction start to be slow at the inflection time about 350 h. The variation of water content would be smaller for the soil at deeper position.

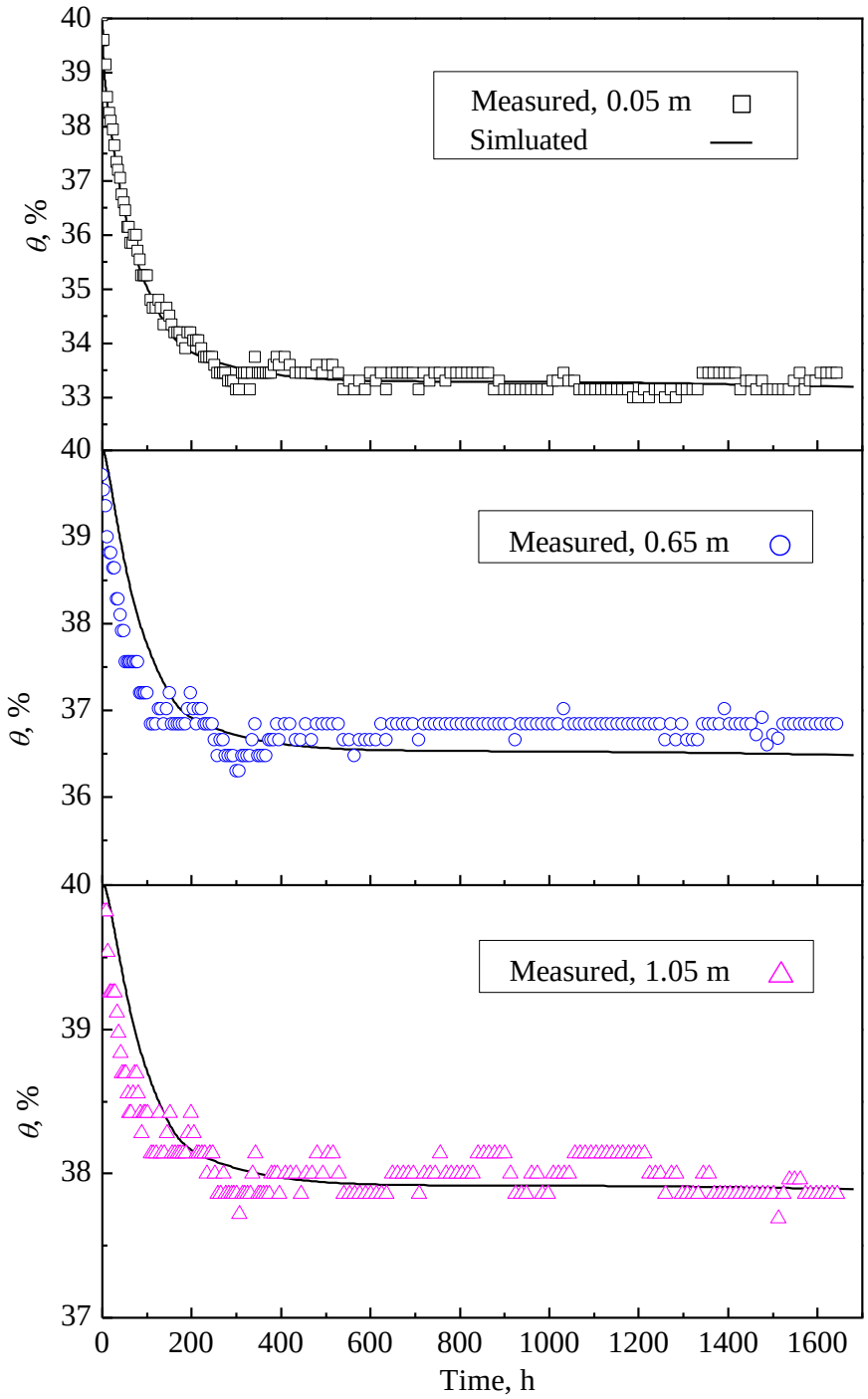

Figure 5.12 Measured and simulated soil water content at different depths versus elapsed time when the water table is 1.5 m

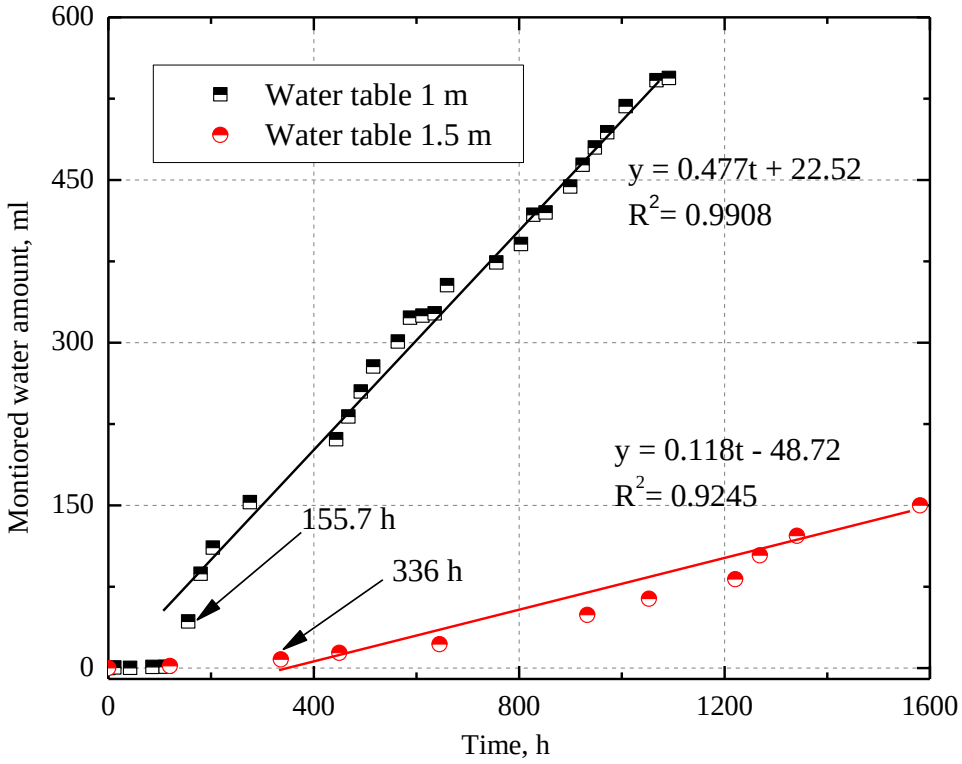

Figure 5.13 Monitored amount of water supplied to the soil column from the boundary

The result in Figures 5.9 to 5.12 provide a verification for the proposed model that it can simulate well soil water dynamic during evaporation process. And also an equilibrium would be emerged after the water supply being activated, and then there is nearly no change in soil water content for the soil column.

Figure 5.13 shows the monitored amount of water that supplied to soil column from bottom versus elapsed time. It is actually the water fluxes at bottom boundary. The result clearly shows there is nearly no supply for the first 155 h and 336 h corresponding to the cases of water table in 1.0 m and 1.5 m, respectively. It indicates the water content gradient is not performed yet to active the water movement at lower boundary. And then a the value of vertical axis increases linearly with the elapsed time, which is the equilibrium state. At that time the water content does not change greatly, and the water supplied amount is considered to be equals to the amount of water evaporated loss. For the case that water table is located in 1.5 m, the gradient is performed later than the 1.0 m case, and the amount of water supplied is less, it may due to more time consumed and energy loss during the water capillary up.

5.5 PARAMETER STUDY

The distribution and variation of soil water content in unsaturated soil are governed by the water flow, which is in affected by many intrinsic and external factors. The intrinsic factors are mainly the hydraulic properties of the soils, including water retention characteristics and the water coefficient of permeability. The external factors mainly refer to climatic conditions, such as rainfall and evaporation intensity, water fluxes pattern.

To improve the understanding of the influence hydraulic properties and evaporation condition on soil evaporation mechanism and hence on the soil water dynamic, the parameter study is carried out based on the proposed model. Soil water characteristic curve and water coefficient of permeability are two essential hydraulic properties for transient flow analysis. Although the diffusion parameter D exists in the Eq. (5.27) of the proposed, it is originally derived from other hydraulic properties as presented in Eq. (5.9). Moreover, for engineering applications, the SWCC can be expressed in terms of desaturation coefficient (α) and water storage capacity (θ_s -θ_r); the permeability can be described in terms of the saturated permeability (k_s) and the desaturation coefficient (α). These three hydraulic parameters (k_s, α, θ_s -θ_r) together with two parameters for specifying the evaporation rate (E) and water table depth (L) are the governing parameters for the 1D evaporation system studied in this section. To obtain an obvious outcome of evaporation, the enlarged value of evaporation rate, E is adopted here.

A homogenous soil layer with water table (L=10 m) is chosen for this parameter study. The experiments shown in Table 5.3 are run to investigate the influence of hydraulic parameters, evaporation condition, and water table, namely k_s, α, θ_s -θ_r, E, and L on soil water profile in unsaturated soil. Series 1, 2, and 3 are considered to investigate individual influence of the three hydraulic parameters (α, θ_s -θ_r, and k_s), respectively. Series 4 and 5 are designed for studying the relative sensitivity of the evaporation rate E and saturated hydraulic conductivity k_s, the last series is primarily for investigating the effect of water table depth. To be simple, a uniform evaporation process lasting for 48 h is simulated for the Series 1, 2, 3, 4.

Table 5.3 Analysis scheme for the parameter study

Series	Case No.	α (m^{-1})	θ_s -θ_r	k_s ($\times 10^{-6}$ m/s)	E ($\times 10^{-6}$ m/s)	L (m)
1	1	1.0	0.3	1.5	5	10
	2	0.5				
	3	0.1				
2	1	0.5	0.2	1.5	5	10
	2		0.3			
	3		0.4			
3	1	0.5	0.3	0.15	5	10
	2			1.5		
	3			15		
4	1	0.5	0.3	3	0.3	10
	2				1	
	3				3	
	4				9	
	5				30	
5	1	0.5	0.3	1.5	5	2
	2					5
	3					10

5.5.1 INFLUENCE OF DESATURATION COEFFICIENT (α)

The desaturation coefficient (α) governs the rate of decrease in water content or hydraulic conductivity with an increasing matric suction or pore water pressure (see Eq. (5.8)), the value of α is related to the grain size distribution of a soil (Zhan and Charles, 2004). Generally speaking, the greater the clay content, the lower the desaturation rate, and hence the more gradually the water coefficient of permeability decreases with an increase in matric suction. Figure 5.14 shows three water content profiles at t = 48 h for different values of α. A small chart is also embedded to illustrate the SWCC of soil (Eq. (5.8b)), where the values of θ_s and θ_r are given to 0.4 and 0.1, respectively. The initial profiles are identical for the three cases from soil saturated. It can be seen that the smaller the α value, the deeper drying front advances. In addition, the three profiles intersect, in other words, the water content

for a smaller α value is large above but smaller below the intersect point than that for a larger α value. This may be explained by considering the embedded small chart: the soil with a larger α value possesses a lower water retention ability than a soil with smaller α. Because of the lower water retention ability, more water tends to be evaporated loss the shallow soil, resulting in a larger reduction in the soil water profile near the soil surface but less reduction in the deep soil layer.

In the current study, the α value has a significant effect on the water content distribution, which is in consensus with Zhan and Charles (2004), while it is apparently contradictory to the conclusion drawn by Kasim et al. (1998). The inconsistent conclusion seems to be caused by the narrow range of α value considered in Kasim et al.'s study (i.e. from 0.15 to 0.25).

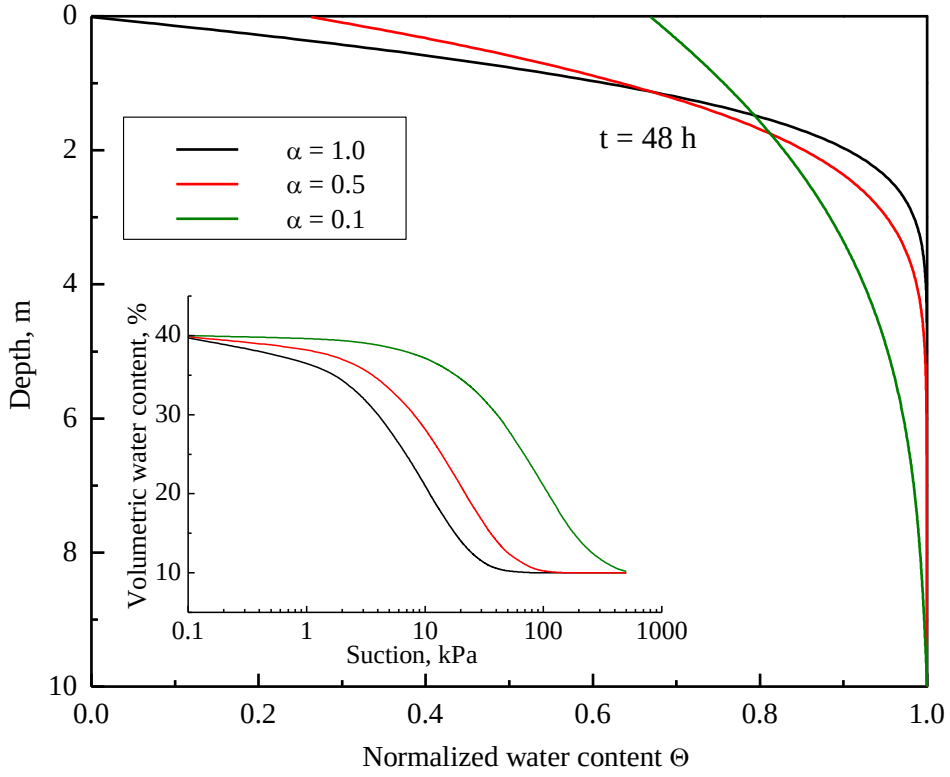

Figure 5.14 Soil water content profiles with respect to different α

5.5.2 INFLUENCE OF WATER STORAGE CAPACITY, (θ_s -θ_r)

Water storage capacity of a soil, (θ_s -θ_r), is equals to the difference between the saturated and residual volumetric water content, it is a measurement of the maximum amount of water that can be absorbed or desorbed by capillary action. It is somewhat

different from the soil's water retention ability. Generally, the value of (θ_s -θ_r) increases with pore sizes. To some extent, it is also related to the void ratio.

Figure 5.15 shows three water content profiles at t = 48 h for different (θ_s -θ_r) values (i.e., 0.2, 0.3, 0.4). For a given value of θ_r = 0.1, small chart showing the SWCC is embedded in Figure 5.15. It clear shows that different values of (θ_s -θ_r) will leads to different relationships between matric suction and volumetric water content. Figure 5.15 illustrates that (θ_s -θ_r) mainly affects the magnitude of the water content but not the shape of the profiles. A larger value of (θ_s -θ_r) represents a higher water storage capacity, which result in a low advance rate of drying front. The lower advance rate of drying front is not due to a low hydraulic conductivity, but due to the storage requirement of the shallow depth. Since the horizontal axis value of Θ is related to the (θ_s -θ_r) as formulated by Eq. (5.10), which may result in the intersections for the soil profile curves. In addition, the effect of (θ_s -θ_r) appears to be not so great as the effects of α value on water content profile.

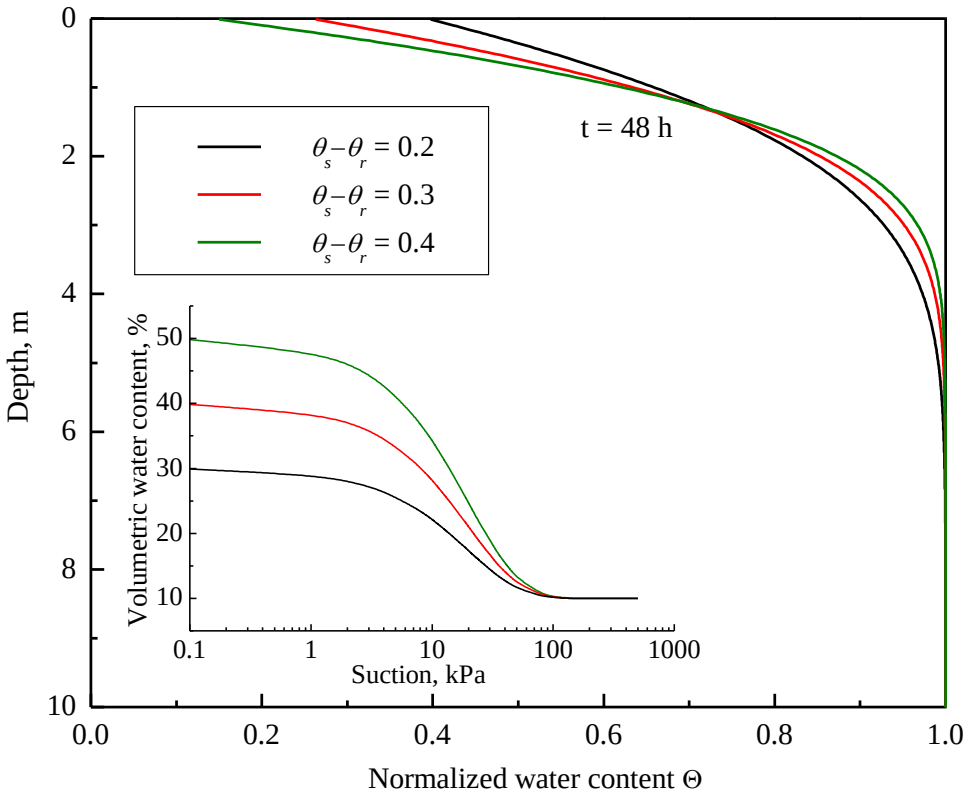

Figure 5.15 Soil water content profiles with respect to different (θ_s -θ_r)

5.5.3 INFLUENCE OF SATURATED PERMEABILITY (K_s)

Two extreme cases of the evaporation problem can be first considered: the permeability tending to zero and that tending to infinity. At the former extreme there will be little water evaporated out from the soil stratum, which would only occurs at the shallow depth, and hence little drop in the initial soil water content profile. At the latter extreme, water will be evaporated loss easily but will immediately capillary up through the boundary water table. So again, there is little decrease in the initial water content profile. However, at intermediate values of permeability water will evaporated loss with not activating the water supply. This implies that a critical saturated permeability may exist and result in the greatest reduction of water content profile.

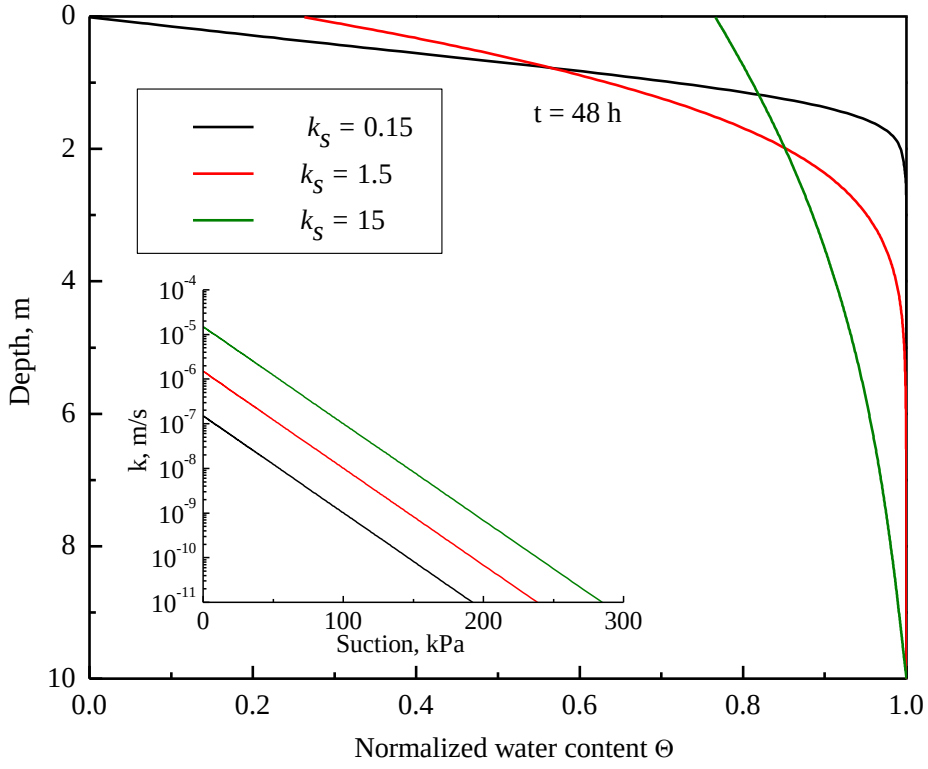

Figure 5.16 Soil water content profiles with respect to different k_s

Figure 5.16 shows a series of water content profile with respect to three different values of saturated permeability (i.e., k_s = 1.5×10^{-7}, 1.5×10^{-6}, and 1.5×10^{-5} m/s). The embedded small chart illustrate the relationship between the permeability and the water content for different values of k_s. As mentioned before, the initial

condition is uniformly saturated for the three cases. Figure 5.16 shows that the saturated hydraulic has a significant influence on the water content redistribution. First, the greater the values of k_s, the deeper the drying front. On the other hand, if the k_s values is relatively small with respect to the applied evaporation rate, the water content near the ground surface decreases greatly, however, the drying front is relatively shallow after a certain duration of evaporation. This is because the evaporation mainly occurs in the shallow water layer due to the low k_s values, and then gradually extends to the soil below. In contrast, for a relatively large value of k_s the capillary would be easier, and hence the evaporated water are distributed more uniformly over the depth, so a smaller reduction in water content profile will be observed in the shallow soil layer.

As mentioned previously, there is a critical saturated permeability, which leads to greatest reduction in soil water profile in a evaporation system. A further observation of Figure 5.16 indicates that the area between initial profile and the one at t = 48 h tends to be largest for $k_s = 1.5\times10^{-6}$ m/s, which means that this value brings about the greatest total reduction in water content profile among the three cases considered. This value is closest to the imposed evaporation rate. This indicates that the critical value may be close to the saturated permeability.

5.5.4 INFLUENCE OF EVAPORATION RATE (E)

The evaporation rate is the main external factor that affecting soil water redistribution during evaporation process. In order to evaluate the influence of E, five cases are investigated in Series 4 (Table 5.3), the value of E is set to different times per k_s. Figure 5.17 shows the result of simulation. First, it can be seen that E affects the water content profile significantly. It is easily imagined that the larger the E value, the more reduction of water content profile would be caused by the E. When the E value is smaller than the saturated permeability k_s, i.e., $E/k_s<1$, the difference among water content profiles is small, the normalized water content Θ still can retain at around 0.7 after 48 h evaporation for the case of $E/k_s=1$. If the value of E is greater than k_s, at this condition the water supply cannot achieve the evaporative demand, the water content will reduce quickly, and a dry layer would be performed after a period, for example the curve of water content profile at $E/k_s=10$.

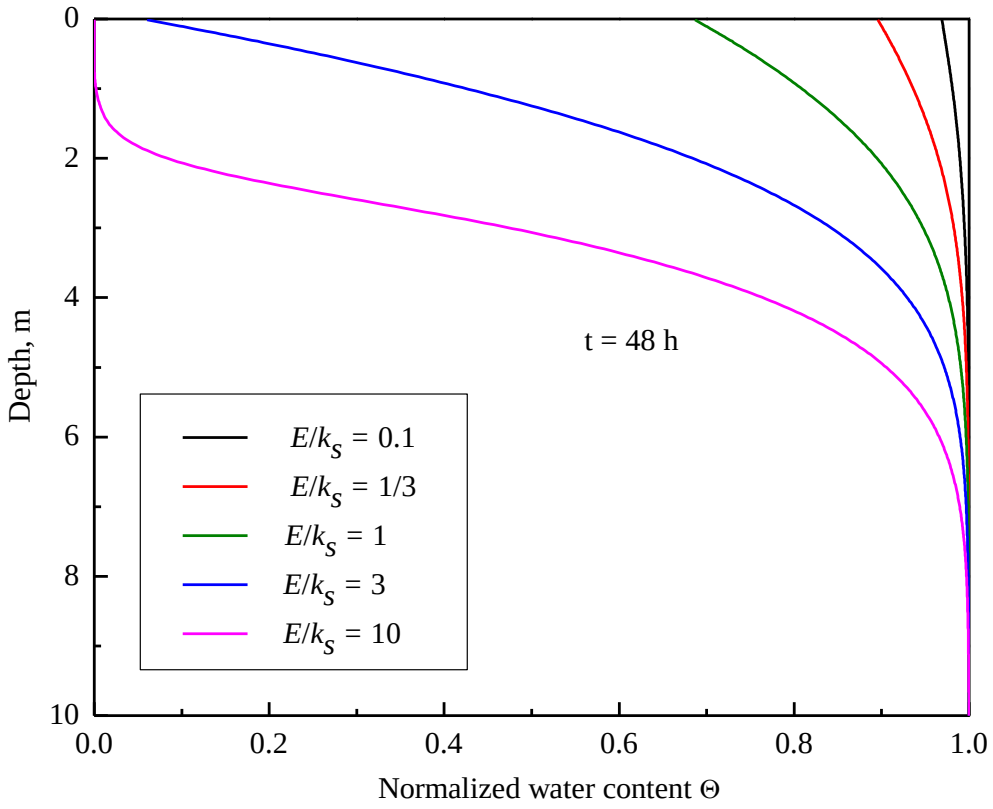

Figure 5.17 Soil water content profiles with respect to different E/k_s

5.5.5 INFLUENCE OF WATER TABLE (L)

The depth of water table is another external factor that affects the soil water redistribution. In general, it would be easy to reach an equilibrium state where the water content will be nearly stable. To investigate the mechanism of water table depth affecting soil water profile, the parameter study is conducted with the indexes set as Series 5 in Table 5.3, three degrees of water table depth is adopted, 2 m, 5 m, and 10 m, respectively.

Firstly, for each case, the variation of water content at two depths of 0.2 m and 1m is computed and plotted in Figure 5.18. The duration of evaporation for simulation is 300 h. It shows that the lower depth the water table, the earlier the soil reaches equilibrium state. For the case of L = 2 m, similar time is consumed to achieve the equilibrium state for the different depths of 0.2 and 1 m, however, the finial water content state is varies with the depth. It also can be seen that the curves are almost overlaid each other for L = 5 m and L = 10 m. It is to say, 5 m is already the extreme water table condition for the monitor depth both 0.2 m and 1 m. It can be

concluded soil water content at depth of z m would be unaffected by the water table L in the case of $z/L \leq 0.2$.

To investigate the influence of z/L, the soil water content at different depths are collected to analyze. Figure 5.19 shows the variation of water content respect to different value of z/L. In this Figure, the solid line or dot in black, magenta, and blue are corresponded to the z/L at 0.1, 0.4 and 0.8, respectively. It is deduced that the lower ratio of z/L always results in greater reduction of soil water profile. Comparing the curves in same z/L value, the water content with larger water table depth usually reaches equilibrium state at earlier time.

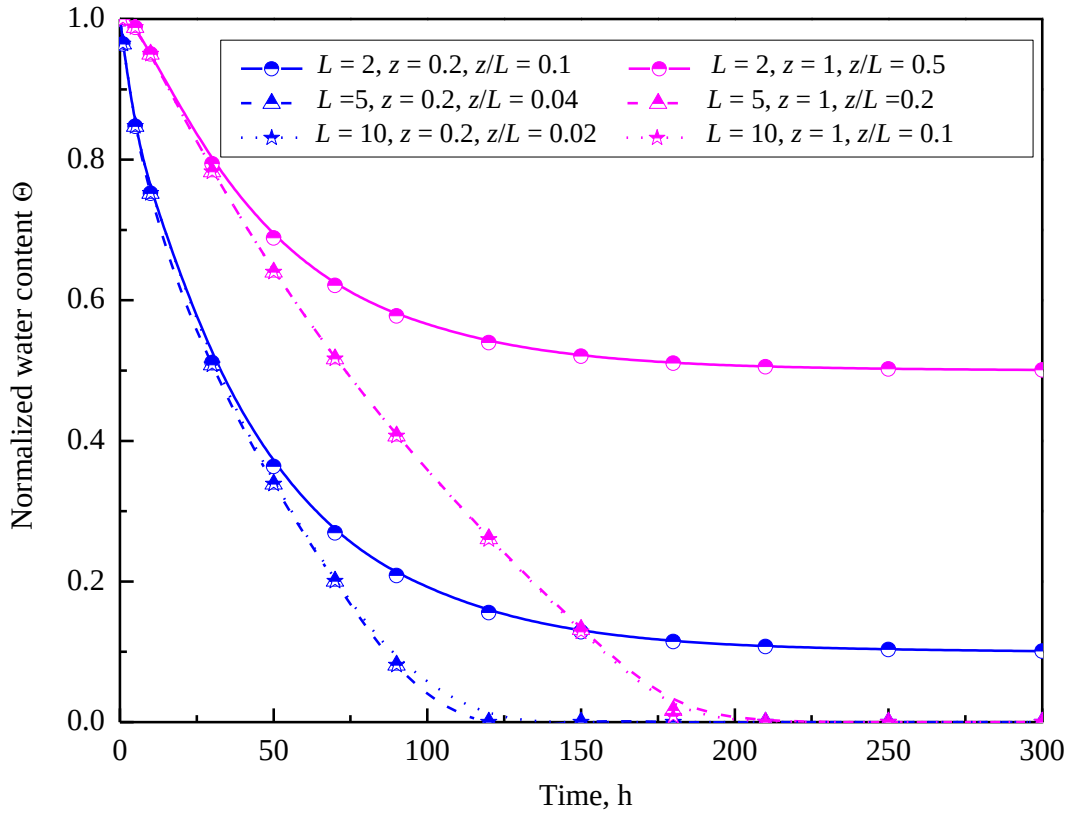

Figure 5.18 Variation of soil water content at depths of 0.2 m and 1 m for different water table conditions

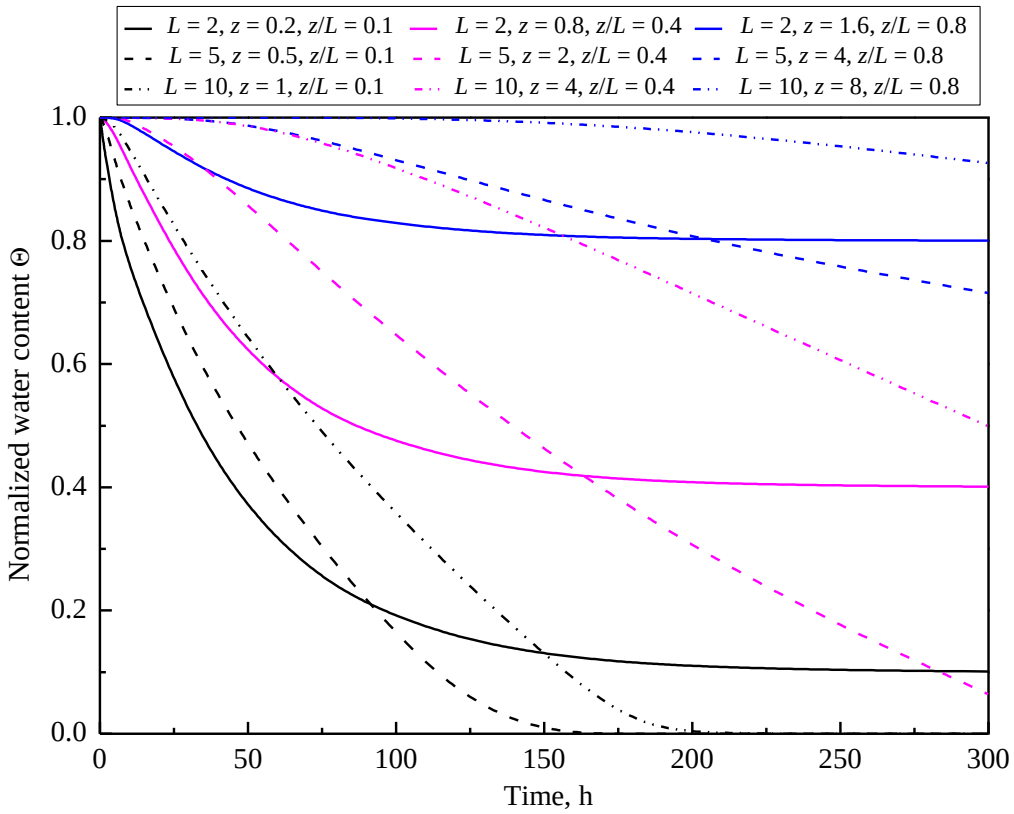

Figure 5.19 Variation of soil water content versus elapsed time for different rate of *z*/*L*

5.6 SUMMARY

To investigate the water content distribution during evaporation process that is the soil water properties variation reflected to the evaporation process, This chapter is extended from the aspects as: analytical development for modeling soil water dynamic, the laboratory experiment to verify the proposed model, and finally the parameter study based on the model. The main conclusions can be remarked like that:

(1) Based on some assumptions and linearization of Richards' equation, the analytical models for two evaporation problems are developed, which are the evaporation process from infinite soil domain, evaporation process with water table. In this model, the basic hydraulic parameters k_s, α, (θ_s -θ_r) and constant evaporation rate E are the inputs for simulating instantaneous water content profile. And the model in these two cases can comprise the normal problem dealing with evaporation problem.

(2) The column experiments were conducted to verify the proposed model in

two groups. In first group, the atmosphere condition was controlled in three cases with no water supply to the soil column, while the water table was the key parameter in the second group. By comparing the experimental result and the simulation, the proposed model is found to be competent for simulating soil water distribution during evaporation process.

(3) Finally, the parameter study is conducted for investigating the influence of soil hydraulic properties (k_s, α, (θ_s -θ_r)) and external factors (E, L) on soil water distribution during evaporation. The new findings from are summarized as follows, among the three hydraulic parameters, the effects of α value and k_s on soil water profile response are much more significant than that of (θ_s -θ_r). The smaller value of desaturation coefficient α, the deeper drying front advances; the greater the values of k_s, the deeper the drying front; (θ_s -θ_r) mainly affects the magnitude of the water content but not the shape of the profiles. E affects the water content profile significantly, the larger the E value results in the more reduction of water content profile. In the case of $z/L \leq 0.2$, soil water content at depth of z would be unaffected by the water table L, and the lower ratio of z/L always results in greater reduction of soil water profile.

REFERENCE

Abramowitz, M., and Stegun, I.A. (1965): Handbook of mathematical functions. Dover Publication, New York.

Basha, H.A. (2003): Multidimensional linearized nonsteady infiltration toward a shallow water table. Water Resource Research, 36(9), 2567-2573.

Bonsu, M. (1997): Soil water management implications during the constant rate and falling rate stages of soil evaporation. Agric. Water Management, 33, 87-97.

Brutsaert, W., and Chen, D., 1995: Desorption and the two stages of drying of natural tallgrass prairie. Water Resources Research, 31(5), 1305-1313.

Carslaw, H.S. and Jaeger, J.C. (1959): Conduction of heat in solids, 2nd edition, Clarendon, Oxford, England.

Chen, J.M., Tan, Y.C., and Chen, C.H., and Parlange, J.Y. (2001): Analytical solutions for linearized Richards' equation with arbitrary time-dependent surface fluxes. Water Resource Research, 37(4), 1091-1093.

Chen, J.M., Tan, Y.C., and Chen, C.H. (2003): Analytical solutions of one dimensional infiltration before and after ponding. Hydrological Process, 17,

815-822.

Gardner, W.R. (1958): Some steady-state solutions of the unsaturated moisture flow equation with application to evaporation from a water table. Soil science, 85, 228-232.

Gardner, W.R. (1959): Solutions of the flow equation for the drying of soils and other porous media. Proceedings - Soil Science Society of America, 23(3), 183-187.

Ghotbi, A.R., Omidvar, M., and Barari, A. (2011): Infiltration in unsaturated soils-an analytical approach. Computers and Geotechnics, 38, 777-782.

Hill, D. (1971): Soil and water, physical principles and processes. New York: Academic Press, Inc, 1971.

Kasim, F.B., Fredlund, D.G., and Gan, J.K.M. (1998): Effect of steady state rainfall on long term matric suction conditions in slopes. Proc., 2nd int. conf. on unsaturated soil, vol. 1, Beingjing, 78-83.

Menziani, M., Pugnaghi, S., Vincenzi, S., Santangelo, R. (2005): Water balance in surface soil: analytical solutions of flow equations and measurements in the Alpine Toce Valley. In:de Jong, C., Collins, D., Ranzi, R. (Eds.), Climate and Hydrology in Mountain Areas. Wiley, New York, 84-100.

Menziani, M., Pugnaghi, S., Vincenzi, S. (2007): Analytical solutions of the linearized Richards' equation for discrete arbitrary initial and boundary conditions. Journal of Hydrology, 332, 214-225.

Nachabe, M.H., Islas, A.L., and Illangasekare, T.H. (1995): Analytical solutions for water flow and solute transport in the unsaturated zone. Models for Assessing and Monitoring Groundwater Quality (Procsedings of a Boulder Symposium July 1995). IAHS Publ. no. 227.

Nasseri, M., Daneshbod, Y., Pirouz, M.D., et al. (2012): New analytical solution to water content simulation in porous media. Journal of Irrigation and Drainage Engineering, 138(4), 328-335.

Richard, B. (2007): Applied partial differential equations, with Fourier series and boundary value problems (fourth edition). China Machine Press.

Richards, L.A. (1931): Capillary conduction of liquids through porous mediums. Physics, 1: 318-333.

Ritchie, J.T. (1972): Model for predicting evaporation from a row crop with incomplete cover. Water Resources Research, 8, 1024-1213.

Serrrano, S.E. (1998): Analytical decomposition of the nonlinear unsaturated flow equation. Water Resources Research, 34(3), 392-407.

Shokri, N., and Or, D., 2011: What determines drying rate at the onset of diffusion controlled stage-2 evaporation from porous media? Water Resource Research, 47, W09513, doi:10.1029/2010WR010284.

Srivastava, R., and Jim Yeh, T.C. (1991): Analytical solutions for one dimensional, transient infiltration toward the water table in homogenous and layer soils. Water Resources Research, 27(5), 753-762.

Suleiman, A.A. and Ritchie, J. T., 2003: Modeling soil water redistribution during second stage evaporation. Soil Science Society of America Journal, 67, 377-386.

Yanful, E.K. and Mousavi, S.M. (2003): Estimating falling rate evaporation from finite soil columns. The Science of the Total Environmental, 313, 141-152.

Yanful, E.K. Mousavi, S.M., Yang, M.D. (2003): Modelling and measurement of evaporation in moisture-retaining soil covers. Advances in Environmental Research, 7, 783-801.

Yuan, F., and Lu, Z. (2005): Analytical solutions for vertical flow in unsaturated, rooted soils with variables surface fluxes. Vadose Zone Journal, 4, 1210-1218.

Yunusa, I.A.M., Sedgley, R.H., and Tennant, D. (1994): Evaporation from bare soil in south-western Australia: a test of two models using lysimeter. Australia Journal of Soil Research, 32, 437-446.

Zhan, L.T., and Charles, W.W.Ng (2004): Analytical analysis of rainfall infiltration mechanism in unsaturated soils. International Journal of Geomechanics, 4(1), 273-284.

CHAPTER 6

IN SITU EVALUATION OF SOIL-ATMOSPHERE INTERACTION

6.1 INTRODUCTION

Climate conditions have an important influence on the behavior of soil through soil-atmosphere interaction. For example, the evaporation and perception and evaporation always change the water content distribution or the pore water pressure profile as shown in Figure 6.1. To understand the evaporation process in natural condition, evaporation mechanism and soil water dynamic during a given period are evaluated together with analyzing the perception process. Based on the lysimeter test that conducted in field, the simulation and analysis are presented in this chapter.

Lysimeters are still considered as the standard method to directly measure actual evaporation. Unlike laboratory experiments, which are mostly performed under very controlled conditions (e.g. homogeneous, saturated steady-state flow conditions, and controlled uniform climatic conditions), lysimeter experiments generally simulate actual field conditions. Lysimeter experiments are suitable for verification of results obtained in the laboratory and for demonstrating similarities and differences between field experiments and laboratory experiments. Lysimeter tests therefore play an important role in the interpretation of laboratory test results with respect to field conditions.

Many studies involving lysimeter can be found in literature, and each study provides useful information about the use, design and operation of lysimeter. Much of the experience of lysimeter tests has been associated with soil science. Lysimeter have a long history of development and different designs have been used (Howell et al., 1991). They have been designed in different shapes and sizes. Shapes include square, circular and rectangular. The size of lysimeter also varies significantly. The size is a function of the intended use and the required or desired resolution (Marek et

al., 1988; Young et al., 1997; Schneider et al., 1998; Yang et al., 2003; Marek et al., 2006). Lysimeter can be weighing and non-weighing. The non-weighing types are used to determine evaporation as a residual by measuring all other components of the soil water balance, including water inputs (rain and irrigation), outputs (drainage and runoff), and change in soil water storage. Weighing lysimeter, on the other hand, measure evaporation directly by measuring the change in mass of an isolated soil volume. The evaporation calculated from the mass changes, however, needs to be adjusted to account for mass changes caused by factors other than ET, such as drainage or water input (Malone et al., 2000). Weighing lysimeter have been designed using different weighing mechanisms. Weighing mechanisms include hydraulic, suspended load cells, deck scales, load cells installed at the bottom of the lysimeter, single load cell with counter-balance, and flexure level action balance with a load cell (Payero and Irmak, 2008).

In order to model the changes in water content and suction due to climate effects in a soil profile during a given period, it is necessary to consider two significantly different boundary conditions. Lysimeters are set up to supply data that correspond closely to those that would be obtained under natural conditions. For a given soil, when the evaporation is calculated, the boundary in term of water flux is determined. Further coupled analysis using numerical simulation approach or analytical approach can be performed in order to determine the soil water variations. This is the common practice in the field of agronomy, in this chapter, we will also follow the approach to introduce the in situ lysimeter test.

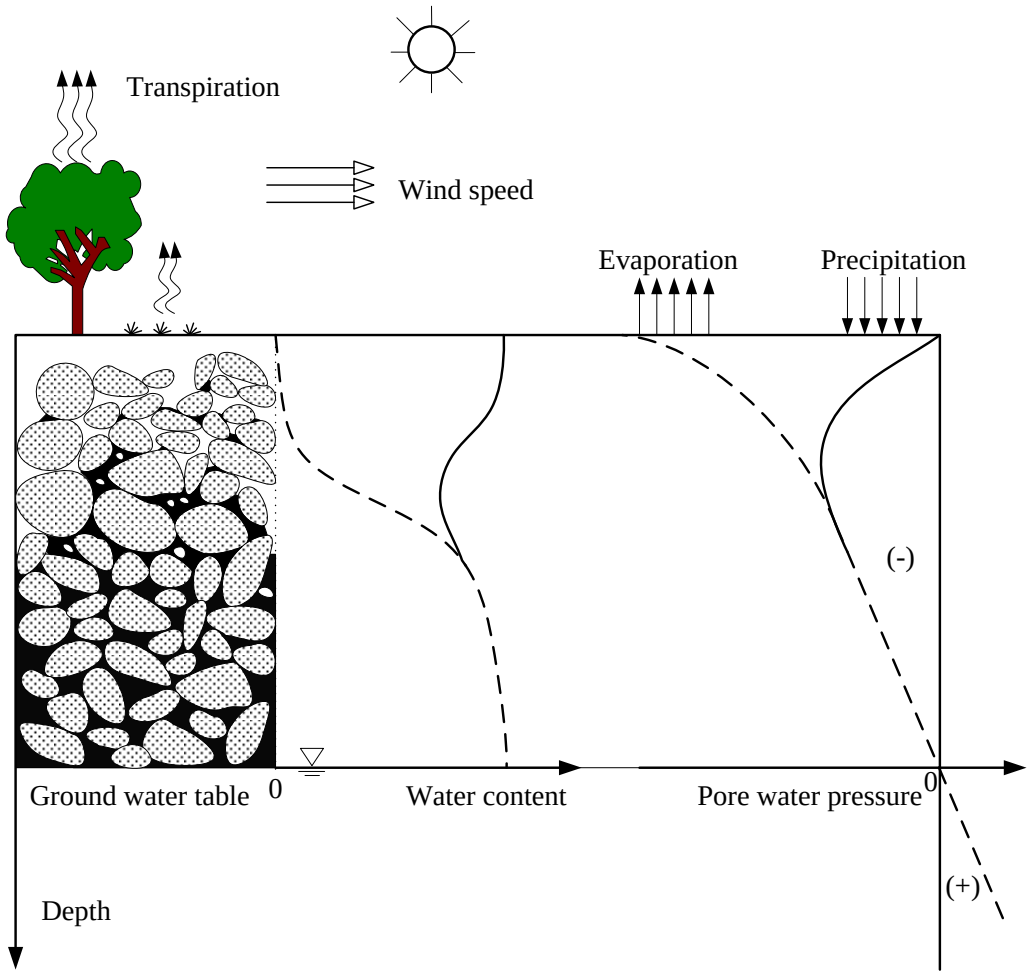

Figure 6.1 Schematic diagram of soil water distribution due to soil-atmosphere interaction

6.2 IN SITU LYSIMETER EXPERIMENT

6.2.1 DESIGN AND CONSTRUCTION

The general concept of a weighing lysimeter requires four major elements. These include the container to hold the soil, water and vegetation; a rigid foundation; the force measuring or weighing system; and the data acquisition and analysis system. Accessory instrumentation is also required to measure and record climatic data. The design criteria for the lysimeter developed in this study are that (1) able to continuously monitor evaporation at the resolution of an hour; (2) easily and rapidly deployed; (3) economical to construct and install. To meet these requirements as well as those of lysimeters in general, a number of constraints must be optimized. A field

lysimeter facility was developed by geotechnical engineering laboratory aiming to obtain high sensitivity and precision combined with a low construction cost and simplicity of installation. The studied area is located at Ito campus of Kyushu University, Nishi-ku, Fukuoka-shi, Japan (33.3°N, 130.2°E). The location of the studied area is presented in Figure 6.2. This site is a field testing area of Kyushu University, moreover, geotechnical engineering research laboratory developed several field testing system in this area. This location will facilitate providing the necessary management to insure continuous and reliable operation.

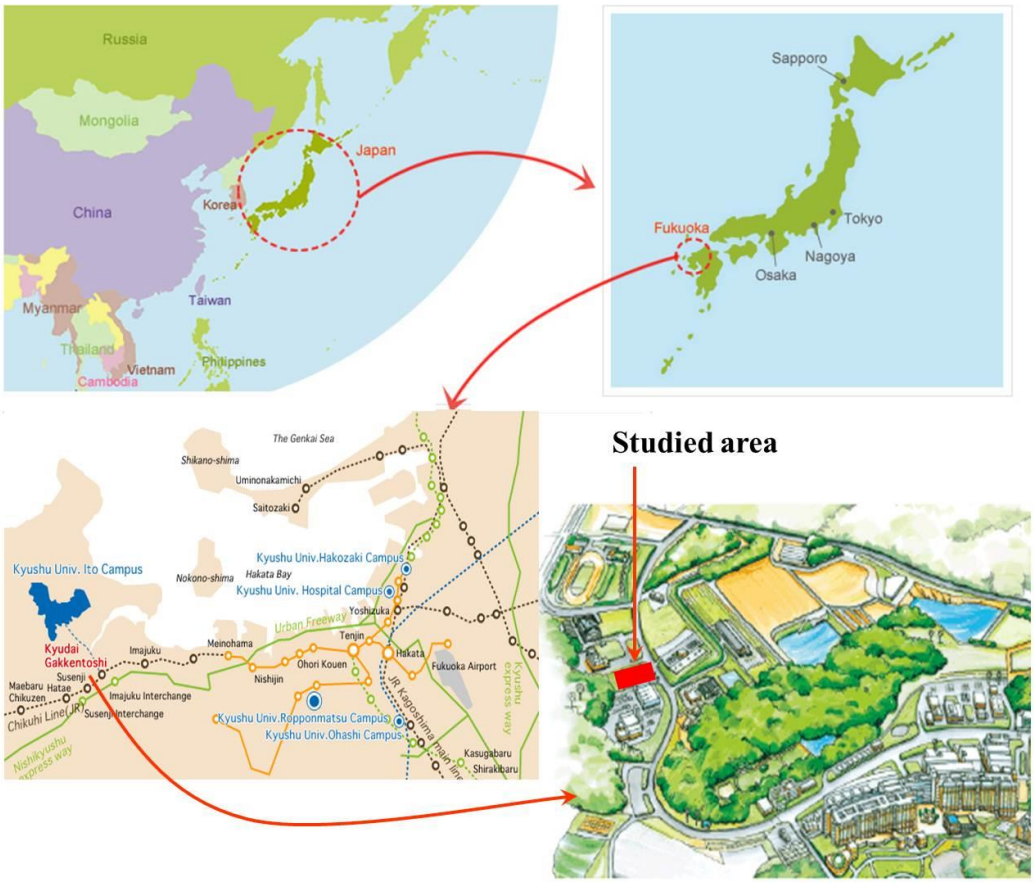

Figure 6.2 The location of studied area

No.	Accessory	No.	Accessory
a	Data logger	h	Protection shield
b	Computer	i	Soil column
c	GL220	j	Load cell
d	Data logger	k	Thermocouples
e	Drainage tank	l	Water sensor
f	Plastic tube	m	Weather station
g	Scale		

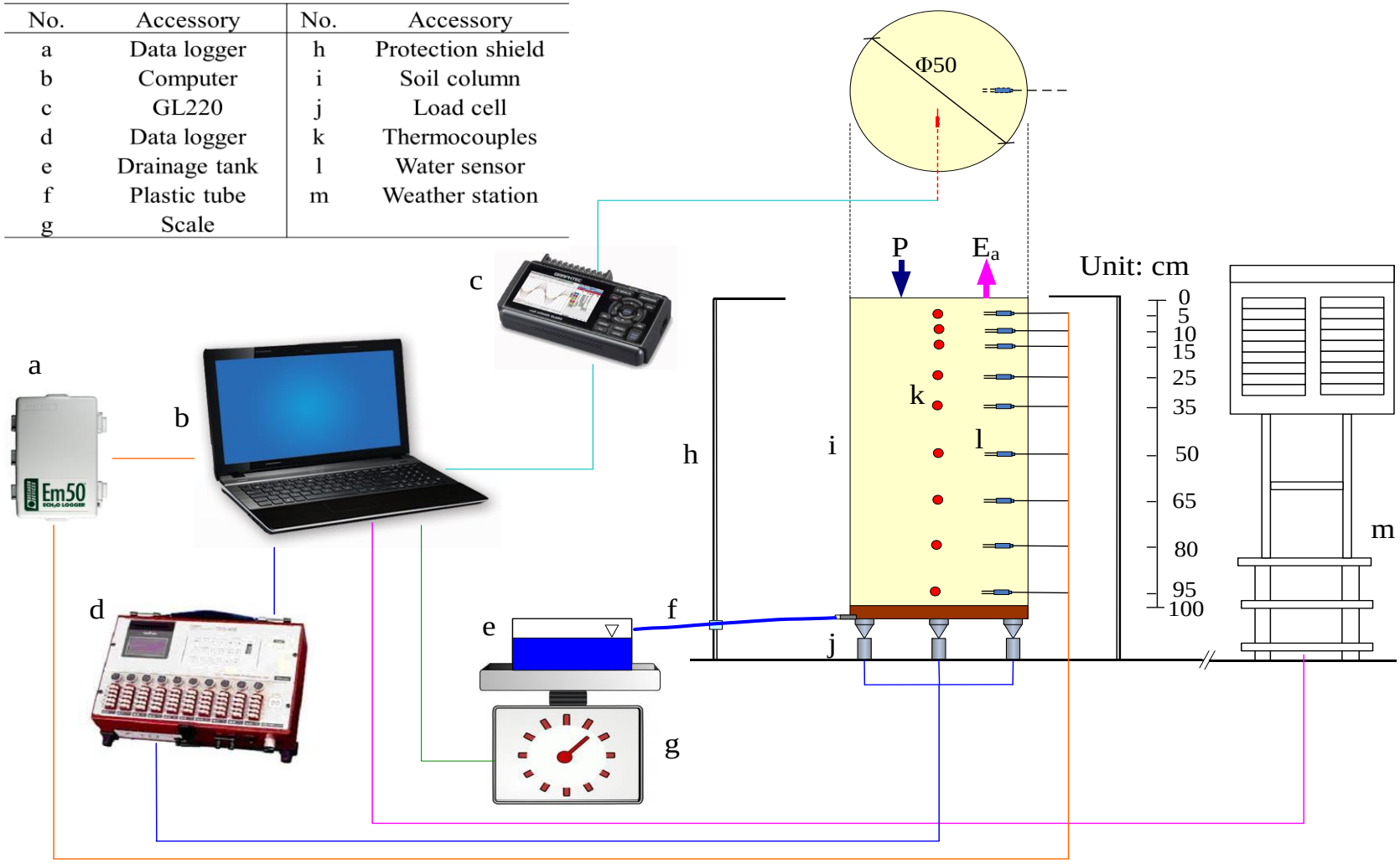

Figure 6.3 Schematic illustration of lysimeter tests

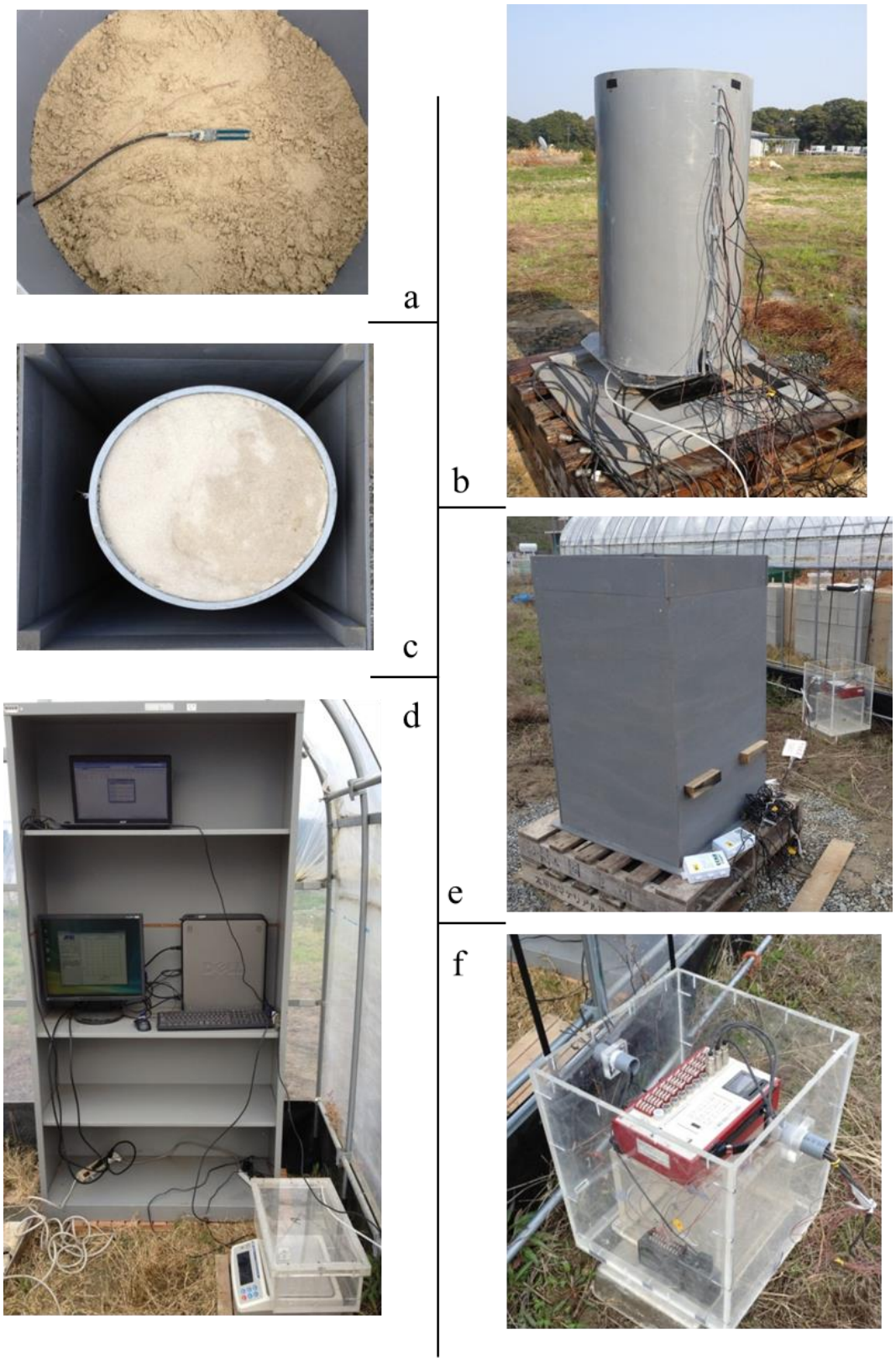

Figure 6.4 Photos of the lysimeter test, (a) thermocouple and water moisture probe, (b) soil column, (c) bird view of lysimeter, (d) data acquisition system, (e) final appearance

A layout of the instrumentation is presented in Figure 6.3, the photo graphics of the equipment are presented in Figure 6.4. A Cylindrical undisturbed lysimeters is performed, whose soil container is made of PVC material (height 105 cm, diameter 50 cm, and wall thickness 1.5 cm). At the bottom of cylinder, a 5 cm drainage layer is set and connected to a polyethylene tube allowing the water flow out. A steel plate is assembled at the bottom of lysimeter to support the reinforce of system and to prevent the bottom plastic plate from bending. Three electronic load cells (Kyowa Co. Ltd) are equipped as equilateral triangle on the steel plate such that the lysimeter can stand stably. A plank protection shield is to insure the lysimeter from the influence of wind speed during weight measuring. The height of protection shield is 105 cm, the length and width are same at 60 cm. Nine thermocouples (Graphtec corporation) and nine water moisture probes (EC-5, Decagon Devices) are inserted to the cylinder to measure the instantaneous temperature and volumetric water content as shown in Figure 6.3, respectively.

A cuboid Tank (height 20cm; weight 20cm; length 40cm) made of transparent acrylic material allows for collecting all the water percolated. A polyethylene tube connected the tank to the bottom of the tank to be used as drains. A scale (GX-32K, AND Co. Ltd, 0.1g solution) gives a continuous weight measurement of both tank and collected water. The outputs of the load cells are recorded in a specific time interval using a TDS-102 data logger (Kyowa co. Ltd), the load cells are connected directly to the data logger, and the output of each load cell is recorded separately in addition to the sum of the outputs of all three load cells. The thermocouples are connected to a midi Data Logger (GL220, Graphtec corporation) for the acquisition of temperature data. Two automatic ECH2O dielectric aquameters (Decagon Devices) are connected with the soil moisture probe to collect the water content. Then all the data is accessed and stored by computers by specific data acquisition software. For the accuracy of lysimeter, Payero and Irmak (2008) indicated that lysimeter accuracy depends on the lysimeter area, mass, and the type of scale. In this study, the total solution of the load cells are 75 g that equals to 0.38 mm of water change in soil specimen.

The weather data was available from Ito campus of Kyushu University and weather station in Itoshima city belonging to Japan meteorological Agency, which is about 3 km away from the field test area. The weather station can provide the climatic parameters as rainfall; air temperature; air humidity; solar radiation; wind speed. Daily meteorological variables used in this study are summarized in Table 6.1.

Table 6.1 Weather variables recorded by the weather station

Items	Reporting interval
Precipitation, mm	Daily total, hourly
Air temperature, °C	Daily average, daily max/min, hourly
Relative humidity, %	Daily max/min ,hourly
Solar radiation, kW/m^2	Daily total, hourly
Wind speed, m/s	Daily average hourly

6.2.2 EXPERIMENTAL PROCEDURE

A solid foundation to support the mass of the lysimeter boxes was firstly constructed. Two leveled wooden frames (100 cm × 100 cm × 15 cm height) were constructed on top of the foundation. The surface of the wooden frames is set as even level. Then lysimeter was installed stably. Sampling or insulation of test material for the lysimeter is an important step in the lysimeter-leaching methodology. In this step, the characteristics of the test material can be altered by affecting either the physical properties as for example the macro pore structure by contaminating the sample. In this study, the K-7 sand was selected as the material due to its fine permeability and low swelling and shrinkage properties during wetting or drying. When packing the dry soil into the container, each time a layer of approximately 10 cm was added, and the compaction energy applied to the soil surface to achieve the maximum dry density. At this time, the soil moisture probes and the thermocouples access tube were installed at different heights. When all the soil layers were in place, soil surface was made to be calm with reserving 2 cm from top edge of the container, which ensures the soil not being flowed out during test. After the fabrication of the lysimeter, water was supplied smoothly from the soil surface to saturate specimen. The infiltration process lasted about half hour until the water percolated from the drainage tube at the bottom of the container. Then water supply was stopped and the soil surface was covered by a plate. The drainage process continued about 3 days and then the initial condition was performed. At last, the protection shield was installed on the bottom plate, and all the probes were connected to corresponding data logger.

Following installation of the lysimeter in the field, a calibration routine was followed to ensure the proper functioning and accuracy of the load cells. A series of known weights was placed one at a time on the lysimeter, and the total lysimeter weight was recorded. The weights were then removed one at a time, and the total

lysimeter weight was recorded. The changes in weight recorded by the load cells were then calculated and compared to the known changes in weight.

The lysimeter was installed in 23rd, March of 2013, and the test started from 27th, March to 15th, June of 2013, the duration was nearly 80 days. The measured data included: the weights of lysimeter, weight of percolated water, the instantaneous data of soil water content and soil temperature profile, the weather indexes. All the data were registered electronically at 15 min intervals.

6.3 NUMERICAL SIMULATION FOR FIELD TEST

6.3.1 DESCRIPTION OF HYDRUS-1D CODE

The coupled movement of liquid water, water vapor, and heat in the subsurface, as well as interactions of these subsurface processes with the energy and water balances at the soil surface, is implemented in the HYDRUS-1D code. The HYDRUS-1D is widely used, well-documented, and tested public domain code for simulating water and solute transport in soil (Saito et al., 2006). Therefore, HYDRUS-1D is adopted as the countermeasure for numerical simulation to supply a comparison with the result of lysimeter test.

The HYDRUS-1D program may be used to analyze water and solute movement in unsaturated, or fully saturated porous media (Šimunek et al., 2005). The program numerically solves the Richards' equation for saturated-unsaturated water flow and Fickian-based advection dispersion equations for heat and solute transport. The governing flow and transport equations are solved numerically using Galerkin type linear finite element schemes. Integration in time is achieved using an implicit (backwards) finite difference scheme for both saturated and unsaturated conditions. Additional measures are taken to improve solution efficiency for transient problems, including automatic time step adjustment and adherence to present ranges of the Courant and Peclet numbers. Possible options for minimizing numerical oscillations in the transport solutions include upstream weighing, artificial dispersion, and/or performance indexing.

6.3.2 INPUT DATA

The hydraulic data of K-7 sand is summarized in Table 6.2, which is the input data of numerical simulation. The soil water retention curves were measured in the

laboratory using the Tempe Cell (Liu, 2010). The pore size distribution model of Mualem is used to predict the isothermal unsaturated hydraulic conductivity function from the saturated hydraulic conductivity as show in Eq. (6.1), the van Genuchten's model of the soil water retention curve is adopted as Eq. (6.2) (Mualem, 1976; van Genuchten, 1980).

$$k = k_s \Theta^l [1-(1-\Theta^{\frac{1}{m_v}})^{m_v}]^2 \tag{6.1}$$

$$\Theta = \frac{1}{[1+(-\alpha_v h)^{n_v}]^{m_v}} \tag{6.2}$$

Where k is unsaturated hydraulic conductivity, k_s is saturated hydraulic conductivity, Θ is normalized water content, l is pore connectivity parameter, α_v, n_v, m_v are fitting parameters. α_v is related to the air entry value, n_v is related to the pore size distribution of the soil, it reflects the slope of soil water retention curve, m_v is related to the overall symmetry of the soil water retention curve. The thermal properties of sand soil implanted in HYDRUS-1D are recommended in this study.

The upper boundary condition is the atmospheric boundary condition with surface layer, which consider no water runoff occurs during the tests. The boundary condition is the seepage face. Boundary conditions at the soil surface for liquid water, water vapor, and heat transport were determined from the surface water and energy balance equations. The initial water contents and soil temperature are determined from measured values at the first day. The soil profile is considered to be 100 cm deep, with observation nodes located at depths of 5 cm, 10 cm, 15 cm, 25 cm, 35 cm, 50 cm, 65 cm, 80 cm, and 95 cm. They are corresponded to the positions for thermocouples and soil water probe. A constant nodal spacing of 0.5 cm is used leading to 200 discretization nodes across the problem. Calculations are performed for a period of 81 days same with the monitored period.

Table 6.2 Parameters used for the numerical simulation of field lysimeter test

Soil	θ_r	θ_s	α_v	n_v	k_s	l
K-7	0.01	0.42	0.016	3.42	130	2.3

6.4 RESULT AND DISCUSSION

6.4.1 ANALYSIS OF FIELD MONITORED DATA

Meteorological data were recorded from 27th, March to 15th, June of 2013, which are presented in Figure 6.5. Six significant rainfall evens that over 20 mm/d were recorded as marked in Figure 6.5(a). The precipitation in April and June were 3.78 mm/d and 4.50 mm/d respectively, higher than that value in May of 1.07 mm/d (Figure 6.5 (b)). The solar radiation is almost constant for these days at about 0.21 kW/m^2. The air temperature varies between 3.4 °C and 30.7 °C, with a daily variation range at about 10 °C. Figure 6.5 (c) clearly shows that the average temperature has an increasing tendency during the period. The relative humidity in air varied between 30% and 90% (Figure 6.5 (d)). It remains more or less constant until to the end of May, and then it goes up day by day in June. The average wind speed was about 2.18 m/s, but several high speeds were recorded, for example, it reached 5.9 m/s and 5.5 m/s at 14th and 19th of April respectively.

Figure 6.6 presents the variation of soil volumetric water content over the whole monitoring period at different depths. Figure 6.6 (a) shows that the soil at the top 25 cm was observed a sharp increase in water content corresponding to each rainfall event. The heavier precipitation resulted in greater increase of soil water content. And also the more near to the soil surface, the greater increase occurs. The soil at 5 cm produced 13% increase of volumetric water content in average, while they were 9%, 5% and 3% for the soil at 10 cm, 15 cm, and 25 cm respectively.

It presents a gradual decrease of volumetric water content at the top 25 cm after rainfall, it is due to the infiltration to the deeper layer and the evaporation to the atmosphere. A higher rate of water content decrease was observed for the soil at lower position, which is mainly caused by the evaporation process since the infiltration can be regarded as same.

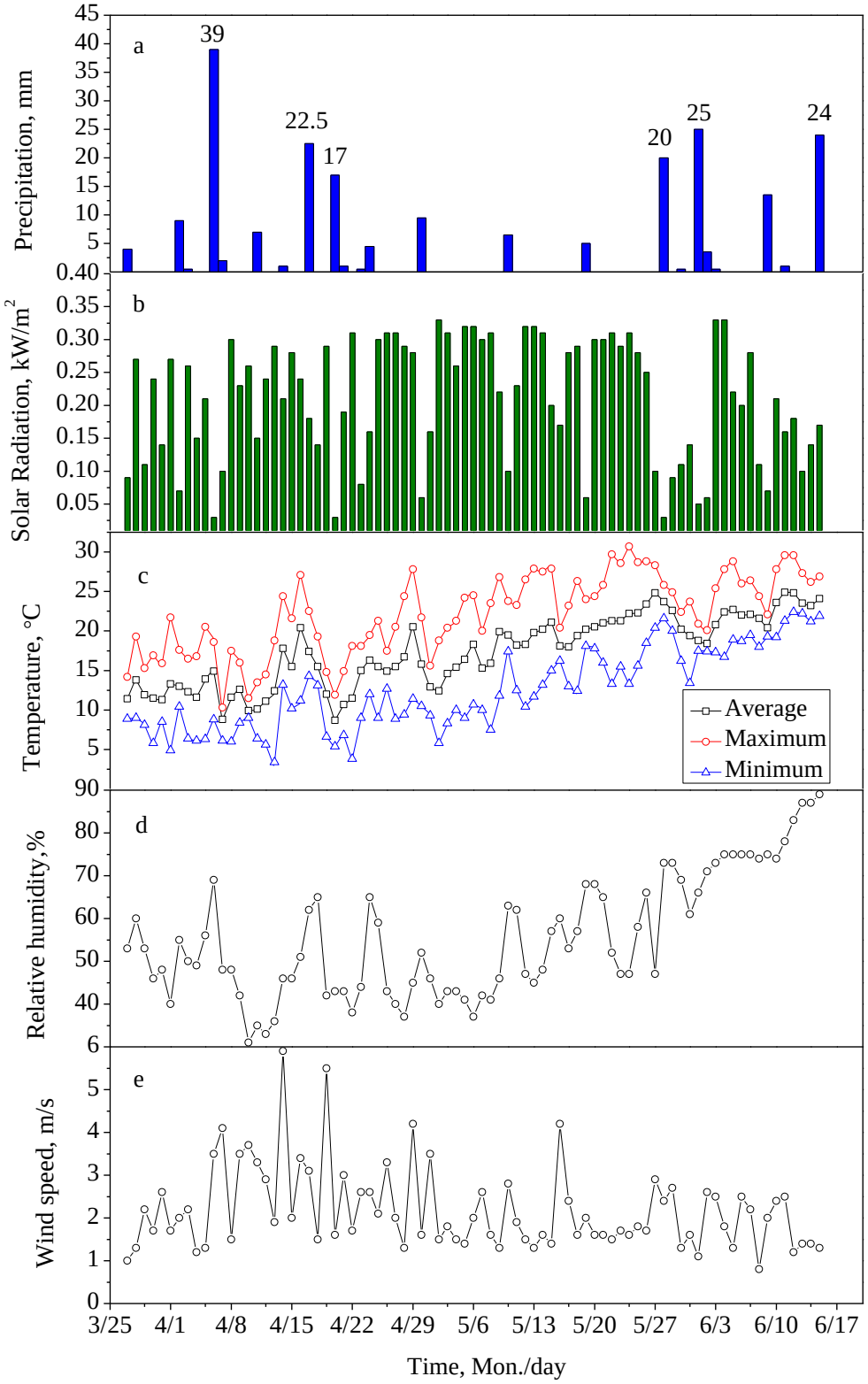

Figure 6.5 Meteorological data from Mar. 27, 2013 to Jun. 15, 2013. (a) precipitation, (b) solar radiation, (c) temperature, (d) relative humidity, (e) wind speed

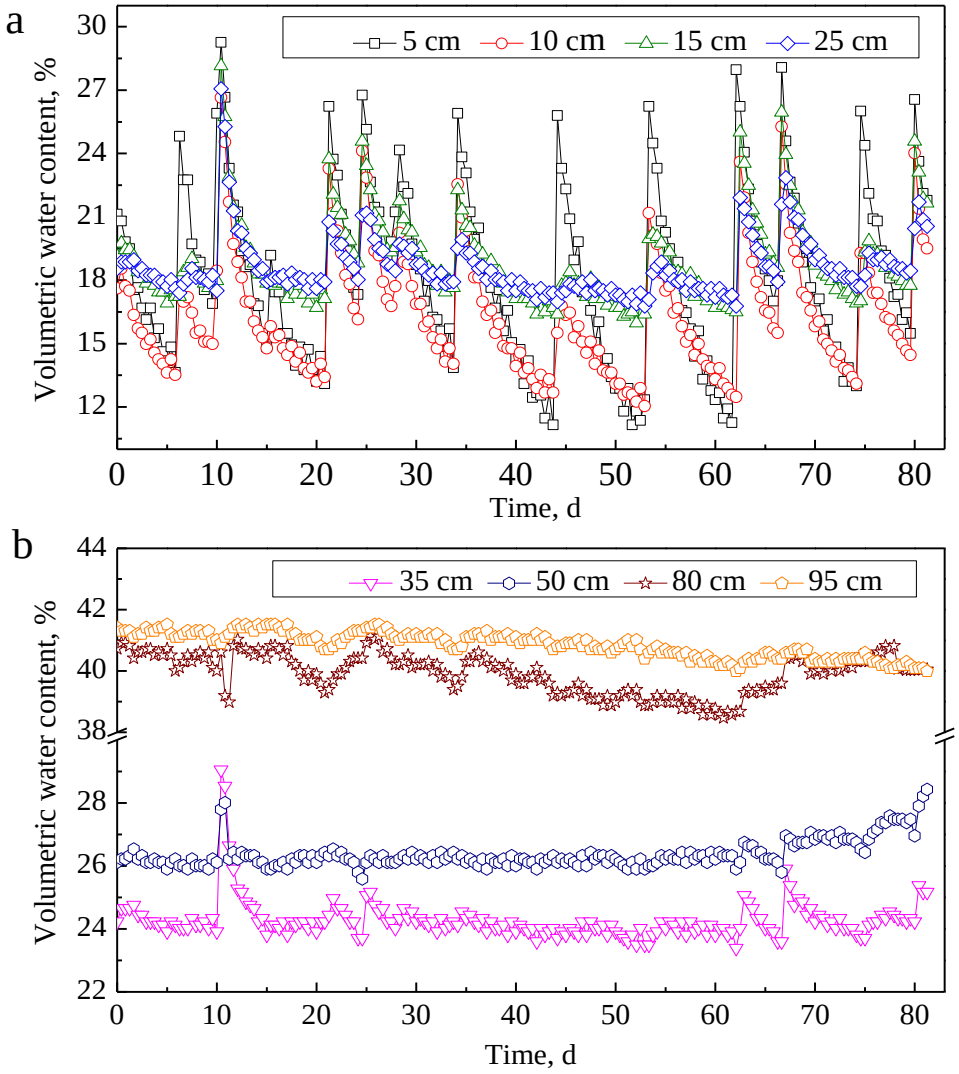

Figure 6.6 Variation of measured volumetric water content at different depths: (a) 5 cm ~ 25 cm, (b) 35 cm ~ 95 cm

Figure 6.6 (b) shows that no significant change of water content at depths of 35 cm and 50 cm was observed expect for the heavy rainfall event, for example, the rain fall in April 6th resulted in about 5% and 2% increase of water content for 35 cm and 50 cm respectively. at other days, constant values of 24% and 26% were recorded for these two depths. Due to the experimental problem, the water content probe at 65 cm could not supply satisfied result. No significant changes occurred in the depths of 80 cm and 95 cm, where the soil was stayed nearly saturation.

From the observations above, it seems that the a linear correlation between the precipitation/evaporation and volumetric water content changes at the top 25 cm, and

the lower soil depth, the greater change. No significant influence would produce for the precipitation/evaporation to the soil at deeper than 35 cm under the studied atmosphere condition.

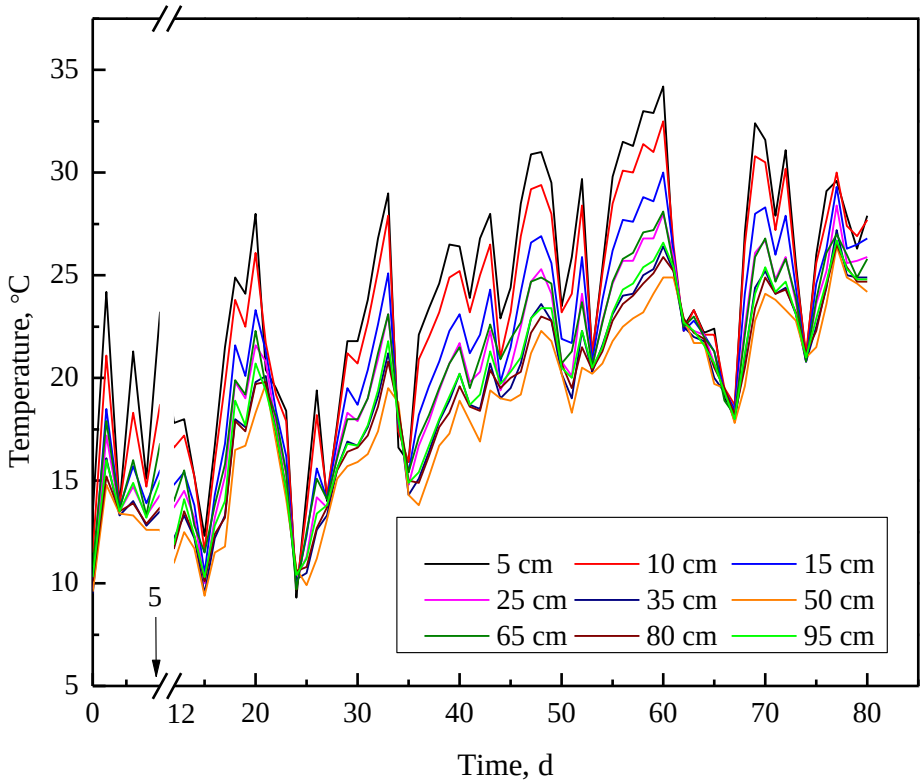

Figure 6.7 Monitored soil temperature variations at different depths during the test

Figure 6.7 presents the soil temperature measured at different depths during the test, where the daily temperature data at 14:00 pm are plotted against the elapsed time. Soil water temperature was not recorded from 04:00 of April 2nd to 16:00 of April 8th due experimental problems. It appears clearly that the lower the soil depth, the greater variation of soil temperature. The temperature at 50 cm seems to be the lowest value all the time, which may be due to the influence of external condition at lower boundary. Comparing with the time for precipitation, it also shows that the soil water content decreases after rainfall, and the temperature gradient becomes non-significant, that means the rainfall produce the tendency to uniform soil temperature profile.

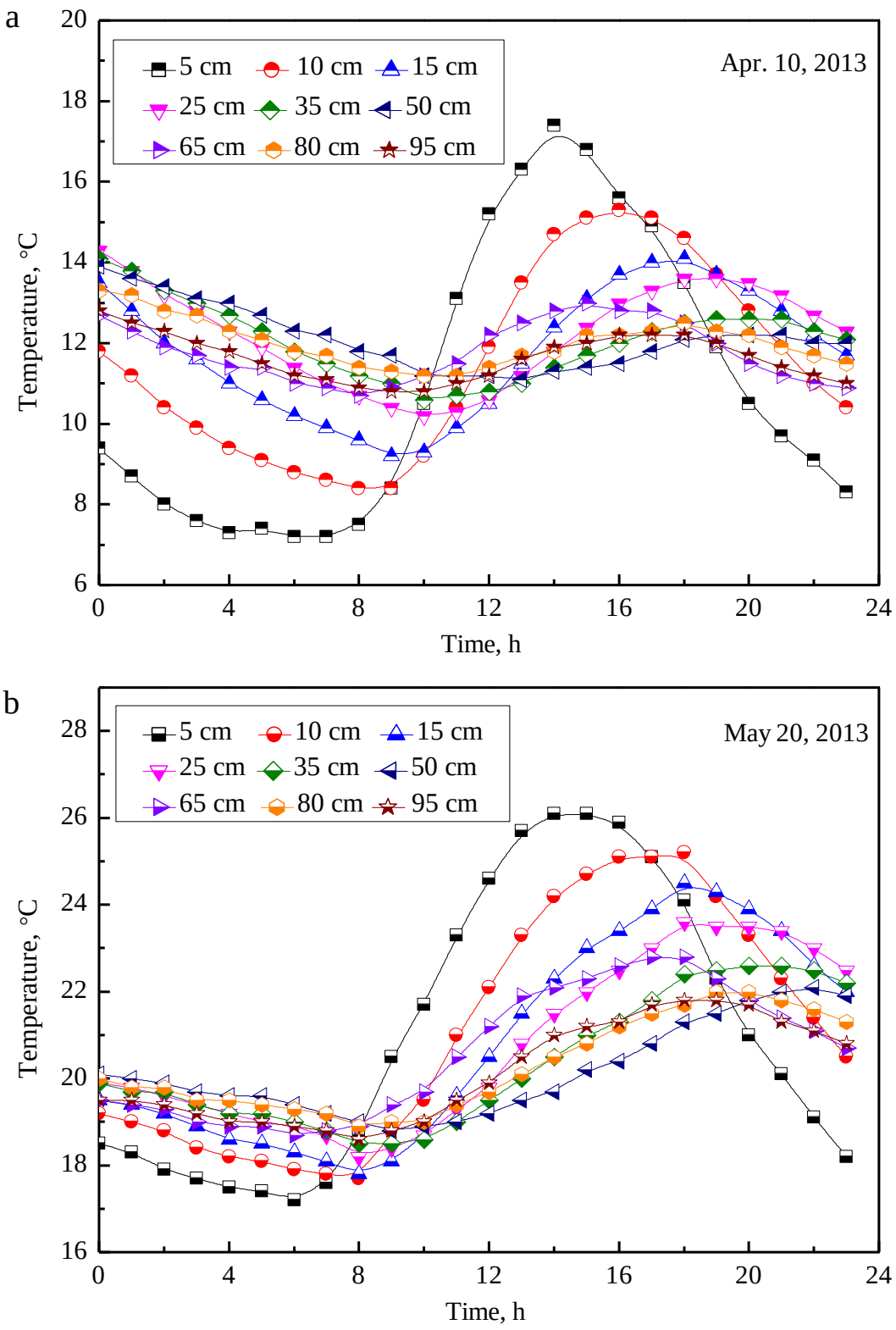

Figure 6.8 Monitored soil temperature variation in one day for the selected two days, (a) Apr. 10th, 2013 and (b) May 20th, 2013

Figure 6.8 shows the temperature variations of soil at different depths in 24 h for the selected two days, April 10th and May 20th. The soil temperature shows a typical sinusoidal behavior at all nine depths. The soil at top surface maintains a greater range for temperature change from day to night. It produces a lowest temperature during night and a highest value at daytime. The amplitude of daily temperature variations decreased with depth due to attenuation of the transported heat energy. Also, it is observed that the soil temperature increases gradually from top soil to the deeper one. Temperature difference of 5 °C between top and low boundary would be performed during daytime. The temperature gradient at the top 25 cm is several times greater than that of deeper soil.

6.4.2 VARIATION OF SOIL TEMPERATURE AND WATER CONTENT

Figure 6.9 compare the simulated and measured soil temperature at three depths 5 cm, 50 cm, and 95 cm. The symbols represent the temperature measured at 14:00 pm of each day. On the whole, satisfactory agreement is obtained between the measured and calculated data. Nevertheless, the simulation for soil temperature at 5 cm only give a good trend of temperature variation, it is difficult to obtain accurate simulation over the whole monitoring period. For the soil temperature at 50 cm and 95 cm, the predicted soil temperature follow fairly well the measured values during the entire simulation period. However, in some period the simulated temperature amplitude is apart from the measured value. A greatest difference about 3 ~ 5 °C would be resulted in.

Figure 6.10 shows the temperature profiles at different selected days. It can be observed that all the simulated temperature profiles fit well with the measured value, expect for the profile at 5 days. From the simulation, temperature of top layer is lower than that of bottom soil; however, it is actually the inverse. This disagreement would be caused by the rainfall event at that day. It also indicates that the soil temperature changed at all the depths. The whole temperature profile increases from 5 days to 60 days, while the temperature profile at finial condition shows a decreasing tendency, moreover, the temperature gradient along the depth is not obvious, thus it is deduced to be influenced by the rainfall.

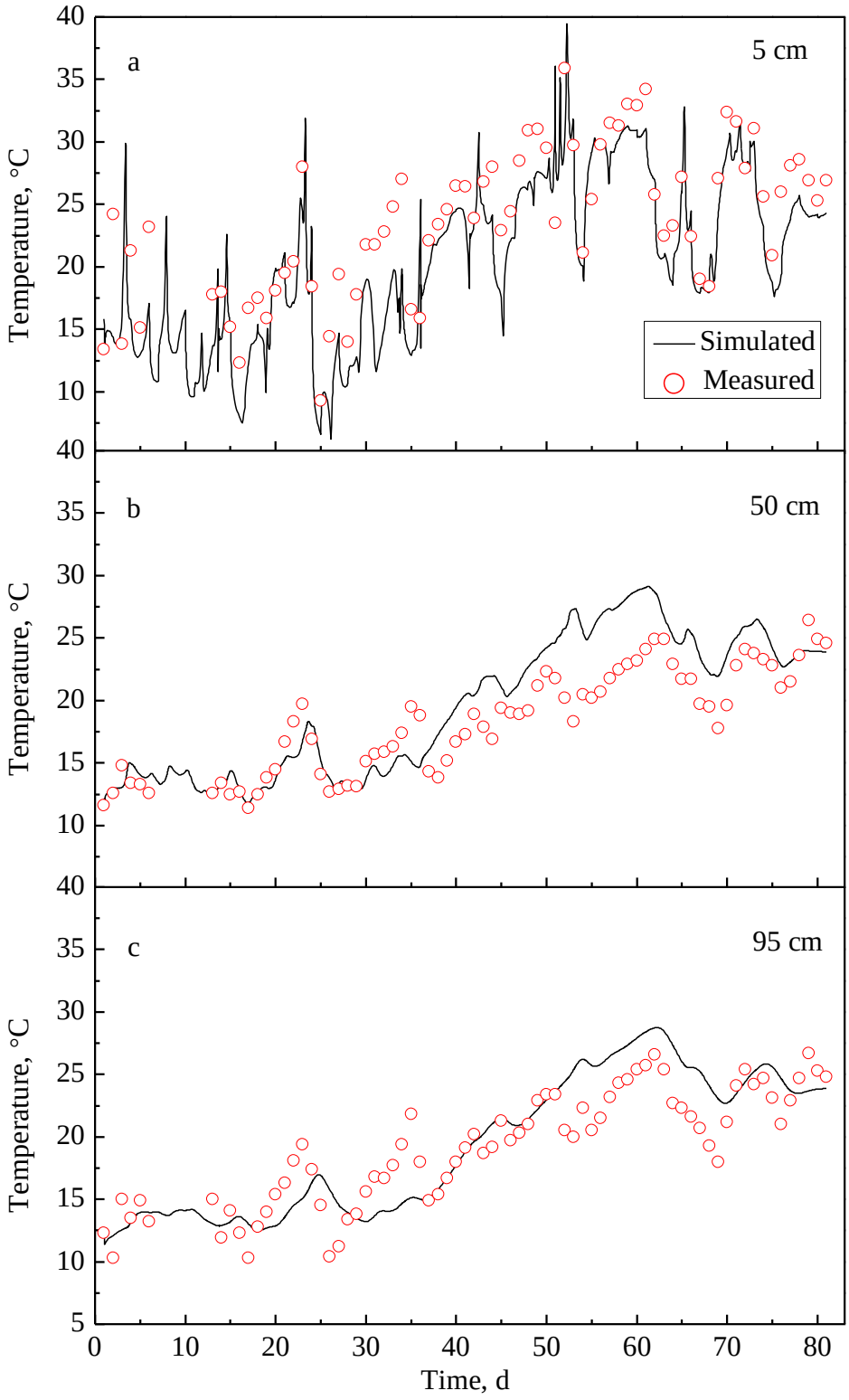

Figure 6.9 Comparison between numerical simulation and measurement for the soil temperature at three depths, (a) 5 cm, (b) 50 cm, and (c) 95 cm

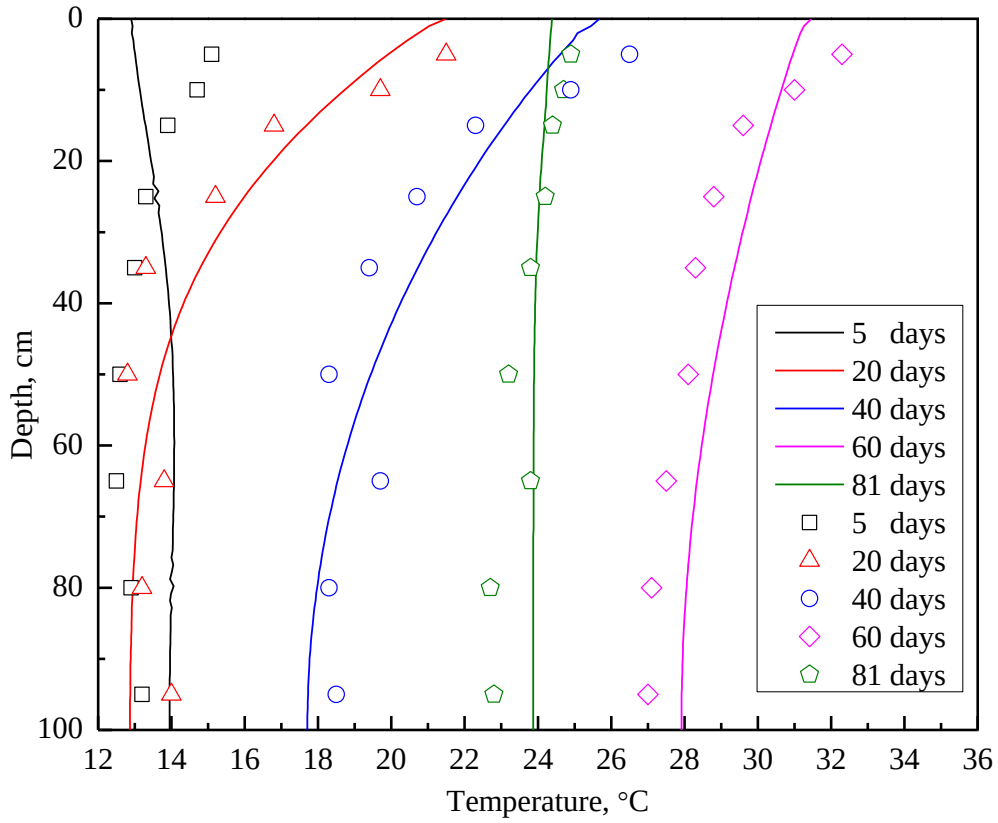

Figure 6.10 Comparison between simulated and measured soil temperature profile for the selected time, the solid lines represent numerical simulation result, symbols are the measured data

Figure 6.11 shows the comparison between simulated and measured volumetric water content at three selected depths: 5 cm, 15 cm, and 50 cm. Simulations are in rough agreement with measurements. For water content at 5 cm and 15 cm, some peaks and valleys at simulated curve is inconsistent with the measured value. For example, for the shape increase of water content at 12 days, the numerical simulation produces underestimation for both 5 cm and 15 cm. For the water content at 55 days, a significant overestimation is observed thereafter. In brief, rapid increases in water content at 5 cm and 15 cm depth after each rainfall are predicted reasonably well. The simulated and measured water content at 50 cm are almost constant during the simulation period while little difference exists between two curves.

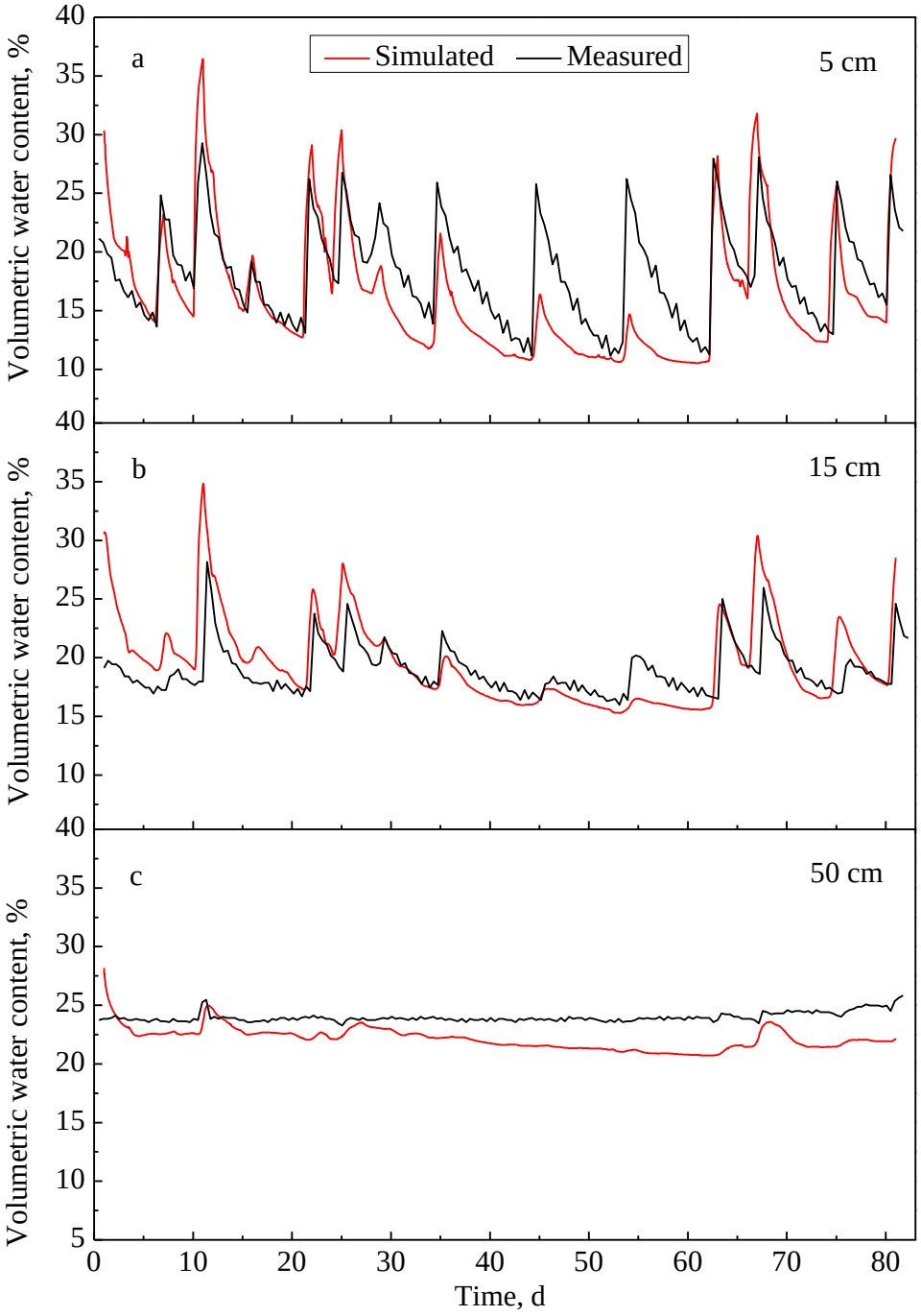

Figure 6.11 Comparison between simulated and measured water content at three different depths, (a) 5 cm, (b) 15 cm, and (c) 50 cm

Figure 6.12 displays the simulated and measured water content profile at five different days. Good agreement can be observed between the solid lines and symbols. A small difference between symbols and lines can be appreciated. It shows that the volumetric water content increase linearly with the soil depth, a linear correction can

be obtained except the profile at 81 days. Due to the influence of rainfall, the water content profile changes at the 81 days, the water content of top 40 cm increases significantly. Moreover, it indicates that the deeper the soil water content, the smaller gradient of the water content. That is because the soil at deeper layer maintain at a condition nearly saturated, the rainfall and evaporation cycle has little influence.

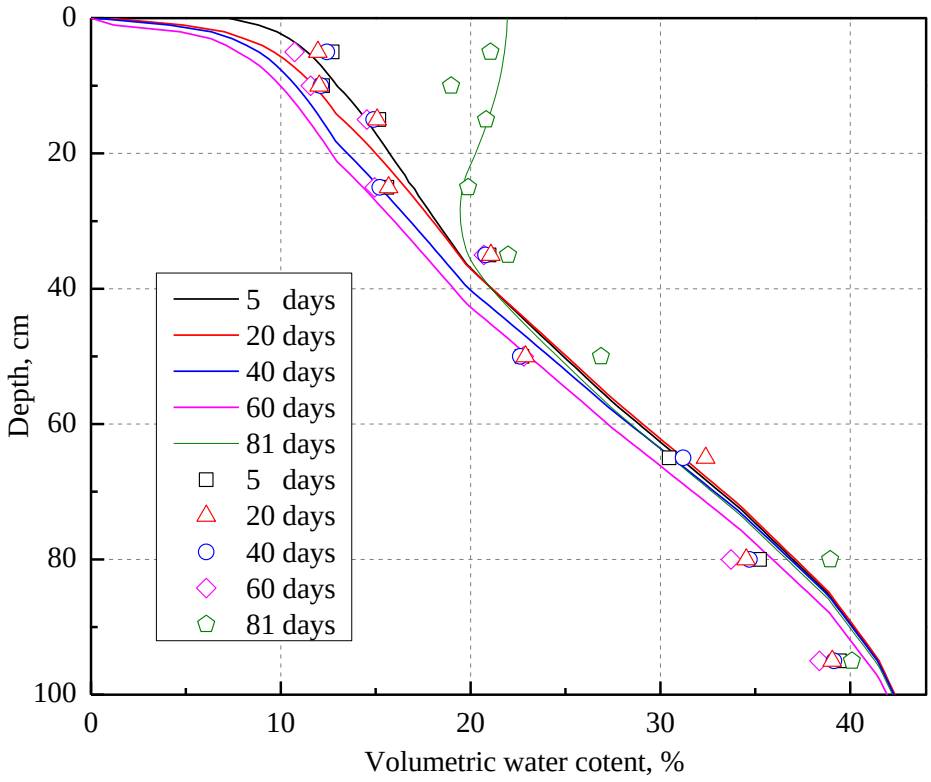

Figure 6.12 Comparison between simulated and measured soil water content profile

6.4.3 DRAINAGE AND EVAPORATION

Figure 6.13 presents the comparison between the calculated and the measured cumulative water drainage from the bottom. The solid line follows fairly well the tendency of measured cumulative drainage. There is a little difference between the total amount of water flowed out, the measured value is about 12.2 cm during 81 days, while the simulated result is around 11.6 cm. The greatest difference appears at about the 65 days, where the disagreement is large to 3.5 cm. In addition, in the first 10 days, a gap between the measured and simulated value is observed, the difference is around 2.5 cm, the percolation would occur due to the high water content profile that is the initial condition of numerical simulation, however, no water flowed out in

actual testing condition. It shows that the percolation always occurs after each rainfall event. For the heavy rainfall event, about 2 days are consumed for the soil water flowing out and achieving an equilibrium state. At that time, amount of water drainage is close to rainfall amount, because the soil body is nearly saturated with no more water can be retained, the soil can be considered as a media for water migration from top to bottom.

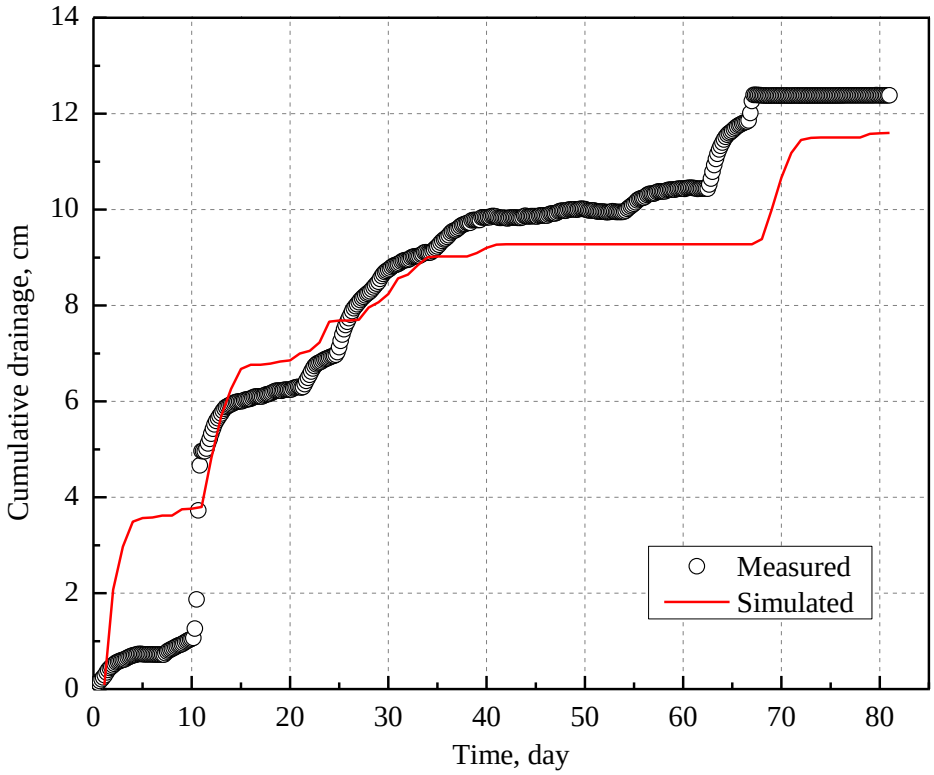

Figure 6.13 Variation of cumulative drainage: comparison between simulation and measurement

The indirectly determination of the evaporation from lysimeter test is reviewed in chapter (refer to Eq. (2.1)), we rewrite that formula here. Considering the conservation of mass of water into and out of the lysimeter, the evaporation may be obtained as follows:

$$E = P - G_p - \Delta S - R_{off} \tag{6.3}$$

where E = evaporation, P = precipitation, G_p = basal percolation, ΔS = changes in moisture storage, R_{off} = surface water runoff. The rainfall can be measured from the weather station and no runoff is assumed during the test, that is to say, all the

precipitation is infiltrated into the soil. The percolation is channeled form the lysimeter by gravity and measured in a drainage tank, the water storage is estimated from the water content profile that measured by the water moisture probe.

The lysimeter in this study, a kind of weighting lysimeter, allow direct measurement of evaporation as it can measure the total weight of soil and stored water. Changes of soil water storage in a lysimeter can be determined by integrating profiles of water content measured using nests of probes. Consequently, the remaining changes in mass can be attributed to losses by evaporation.

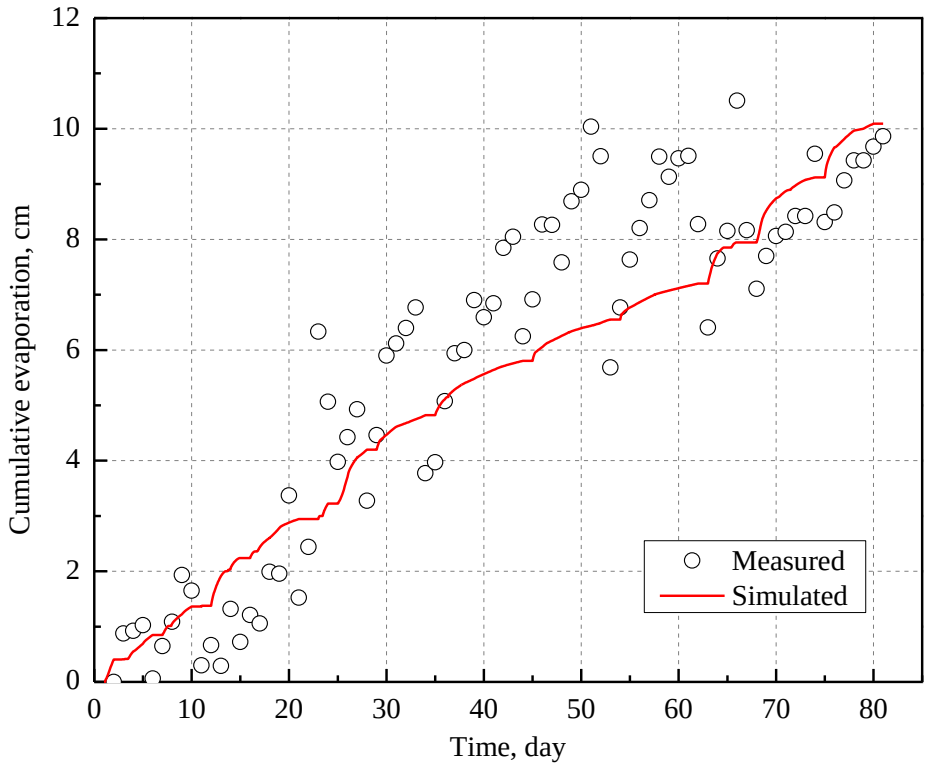

Figure 6.14 Variation of cumulative evaporation from soil surface: comparison between simulation and measurement

The comparison between simulated and measured cumulative evaporation is displayed in Figure 6.14. The simulated cumulative evaporation increases linearly with the elapsing time. It shows that the cumulative evaporation increases with pause for each rainfall event. The total amount of water evaporated loss is about 10 cm, equals to 1.25 mm/d in average during the field test. The symbols in Figure 6.14 are dispersed each other, which due to the error when integrating profiles of water content, deviation of total weight caused by the sensitivity of load cell is also

attribute to this error. Although the measured volumetric water content is discrete, it clearly shows the linear correlation and is agreed well by the simulated result. A conclusion remark is that a significant error would be resulted in using the weighting lysimeter, an optimal design are conducted with both considering the test section and capacity of scales.

6.5 SUMMARY

In this chapter, a lysimeter test conducted in Ito campus of Kyushu University is described, it provide an extensive database of environmental parameters and the reaction of soil properties, the thermal and hydrological phenomena are discussed in this study. These data are also used to compare with and valid the numerical simulation based on HYDRUS-1D code. The conclusions can be summarized as following:

(1) For the volumetric water content, the most significant variation were in the near surface area, it is limited for the soil deeper than 35 cm. the lower the soil depth, the greater change in water content responding to evaporation or precipitation. Soil temperature increases gradually from top soil to the deeper one with temperature gradient of about 0.05 °C/cm. it appears that all the depths are affected, this suggests that temperature is more sensitive to climate change than volumetric water content. The rainfall event shows the function of eliminating temperature gradient and unifying the water content profile, while the evaporation process enlarge the gradient of temperature and water content.

(2) Comparing the simulation results with field measurement, it is found that HYDRUS-1D Code provides a rough simulation for the variation of temperature and water content. Further effort is needed on dealing with the upper boundary.

(3) Although the adopted code provides a relatively direct countermeasure, a two-dimensional or three dimensional model is necessary for a full geometry analysis. In addition, an analytical approach is also necessary to develop for revealing the mechanism of soil-atmosphere interaction in field test.

REFERENCE

Howell, T.A., Schneider, A.D., Jensen, M.E. (1991): History of lysimeter design and use for evapotranspiration measurements. In: Proceedings of the conference on lysimeters for evapotranspiration and environmental measurements, IR

Div/ASCE/Honolulu, 23-25.

Liu, Q (2010): Development and evaluation of self-watering system in unsaturated arid ground. Ph.D. dissertation, Kyushu University, Fukuoka.

Malone, R.W., Bonta, J.V., Stewardson, D.J., Nelsen, T. (2000): Error analysis and quality improvement of the Coshcton weighing lysimeters. Trans ASAE 43:271-280.

Marek, T.H., Schneider, A.D., Howell, T.A., and Ebeling, L.L. (1988): Design and construction of large weighing monolithic lysimeters. Trans ASAE 31:477-484.

Marek, T.H., Piccinni, G., Schneider, A.D., Howell, T.A., Jett, M., Dusek, D.A. (2006): Weighing lysimeters for the determination of crop water requirements and crop coefficients. Appl Eng Agric 22:851-856.

Mualem, Y. (1976): A new model for predicting the hydraulic conductivity of unsaturated porous media. Water Resource Research, 12, 513-521.

Payero, J.O. and Irmak, S. (2008): Construction, installation, and performance of two repacked weighing lysimeters. Irrigation Science, 26, 191-202.

Payero, J.O., and Irmak, S. (2008): Construction, Installation, and Performance of Two Repacked Weighing Lysimeters. Irrigation Science, 26, 191-202.

Saito, H., Šimunek, J., and Mohanty, B.P. (2006): Numerical analysis of coupled water, vapor, and heat transport in the vadose zone. Vadose Zone Journal, 5, 784-800.

Schneider, A.D., Howell, T.A., Moustafa, A.T.A., Evett, S.R., Abou-Zeid, W. (1998): A simplified weighing lysimeter for monolithic or reconstructed soils. Appl Eng Agric 14:267-273.

Šimunek, J., van Genuchten, M.Th., and Šejna, M. (2005): The HYDRUS-1D software package for simulating the. One-dimensional movement of water, heat, and multiple solutes in variably-saturated media. Version 3.0. *HYDRUS Software Series 1*, Department of Environmental Sciences, University of California Riverside, Riverside, California, USA.

van Genuchten, M.Th. (1980): A closed form equation for predicting the hydraulic conductivity of unsaturated soils. Soil Science Society of America Journal, 44, 892-898.

Wilson, G.W., Fredlund, D.G., and Barbour, S.L. (1997): The effect of soil suction on evaporative fluxes from soil surfaces. Canadian Geotechnical Journal, 34, 145-155.

Yang, S.L., Aydin, M., Yano, T., Li, X. (2003): Evapotranspiration of orange trees in

greenhouse lysimeters. Irrig Sci 21:145-149.

Young, M.H., Wierenga, P.J., Mancino, C.F. (1997): Monitoring near-surface soil water storage in turfgrass using time domain reflectometry and weighing lysimetry. Soil Sci Soc Am J 61:1138–1146.

CHAPTER 7

CONCLUSIONS AND FUTURE WORK

7.1 CONCLUSIONS

The primary objective of this thesis is to identify the dominant mechanisms of evaporation from soil surface and to propose the methodology for determining evaporation rate and simulating soil water redistribution. A study of the fundamental mechanisms involved in evaporation characteristics and soil water properties is investigated through both experimental and theoretical approaches. The main conclusion can be drawn as follows,

(1) A climate control apparatus is newly developed for investigating the soil surface evaporation, it has functions of controlling the wind speed (0-3.6 m/s), relative humidity (30-80%), and temperature (20-30 ℃), it is also flexible to response to different experimental demands, for example, the pan soil evaporation test, column soil evaporation test with or without water supply. In addition, it provides the soil evaporation rate in high precision 0.01 mm/h comparing to regular evaporation devices.

(2) Higher atmosphere temperature results in the faster reduction of mean water content and shorter time for reaching the residual stage, time would shorten 4% in average for temperature increasing 1 °C. An increase in wind speed always causes linearly increases in evaporation rate, however, relative humidity controls the average gradients. It appears to be a nonlinear relationship between evaporation rate and relative humidity, an inflection point exists properly at about 60%. Soil structure (dry density) has little influence on the evaporation rate.

(3) Theoretical derivation of E_a/E_p from aerodynamic approach and molecular physic approach shows that only the water content cannot be identified as the

independent variable to formulate the evaporation from all soil surfaces. Additional parameters for soil texture and wind speed must be taken into account as well.

(4) A methodology for determining soil evaporation is presented by defining a critical water content θ_c and setting up the empirical formulation of θ_c for different soil textures and wind speeds. Three easily measured indexes are inputs in this method: the moisture of top 1cm soil, aerodynamic resistance (wind speed), and field capacity as a constant for specified soil texture. Although this parameterization is empirical form, its accuracy for estimating evaporation is evaluated that it agrees well with the experimental data for different soil types.

(5) Based on some assumptions, the analytical models for simulating the soil water redistribution in two categories are developed respectively, which are the evaporation process from infinite soil domain, and evaporation process with water table. In this model, the basic hydraulic parameters k_s, α, (θ_s -θ_r), constant evaporation rate E, and water table depth L are the inputs for simulating instantaneous water content profile. The model in these two cases can comprise the normal problem dealing with evaporation problem. This proposed model is validated by the soil column evaporation test under the climate control apparatus for various experimental conditions.

(6) Some new findings through parameter study based on the proposed model are summarized as follows, among the three hydraulic parameters, the effects of α value and k_s on soil water profile response are much more significant than that of (θ_s -θ_r). The smaller value of desaturation coefficient α, the deeper drying front advances; the greater the values of k_s, the deeper the drying front; (θ_s -θ_r) mainly affects the magnitude of the water content but not the shape of the profiles. E affects the water content profile significantly, the larger the E value results in the more reduction of water content profile. In the case of $z/L \leq 0.2$, soil water content at depth of z would be unaffected by the water table L, and the lower ratio of z/L always results in greater reduction of soil water profile.

(7) The field lysimeter test shows that the most significant variation of volumetric water content are in the near surface area, it is limited for the soil deeper than 35 cm. the lower the soil depth, the greater change in water content responding to evaporation or precipitation. Soil temperature increases gradually from top soil to the deeper one with temperature gradient of about 0.05 °C/cm. it appears

that all the depths are affected, this suggests that temperature is more sensitive to climate change than volumetric water content. The rainfall event shows the function of eliminating temperature gradient and unifying the water content profile, while the evaporation process enlarge the gradient of temperature and water content.

(8) Comparing the simulation results with field measurement from the aspects of water content and temperature variations, drainage and evaporative flux, it is found that HYDRUS-1D Code provides a rough simulation for the variation of temperature and water content. Further effort is needed on dealing with the upper boundary.

7.2 FUTURE WORK

The study presented in this dissertation has provided some insight in understanding and modeling the evaporation from soil surface, moreover, the objectives stated in Chapter 1 has been achieved. However, there are still many questions unanswered. The following suggestion are therefore made for future research on soil-atmosphere interaction and further development of the proposed model,

(1) Although the proposed empirical method to determine evaporation rate from soil surface has been validated based on the experimental result of three different types of soil. However, more experimental evidences from various soils are needed to general this methodology.

(2) This study focuses on the evaporation from homogeneous soil, the theoretical and experimental work are mainly conducted to the single soil layer. In contrast, the soil property in field shows strong vertical and lateral inhomogeneity. The proposed model should be further extended to heterogeneous soil body. Moreover, the final and possibly most difficult extension of this study is the provision for vegetation. The vegetated soil surface would produce the transpiration term, the root uptake also has influence on the soil water distribution, which should be evaluated in the future to make the model more close to actual situation.

(3) The laboratory test and theoretical work conducted for this study are for evaporation only. The existing theory is also applicable for infiltration events. Combined infiltration-evaporation should be carried out. The effect of

hysteresis with respect to the soil water retention curves must also be addressed. The verification of the proposed analytical approach should be carried out in the field condition. The comparison among analytical approach, numerical simulation and field lysimeter test should be analyzed.

(4) The laboratory and field test are conducted using a material resistant to volume change during desiccation. Since clay and silt always exhibit relatively large volume change during evaporation, further test is required to study the effect of shrinkage and cracking.

(5) It would also be beneficial to extend the research to examine the effect of pore-fluid chemistry on the behavior of soils subjected to evaporative conditions. In addition, the salinization is highly closed to evaporation process, the mechanism of which should be studied together in the future, especially for the case of arid and semi-arid region.